CHAPTER SIX

Compressible Flows via Finite Difference Methods

In general, the physical behavior of compressible flows is more complicated than in incompressible flows. Compressible flows may be viscous or inviscid, depending on flow velocities. Compressible inviscid flows are analyzed using the potential or Euler equations, whereas compressible viscous flows are solved from the Navier-Stokes system of equations. Shock waves may occur in compressible flows and require special attention as to the solution methods. Furthermore, shock wave turbulent boundary layer interactions in compressible viscous flows constitute one of the most important physical phenomena in computational fluid dynamics. Let us consider air flows at speeds greater than 100 m/s, which corresponds to a Mach number of approximately 0.3, but less than 1700 m/s, or approximately Mach 5. Air flows in this range ($0.3 \leq M \leq 5$) may be considered as compressible and inviscid. This range is usually subdivided into regions identified as subsonic ($0.3 < M < 0.8$), transonic ($0.8 \leq M \leq 1.2$), and supersonic ($1.2 < M \leq 5$). For $M > 5$, the flow is referred to as hypersonic. Hypersonic flows around a solid body are usually coupled with viscous boundary layers. Effects of dilatational dissipation due to compressibility, high temperature gradients, vortical motions within the secondary boundary layers, radiative heat transfer, vibrational and electronic energies, and chemical reactions are examples of some of the complex physical phenomena associated with hypersonic flows.

In order to take into account the compressibility and variations of density in high-speed flows, we utilize the conservation form of the governing equations, using the density-based formulation. This is in contrast to the pressure-based formulation for incompressible flows discussed in Chapter 5. For compressible flows, we encounter some regions of the flow domain (close to the wall, for example) in which low Mach numbers or incompressible flows prevail. In this case, the density-based formulations become ineffective, with the solution convergence being extremely slow. To resolve such problems, various schemes have been developed. Among them are the preconditioning process for the time-dependent term toward improving the stiff convection eigenvalues and the flowfield-dependent variation (FDV) methods allowing the transitions and interactions of various flow properties as well as all speed flows.

For simple cases of compressible inviscid flows (irrotational, isentropic, isothermal), the potential equation can be used, whereas the Euler equations are preferred for more general compressible inviscid flows. For compressible viscous flows, various approximate governing equations such as boundary layer equations or parabolized

Navier-Stokes system of equations are utilized. However, the most general and complete analysis is to invoke the full Navier-Stokes system of equations, which is the emphasis in this book.

FDM formulations and solution procedures for the potential equation are presented in Section 6.1, with Euler equations and the Navier-Stokes system of equations in Sections 6.2 and 6.3, respectively. The solution of the Navier-Stokes system of equations for compressible and incompressible flows using the preconditioning process will be presented in Section 6.4, followed by the flowfield-dependent variation (FDV) methods in Section 6.5 and various other methods in Section 6.6. Finally, the boundary conditions for compressible flows in general are discussed in Section 6.7.

6.1 POTENTIAL EQUATION

6.1.1 GOVERNING EQUATIONS

The governing equation for steady-state compressible inviscid flows may be represented by the potential equation of the form (2-D),

$$\left[1-\left(\frac{u}{a}\right)^2\right]\frac{\partial u}{\partial x}+\left[1-\left(\frac{\mathrm{v}}{a}\right)^2\right]\frac{\partial \mathrm{v}}{\partial y}-\frac{u\mathrm{v}}{a^2}\left(\frac{\partial u}{\partial y}+\frac{\partial \mathrm{v}}{\partial x}\right)=0 \tag{6.1.1a}$$

or

$$\left[1-\left(\frac{u}{a}\right)^2\right]\frac{\partial u}{\partial x}+\left[1-\left(\frac{\mathrm{v}}{a}\right)^2\right]\frac{\partial \mathrm{v}}{\partial y}-\frac{2}{a^2}u\mathrm{v}\frac{\partial u}{\partial y}=f \tag{6.1.1b}$$

with

$$f=\frac{1}{a^2}u\mathrm{v}\left(\frac{\partial \mathrm{v}}{\partial x}-\frac{\partial u}{\partial y}\right) \tag{6.1.2}$$

and $f=0$ for irrotational flow. In terms of the velocity potential function ϕ, (6.1.1) may be written as

$$\phi_{,ii}-\frac{1}{a^2}\phi_{,i}\phi_{,j}\phi_{,ij}=0$$

or

$$\left(1-M_x^2\right)\frac{\partial^2\phi}{\partial x^2}+\left(1-M_y^2\right)\frac{\partial^2\phi}{\partial y^2}-\frac{2}{a^2}\frac{\partial\phi}{\partial x}\frac{\partial\phi}{\partial y}\frac{\partial^2\phi}{\partial x\partial y}=0 \tag{6.1.3}$$

with $u=\partial\phi/\partial x$, $\mathrm{v}=\partial\phi/\partial y$, $M_x=u/a$, and $M_y=\mathrm{v}/a$.

For small perturbation approximations in irrotational flow, we obtain

$$\left(1-M_\infty^2\right)\frac{\partial^2\phi}{\partial x^2}+\frac{\partial^2\phi}{\partial y^2}=M_\infty^2\left(\frac{1+\gamma}{U_\infty}\right)\frac{\partial\phi}{\partial x}\frac{\partial^2\phi}{\partial x^2} \tag{6.1.4}$$

For unsteady flows, using the first and second laws of thermodynamics for isentropic and irrotational flows, (6.1.1) is modified to

$$\phi_{,ii}-\frac{1}{a^2}\phi_{,i}\phi_{,j}\phi_{,ij}-\frac{1}{a^2}\left[\frac{\partial^2\phi}{\partial t^2}+\frac{\partial}{\partial t}(\phi_{,i}\phi_{,i})\right]=0 \tag{6.1.5}$$

where

$$a^2 = \frac{\partial p}{\partial \rho} = \frac{\gamma p}{\rho} = (\gamma - 1)H = (\gamma - 1)\left[H_0 - \frac{1}{2}\phi_{,i}\phi_{,i} - \frac{\partial \phi}{\partial t}\right]$$

In the case of isentropic flows with stagnation density ρ_0 and stagnation enthalpy H_0, we have

$$\frac{\rho}{\rho_0} = \left[1 - \frac{1}{2H_0}\phi_{,i}\phi_{,i} - \frac{1}{H_0}\frac{\partial \phi}{\partial t}\right]^{\frac{1}{\gamma - 1}} \tag{6.1.6}$$

with

$$H_0 = H + \frac{1}{2}\mathbf{v}\cdot\mathbf{v} \tag{6.1.7}$$

For steady flows, (6.1.6) takes the form

$$\frac{\rho}{\rho_0} = \left[1 - \frac{1}{2H_0}\phi_{,i}\phi_{,i}\right]^{\frac{1}{\gamma - 1}} \tag{6.1.8}$$

or

$$\frac{\rho}{\rho_0} = \left[1 - \frac{\gamma - 1}{2a_0^2}\phi_{,i}\phi_{,i}\right]^{\frac{1}{\gamma - 1}} = \left[1 - \frac{\gamma - 1}{2}M^2\right]^{\frac{1}{\gamma - 1}} \tag{6.1.9}$$

If a nonisentropic process with rotational flows is considered, the momentum equation is written as

$$T\nabla S + \mathbf{v} \times \boldsymbol{\omega} - \nabla H_0 = 0 \tag{6.1.10}$$

where S is the entropy per unit mass. Combining (6.1.10) and (6.1.2), we obtain for two dimensions

$$f = -\frac{1}{V^*}\left(H_{0,i}n_i - \frac{a^2}{\gamma R}S_{,i}n_i\right)\frac{uv}{a^2} \tag{6.1.11}$$

with

$$V^* = vn_1 - un_2$$

It follows from (6.1.10) and (6.1.9) that

$$\frac{\rho}{\rho_0} = \left[\exp\left(\frac{-\Delta S}{c_v}\right)\left(1 - \frac{1}{2H_0}\phi_{,i}\phi_{,i}\right)^{\frac{1}{\gamma - 1}}\right] \tag{6.1.12}$$

where ΔS is the entropy increase over the shock. This is equivalent to a modification of the stagnation density ρ_0

$$\frac{\rho}{\rho_{02}} = \left(1 - \frac{1}{2H_0}\phi_{,i}\phi_{,i}\right)^{\frac{1}{\gamma - 1}} \tag{6.1.13}$$

with

$$\rho_{02} = \rho_{01}\left(\frac{p_{02}}{p_{01}}\right)^{\frac{1}{\gamma}}$$

where the subscripts 1 and 2 denote upstream and downstream of the shock, respectively.

6.1.2 SUBSONIC POTENTIAL FLOWS

For irrotational flow [$f = 0$ in (6.1.3)] with $\Delta x = \Delta y = 1$, the finite difference scheme may be written as

$$\left(1 - M_x^2\right)_{i,j}(\phi_{i+1,j} - 2\phi_{i,j} + \phi_{i-1,j}) + \left(1 - M_y^2\right)_{i,j}(\phi_{i,j+1} - 2\phi_{i,j} + \phi_{i,j-1}) - \frac{1}{2}(M_x M_y)_{i,j}(\phi_{i+1,j+1} - \phi_{i+1,j-1} - \phi_{i-1,j+1} + \phi_{i-1,j-1}) = 0 \tag{6.1.14}$$

It is interesting to note that (6.1.14) is diagonally dominant for subsonic flows, while this is not true for transonic and supersonic flows. This implies that the elliptic nature of (6.1.14) changes to parabolic and hyperbolic forms.

Another scheme is to use the continuity equation,

$$\nabla \cdot (\rho \mathbf{v}) = \nabla \cdot (\rho \nabla \phi) = (\rho \phi_{,i})_{,i} = 0 \tag{6.1.15}$$

Thus, the finite difference form of (6.1.15) may be written as

$$\rho_{i+\frac{1}{2},j}(\phi_{i+1,j} - \phi_{i,j}) - \rho_{i-\frac{1}{2},j}(\phi_{i,j} - \phi_{i-1,j}) + \rho_{i,j+\frac{1}{2}}(\phi_{i,j+1} - \phi_{i,j}) - \rho_{i,j-\frac{1}{2}}(\phi_{i,j} - \phi_{i,j-1}) = 0 \tag{6.1.16}$$

To solve (6.1.16), the so-called Taylor linearization [Murman and Cole, 1971] may be used:

$$\nabla \cdot (\rho^n \nabla \phi^{n+1}) = 0 \tag{6.1.17}$$

or

$$\nabla \cdot \left[\rho\left(|\nabla \phi^n|^2\right)\nabla \phi^{n+1}\right] = 0 \tag{6.1.18}$$

where density is calculated from the known values of the velocities obtained at the previous iteration step n.

6.1.3 TRANSONIC POTENTIAL FLOWS

As the Mach number approaches unity, the potential equation tends toward parabolic, leading to instability or nonconvergence of the numerical scheme. To cope with this difficulty, a number of numerical methods have been developed. They include artificial viscosity, artificial compressibility, artificial flux or upwinding, and iterations with overrelaxation, among others.

(a) Artificial Viscosity with Nonconservative Equation

In order to resolve shock discontinuities, we consider two forms of finite differences:

Central Differences

$$\left.\frac{\partial^2 \phi}{\partial x^2}\right|_{i,j}^{(c)} = \frac{1}{(\Delta x)^2}(\phi_{i+1,j} - 2\phi_{i,j} + \phi_{i-1,j}) \tag{6.1.19}$$

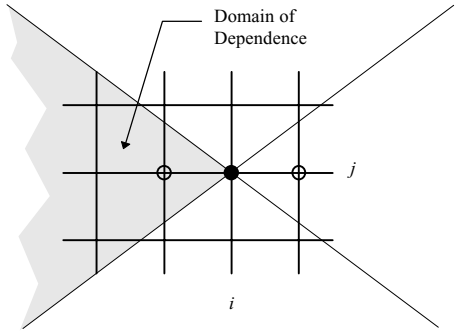

Figure 6.1.1 Region of dependence.

Backward (upwind) Differences

$$\left.\frac{\partial^2\phi}{\partial x^2}\right|_{i,j}^{(B)} = \frac{1}{(\Delta x)^2}(\phi_{i-2,j} - 2\phi_{i-1,j} + \phi_{i,j}) \tag{6.1.20}$$

Obviously, the central difference is in opposition to the physical properties of supersonic flows since only the points located within the region of dependence (Figure 6.1.1) can have an effect on the flow properties at the point under consideration ($\phi_{i,j}$). Subtracting (6.1.19) from (6.1.20), we get

$$\left.\frac{\partial^2\phi}{\partial x^2}\right|_{i,j}^{(B)} - \left.\frac{\partial^2\phi}{\partial x^2}\right|_{i,j}^{(C)} = -\frac{1}{(\Delta x)^2}(\phi_{i+1,j} - 3\phi_{i,j} + 3\phi_{i-1,j} - \phi_{i-2,j})$$

or

$$\left.\frac{\partial^2\phi}{\partial x^2}\right|_{i,j}^{(B)} = \left.\frac{\partial^2\phi}{\partial x^2}\right|_{i,j}^{(C)} - \Delta x\frac{\partial^3\phi}{\partial x^3} \tag{6.1.21}$$

Thus, it is seen that the backward difference amounts to adding an artificial viscosity, $\Delta x\frac{\partial^3\phi}{\partial x^3}$, to the central difference. Therefore, the upwind differencing automatically adds an entropy condition in the form of artificial dissipation terms which are proportional to the mesh size.

For applications to the small perturbation equation, we have the following options [Murman and Cole, 1971]:

$$(1 - M^2)\phi_{xx}^{(B)} + \phi_{yy}^{(C)} = 0 \qquad \text{for } M > 1 \tag{6.1.22}$$

$$(1 - M^2)\phi_{xx}^{(C)} + \phi_{yy}^{(C)} = -\Delta x(M^2 - 1)\phi_{xxx} \qquad \text{for } M > 1 \tag{6.1.23}$$

$$(1 - M^2)\phi_{xx}^{(C)} + \phi_{yy}^{(C)} = 0 \qquad \text{for } M < 1 \tag{6.1.24}$$

To apply these conditions to the full potential equation, we must take into account the local flow direction (Figure 6.1.2). Jameson [1974] introduced "rotational difference scheme" for this purpose.

Choosing the local streamline coordinates as (ℓ, n),

$$(1 - M^2)\phi_{\ell\ell} - \phi_{nn} = 0 \tag{6.1.25}$$

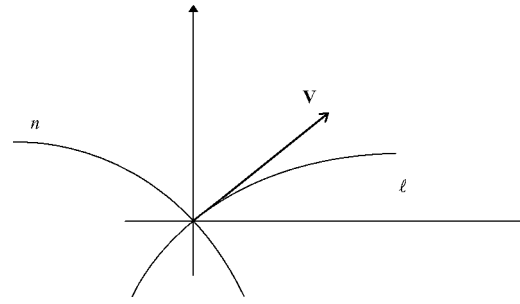

Figure 6.1.2 Local streamlines.

where

$$\phi_{\ell\ell} = \frac{1}{q^2}(u^2\phi_{xx} + 2uv\phi_{xy} + v^2\phi_{yy}) \tag{6.1.26a}$$

$$\phi_{nn} = \frac{1}{q^2}(v^2\phi_{xx} - 2uv\phi_{xy} + u^2\phi_{yy}) \tag{6.1.26b}$$

with $q = (u^2 + v^2)^{\frac{1}{2}}$ and

$$\phi_{xy}^{(C)} = \frac{1}{4\Delta x\Delta y}(\phi_{i+1,j+1} - \phi_{i+1,j-1} - \phi_{i-1,j+1} + \phi_{i-1,j-1})$$

$$\phi_{xy}^{(B)} = \frac{1}{4\Delta x\Delta y}(\phi_{i,j} - \phi_{i-1,j} - \phi_{i,j-1} + \phi_{i-1,j-1})$$

$$= \phi_{xy}^{(C)} - \frac{\Delta x}{2}\phi_{xxy} - \frac{\Delta y}{2}\phi_{xyy}$$

$$\phi_{\ell\ell}^{(B)} = \phi_{\ell\ell}^{(C)} - \frac{u^2}{q}\Delta x\phi_{xxx} - \frac{v^2}{q}\Delta y\phi_{yyy} - \frac{uv}{q}(\Delta x\phi_{xxy} + \Delta y\phi_{xyy})$$

Thus, the rotational difference scheme takes the form

$$(1 - M^2)\phi_{\ell\ell}^{(C)} - \phi_{nn}^{(C)} = g \tag{6.1.27}$$

$$g = \frac{1}{q^2}(1 - M^2)[\Delta x(u^2\phi_{xxx} + uv\phi_{xxy}) + \Delta y(v^2\phi_{yyy} + uv\phi_{xyy})]$$

(b) Artificial Viscosity with Conservative Equation

The potential equation in conservation form with artificial viscosity is written as

$$\nabla \cdot (\rho\nabla\phi + \mathbf{A}) = 0 \tag{6.1.28}$$

where $\boldsymbol{A}$ is the artificial viscosity vector,

$$\boldsymbol{A} = -\mu(u\rho_x\Delta x\mathbf{i}_x + v\rho_y\Delta y\mathbf{i}_y) \tag{6.1.29}$$

$$\rho_x = -\frac{\rho}{a^2}\mathbf{v}\cdot\frac{\partial\mathbf{v}}{\partial x} = -\frac{\rho}{a^2}\left(u\frac{\partial u}{\partial x} + v\frac{\partial v}{\partial x}\right)$$

$$\rho_y = -\frac{\rho}{a^2}\mathbf{v}\cdot\frac{\partial\mathbf{v}}{\partial y} = -\frac{\rho}{a^2}\left(u\frac{\partial u}{\partial y} + v\frac{\partial v}{\partial y}\right)$$

with μ being the switching function,

$$\mu = \max\left[0, \left(1 - \frac{1}{M^2}\right)\right] \tag{6.1.30}$$

and the derivatives of the density are upwind differenced.

(c) Artificial Compressibility

Equation (6.1.28) may be rewritten in the form [Holst and Ballhaus, 1979],

$$\frac{\partial}{\partial x}(\overline{\rho}\phi_x) + \frac{\partial}{\partial y}(\overline{\overline{\rho}}\phi_y) = 0 \tag{6.1.31}$$

where

$$\overline{\rho} = \rho - \mu\rho_x \Delta x \tag{6.1.32a}$$

$$\overline{\overline{\rho}} = \rho - \mu\rho_y \Delta y \tag{6.1.32b}$$

The artificial densities are prescribed at the midpoints $(i \pm \frac{1}{2}, j)$ and $(i, j \pm \frac{1}{2})$.
For $u_{i+\frac{1}{2},j} > 0$

$$\overline{\rho}_{i+\frac{1}{2},j} = \rho_{i+\frac{1}{2},j} - \mu_{ij}\left(\rho_{i+\frac{1}{2},j} - \rho_{i-\frac{1}{2},j}\right) \tag{6.1.33a}$$

For $u_{i+\frac{1}{2},j} < 0$

$$\overline{\rho}_{i+\frac{1}{2},j} = \rho_{i+\frac{1}{2},j} + \mu_{i+1,j}\left(\rho_{i+\frac{1}{2},j} - \rho_{i+\frac{3}{2},j}\right) \tag{6.1.33b}$$

For $\mathrm{v}_{i,j+\frac{1}{2}} > 0$

$$\overline{\overline{\rho}}_{i,j+\frac{1}{2}} = \rho_{i,j+\frac{1}{2}} - \mu_{ij}\left(\rho_{i.j+\frac{1}{2}} - \rho_{i,j-\frac{1}{2}}\right) \tag{6.1.34a}$$

For $\mathrm{v}_{i,j+\frac{1}{2}} < 0$

$$\overline{\overline{\rho}}_{i,j+\frac{1}{2}} = \rho_{i,j+\frac{1}{2}} + \mu_{i,j+1}\left(\rho_{i,j+\frac{1}{2}} - \rho_{i,j+\frac{3}{2}}\right) \tag{6.1.34b}$$

An alternative form for artificial compressibility may be given as

$$\boldsymbol{\nabla} \cdot (\tilde{\rho}\,\boldsymbol{\nabla}\phi) = 0 \tag{6.1.35}$$

where

$$\tilde{\rho} = \rho - \mu\frac{\partial\rho}{\partial\ell}\Delta\ell = \rho - \mu\Delta\ell\left(\frac{u}{q}\rho_x + \frac{\mathrm{v}}{q}\rho_y\right) \tag{6.1.36a}$$

or

$$\tilde{\rho} = \rho - \mu\left(\frac{u}{q}\rho_x\Delta x + \frac{\mathrm{v}}{q}\rho_y\Delta y\right) \tag{6.1.36b}$$

Various switching functions have been suggested for stability, such as

$$\mu = \max\left[0, \left(1 - \frac{M_c^2}{M^2}\right)CM^2\right] \tag{6.1.37}$$

where M_c is a cutoff Mach number of the order of $M \cong 0.95$, $1 \le C \le 2$. The cutoff

Mach number M_c activates the switching function in the small subsonic region $M_c \leq M \leq 1$ close to the sonic lines.

(d) Artificial Flux or Flux Upwinding

For switching at sonic points to avoid unwanted expansion peaks, we may utilize controlled monotone schemes such as those used in Euler equations [Engquist and Osher, 1980; Osher, Hafez, and Whitlow, 1985]. To this end, we may write the continuity equation in the form

$$\frac{\partial \rho}{\partial \ell} = -\frac{\rho q}{a^2}\frac{\partial q}{\partial \ell} \tag{6.1.38}$$

and

$$\begin{aligned}\frac{\partial \rho q}{\partial \ell} &= -\frac{\rho}{a^2}q^2\frac{\partial q}{\partial \ell} + \rho\frac{\partial q}{\partial \ell} = \rho(1-M^2)\frac{\partial q}{\partial \ell} \\ &= q\left(1-\frac{1}{M^2}\right)\frac{\partial \rho}{\partial \ell}\end{aligned} \tag{6.1.39}$$

The corrected upwinded flux $\tilde{\rho} q$ can be written in supersonic regions as

$$\tilde{\rho} q = \rho q - q\left(1-\frac{1}{M^2}\right)\frac{\partial \rho}{\partial \ell}\Delta\ell \tag{6.1.40}$$

or

$$\tilde{\rho} q = \rho q - \frac{\partial}{\partial \ell}(\rho q)\Delta\ell \tag{6.1.41}$$

A modification of (6.1.41) results in

$$\overline{\rho q} = \rho q - \frac{\partial}{\partial \ell}[\mu(\rho q - \rho^* q^*)]\Delta\ell \tag{6.1.42}$$

where $\rho^* q^*$ denotes the sonic flux, $\mu = 0$ for subsonic flow ($M \leq 1, q \leq q^*, \rho \geq \rho^*$) and $\mu = 1$ for supersonic flows ($M > 1, q > q^*, \rho < \rho^*$) (see Figure 6.1.3). The discrete form

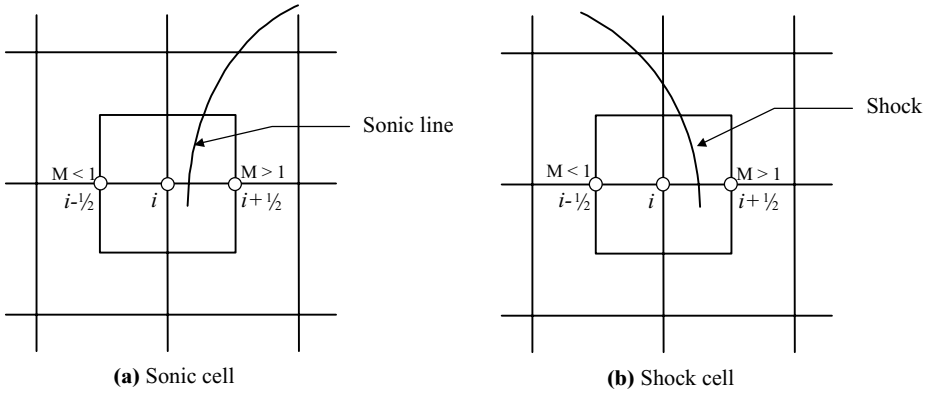

(a) Sonic cell **(b)** Shock cell

Figure 6.1.3 Flux upwinding at sonic and shock point transitions.

of (6.1.42) becomes

$$(\overline{\rho q})_{i+\frac{1}{2},j} = (\rho q)_{i+\frac{1}{2},j} - \mu_{i+\frac{1}{2},j}(\rho q - \rho^* q^*)_{i+\frac{1}{2},j} + \mu_{i-\frac{1}{2},j}(\rho q - \rho^* q^*)_{i-\frac{1}{2},j} \tag{6.1.43}$$

It is similar for other points. Thus, we have
For $M < 1$

$$(\overline{\rho q})_{i+\frac{1}{2},j} = (\rho q)_{i+\frac{1}{2},j} \tag{6.1.44}$$

For $M > 1$

$$(\overline{\rho q})_{i+\frac{1}{2},j} = (\rho q)_{i-\frac{1}{2},j} \tag{6.1.45}$$

For $M = 1$

$$(\overline{\rho q})_{i+\frac{1}{2},j} = (\rho^* q^*) \tag{6.1.46}$$

Notice that this scheme guarantees that expansion shocks will not occur when $(\rho q)_{i+\frac{1}{2},j} < (\rho^* q^*)$.

At a shock transition, we obtain

$$(\overline{\rho q})_{i+\frac{1}{2},j} = (\rho q)_{i+\frac{1}{2},j} + (\rho q - \rho^* q^*)_{i-\frac{1}{2},j} \tag{6.1.47}$$

At shock points, the switching ensures that there is only one mesh point in the shock region since the corresponding cell is treated as fully supersonic or fully subsonic as soon as the shock cell is left. This results in a very sharp shock.

(e) Over-Relaxation Scheme

To solve (6.1.22) in the supersonic region, we write

$$(1 - M^2)\left(\phi^{n+1}_{i-2,j} - 2\phi^{n+1}_{i-1,j} + \phi^{\overline{n+1}}_{i,j}\right) + \left(\phi^{\overline{n+1}}_{i,j+1} - 2\phi^{\overline{n+1}}_{i,j} + \phi^{\overline{n+1}}_{i,j-1}\right) = 0 \tag{6.1.48}$$

where

$$\phi^{n+1} = \phi^n + \omega\left(\phi^{\overline{n+1}} - \phi^n\right) \tag{6.1.49}$$

Denoting that

$$\Delta\phi = \phi^{n+1} - \phi^n \tag{6.1.50}$$

we have

$$(M^2 - 1)_{i,j}(\omega\Delta\phi_{i-2,j} - 2\omega\Delta\phi_{i-1,j} + \Delta\phi_{i,j}) - (\Delta\phi_{i,j+1} - 2\Delta\phi_{i,j} + \Delta\phi_{i,j-1}) = \omega R^n_{i,j} \tag{6.1.51}$$

or

$$(M^2 - 1)\left[\omega E_x^{-1}\delta_x^2 + (1 - \omega)\right]\Delta\phi_{i,j} - \delta_y^2\phi_{i,j} = \omega R^n_{i,j} \tag{6.1.52}$$

where E is the shift operator ($E_x\phi_{i,j} = \phi_{i+1,j}$) and δ^2 is the central second difference

operator. The equivalent artificial time dependent formulation is

$$(M^2 - 1)[\omega\phi_{xxt} + (1 - \omega)\phi_t] - \phi_{yyt} = \frac{\omega}{\tau} R \tag{6.1.53}$$

where

$$\phi_t \cong \frac{\Delta\phi}{\tau} \tag{6.1.54}$$

with τ being a fictitious time step and where ϕ_{xxt} is backward differenced and R is the differential potential equation.

In (6.1.53), ϕ_{yy} is represented by

$$\phi_{yy} = \delta_y^2 \phi^{n+1} + (\omega - 1)\delta_y^2 \phi^n \tag{6.1.55}$$

but the appropriate procedure in the supersonic region is to march in the flow direction, such that $\phi_{i,j}^{n+1}$ can be determined only as a function of the new values $\phi_{i-2,j}^{n+1}$ and $\phi_{i-1,j}^{n+1}$ determined on the previous columns. This implies that ϕ_{yy} should be represented by $\delta_y^2 \phi^{n+1}$ in the supersonic region. Note that the scheme (6.1.48) satisfies this requirement for $\omega = 1$. For a general relaxation procedure, this condition can be satisfied by taking the y-derivative terms at the new level $n + 1$, instead of the intermediate level, introducing a factor ω in front of the y second difference operator of (6.1 52).

The analysis using the potential equation has been well established, but important physical phenomena such as rotational, nonisentropic, or nonisothermal effects are not taken into account in the governing equation. For this reason, the most general approach to the analysis of compressible inviscid flows must resort to the Euler equations. This is the subject of the next section.

6.2 EULER EQUATIONS

Compressible inviscid flows including rotational, nonisentropic, and nonisothermal effects require simultaneous solutions of continuity, momentum, and energy equations. In this approach, however, specialization for small perturbation or linearization outside of transonic flow as done in the potential equation can not be allowed. Thus, the difficulty encountered in transonic flows with shock discontinuities must be resolved with special computational schemes.

The most basic requirement for the solution of the Euler equations is to assure that solution schemes provide an adequate amount of artificial viscosity required for rapid convergence toward an exact solution. Furthermore, eigenvalues and compatibility relations associated with convection terms are important factors in the resolution of shock and expansion waves.

Solution schemes for the Euler equations may be grouped into three major categories: (1) central schemes, (2) first order upwind schemes, and (3) second order upwind schemes and essentially nonoscillatory schemes. These schemes are tabulated in Table 6.2.1 and elaborated in the following subsections.

Table 6.2.1 Various Computational Schemes for Euler Equations

Central Schemes	First Order Upwind Schemes	Second Order Upwind Schemes
1. Combined Space-Time Integration	**1. Flux Vector Splitting**	**1. Extrapolation**
(a) Explicit Schemes	Courant, Isaacson, and Reeves (1952)	**(a) Variable Extrapolation (MUSCL)**
Lax-Friendrichs – First order (1954)	Moretti (1979)	Van Leer (1979)
Lax-Wendroff – Second order (1960)	Steger and Warming (1981)	**(b) Flux Extrapolation**
(b) Two-Step Explicit Schemes	VanLeer (1982)	Van Leer (1979)
Richtmyer and Morton (1967)	**2. Godunov Methods-Riemann Solvers**	**2. Explicit TVD Upwind**
MacCormack (1969)	**(a) Exact Riemann Solvers**	VanLeer (1974)
LeRat and Peyret (1974)	Godunov (1959) – First order	Harten (1983)
(c) Implicit Schemes	VanLeer (1979) – Second order	Osher (1984)
MacCormack (1981)	Woodward and Colella (1984)	Osher and Chakravarthy (1984)
Casier, Deconinck, Hirsch (1983)	Ben-Artzi and Falcovitz (1984)	**3. Implicit TVD Upwind**
LeRat (1979, 1983)	**(b) Approximate Riemann Solvers**	Yee (1986)
2. Separate Space-Time Integration	Roe (1981)	**4. Central TVD Implicit or Explicit**
(a) Implicit Schemes	Enquist and Osher (1980)	Davis (1984)
Briley and McDonald (1975)	Osher (1982)	Roe (1985)
Beam and Warming (1976)	Harten, Lax, Van Leer (1983)	Yee (1985)
(b) Explicit Schemes (Multistage Runge-Kutta)		**5. Essentially Nonoscillatory Scheme**
Jameson, Schmidt, Turkel (1981)		Harten and Osher (1987)
		6. Flux Corrected Transport
		Boris and Book (1973)

6.2.1 MATHEMATICAL PROPERTIES OF EULER EQUATIONS

6.2.1.1 Quasilinearization of Euler Equations

The Euler equations may be linearized in terms of conservation variables or primitive (nonconservation) variables. Consider the conservation form of the Euler equations,

$$\frac{\partial \mathbf{U}}{\partial t} + \frac{\partial \mathbf{F}_i}{\partial x_i} = 0, \quad \text{or} \quad \frac{\partial \mathbf{U}}{\partial t} + \mathbf{a}_i \frac{\partial \mathbf{U}}{\partial x_i} = 0 \quad (i = 1, 2, 3) \tag{6.2.1}$$

with

$$\mathbf{U} = \begin{bmatrix} \rho \\ \rho v_j \\ \rho E \end{bmatrix}, \qquad \mathbf{F}_i = \begin{bmatrix} \rho v_i \\ \rho v_i v_j + p\delta_{ij} \\ \rho E v_i + p v_i \end{bmatrix}, \qquad \mathbf{a}_i = \frac{\partial \mathbf{F}_i}{\partial \mathbf{U}}, \tag{6.2.2}$$

For two dimensions, components of the convection Jacobian $\mathbf{a}_i$ $(i = 1, 2)$ are given by

$$\mathbf{a}_1 = \begin{bmatrix} 0 & 1 & 0 & 0 \\ \dfrac{(\gamma-3)u^2}{2} + \dfrac{(\gamma-1)\mathrm{v}^2}{2} & (3-\gamma)u & -(\gamma-1)\mathrm{v} & \gamma-1 \\ -u\mathrm{v} & \mathrm{v} & u & 0 \\ -\gamma u E + (\gamma-1)uq^2 & \gamma E - \dfrac{\gamma-1}{2}(\mathrm{v}^2+3u^2) & -(\gamma-1)u\mathrm{v} & \gamma u \end{bmatrix} \tag{6.2.3a}$$

$$\mathbf{a}_2 = \begin{bmatrix} 0 & 0 & 1 & 0 \\ -u\mathrm{v} & \mathrm{v} & u & 0 \\ \dfrac{(\gamma-3)\mathrm{v}^2}{2} + \dfrac{(\gamma-1)u^2}{2} & -(\gamma-1)u & (3-\gamma)\mathrm{v} & \gamma-1 \\ -\gamma \mathrm{v} E + (\gamma-1)\mathrm{v}q^2 & -(\gamma-1)u\mathrm{v} & \gamma E - \dfrac{\gamma-1}{2}(u^2+3\mathrm{v}^2) & \gamma\mathrm{v} \end{bmatrix} \tag{6.2.3b}$$

Alternatively, the Euler equations may be written in nonconservation form for isentropic flow in terms of the primitive variable $\mathbf{V}$ as

$$\frac{\partial \mathbf{V}}{\partial t} + \mathbf{A}_i \frac{\partial \mathbf{V}}{\partial x_i} = 0 \tag{6.2.4}$$

with

$$\mathbf{V} = \begin{bmatrix} \rho \\ u \\ \mathrm{v} \\ p \end{bmatrix} = \begin{bmatrix} \rho \\ u \\ \mathrm{v} \\ (\gamma-1)\left(\rho E - \rho \dfrac{(u^2+\mathrm{v}^2)}{2}\right) \end{bmatrix} \tag{6.2.5}$$

$$\mathbf{A}_1 = \begin{bmatrix} u & \rho & 0 & 0 \\ 0 & u & 0 & \dfrac{1}{\rho} \\ 0 & 0 & u & 0 \\ 0 & \rho a^2 & 0 & u \end{bmatrix}, \qquad \mathbf{A}_2 = \begin{bmatrix} \mathrm{v} & 0 & \rho & 0 \\ 0 & \mathrm{v} & 0 & 0 \\ 0 & 0 & \mathrm{v} & \dfrac{1}{\rho} \\ 0 & 0 & \rho a^2 & \mathrm{v} \end{bmatrix} \tag{6.2.6}$$

Introducing a transformation between the conservation and nonconservation variables,

$$\mathbf{M} = \frac{\partial \mathbf{U}}{\partial \mathbf{V}} \tag{6.2.7}$$

or

$$\mathbf{M}=\begin{bmatrix} 1 & 0 & 0 & 0 \\ u & \rho & 0 & 0 \\ v & 0 & \rho & 0 \\ \dfrac{q^2}{2} & \rho u & \rho v & \dfrac{1}{\gamma-1} \end{bmatrix} \quad \mathbf{M}^{-1}=\begin{bmatrix} 1 & 0 & 0 & 0 \\ \dfrac{-u}{\rho} & \dfrac{1}{\rho} & 0 & 0 \\ \dfrac{-v}{\rho} & 0 & \dfrac{1}{\rho} & 0 \\ \dfrac{\gamma-1}{2}q^2 & -(\gamma-1)u & -(\gamma-1)v & \gamma-1 \end{bmatrix} \tag{6.2.8}$$

and combining (6.2.1), (6.2.4), and (6.2.7), we obtain

$$\mathbf{M}\frac{\partial \mathbf{V}}{\partial t}+\mathbf{a}_i\mathbf{M}\frac{\partial \mathbf{V}}{\partial x_i}=0 \tag{6.2.9}$$

Multiplying (6.2.9) by $\mathbf{M}^{-1}$, we obtain the form given by (6.2.4):

$$\frac{\partial \mathbf{V}}{\partial t}+\mathbf{A}_i\frac{\partial \mathbf{V}}{\partial x_i}=0 \tag{6.2.10}$$

with

$$\mathbf{A}_i=\mathbf{M}^{-1}\mathbf{a}_i\mathbf{M}, \qquad \mathbf{a}_i=\mathbf{M}\mathbf{A}_i\mathbf{M}^{-1} \tag{6.2.11}$$

Note that **M** represents the transformation matrix between the conservation variables **U** and the primitive variables **V**.

6.2.1.2 Eigenvalues and Compatibility Relations

In order to examine the oscillatory behavior of the equations such as (6.2.4), we write **V** in the form

$$\mathbf{V}=\overline{\mathbf{V}}e^{\mathbf{I}(\boldsymbol{\kappa}\cdot\mathbf{x}-\omega t)}=\overline{\mathbf{V}}e^{\mathbf{I}(\kappa_i x_i-\omega t)} \tag{6.2.12}$$

Substituting (6.2.12) into (6.2.10) leads to

$$(-\omega+\mathbf{A}_i\kappa_i)\overline{\mathbf{V}}=0 \tag{6.2.13}$$

or

$$|\mathbf{K}-\lambda\mathbf{I}|=0 \tag{6.2.14}$$

with

$$\omega=\lambda\mathbf{I}, \quad \mathbf{A}_i\kappa_i=\mathbf{K}$$

For one dimension, (6.2.14) becomes

$$\begin{vmatrix} u-\lambda & \rho & 0 \\ 0 & u-\lambda & \dfrac{1}{\rho} \\ 0 & \rho a^2 & u-\lambda \end{vmatrix} = 0 \tag{6.2.15}$$

where $\lambda_1 = u$, $\lambda_2 = u + a$, $\lambda_3 = u - a$, constitute eigenvalues.

Return to (6.2.10) for one-dimensional case and write

$$\mathbf{L}^{-1}\frac{\partial \mathbf{V}}{\partial t} + \mathbf{L}^{-1}\mathbf{A}\frac{\partial \mathbf{V}}{\partial x} = 0, \quad \text{with} \quad \mathbf{L} = \frac{\partial \mathbf{V}}{\partial \mathbf{W}} \tag{6.2.16}$$

where $\mathbf{L}^{-1}$ is the matrix which will diagonalize the matrix $\mathbf{K} = \mathbf{A}_i \kappa_i$. Using (6.2.7) in (6.2.16) leads to

$$\mathbf{L}^{-1}\mathbf{M}^{-1}\left(\frac{\partial \mathbf{U}}{\partial t} + \mathbf{A}\frac{\partial \mathbf{U}}{\partial x}\right) = 0 \tag{6.2.17}$$

Similarly, we may define the variable $\mathbf{P}$ in the form

$$\mathbf{P} = \frac{\partial \mathbf{U}}{\partial \mathbf{W}} = \frac{\partial \mathbf{U}}{\partial \mathbf{V}}\frac{\partial \mathbf{V}}{\partial \mathbf{W}} = \mathbf{ML}, \qquad \mathbf{P}^{-1} = \mathbf{L}^{-1}\mathbf{M}^{-1}$$

so that the diagonalized eigenvalue matrix becomes

$$\mathbf{\Lambda} = \mathbf{L}^{-1}\mathbf{M}^{-1}\mathbf{KML} = \mathbf{P}^{-1}\mathbf{KP} \tag{6.2.18}$$

where $\mathbf{P}^{-1}$ and $\mathbf{P}$ denote the left eigenvector and right eigenvector, respectively.

Let us now postulate an existence of the characteristic variables $\mathbf{W}$ such that

$$\delta\mathbf{W} = \mathbf{L}^{-1}\delta\mathbf{V} \tag{6.2.19}$$

Substituting (6.2.19) into (6.2.16) yields

$$\frac{\partial \mathbf{W}}{\partial t} + \mathbf{L}^{-1}\mathbf{AL}\frac{\partial \mathbf{W}}{\partial x} = 0 \tag{6.2.20}$$

which is known as the compatibility equation.

The characteristic variables are also related by

$$\delta\mathbf{W} = \mathbf{P}^{-1}\delta\mathbf{U}, \quad \text{or} \quad \delta\mathbf{U} = \mathbf{P}\delta\mathbf{W} \tag{6.2.21}$$

Thus, the relations between the three sets of variables (Equations 6.2.7, 6.2.19, and 6.2.21) may be summarized as shown in Figure 6.2.1.

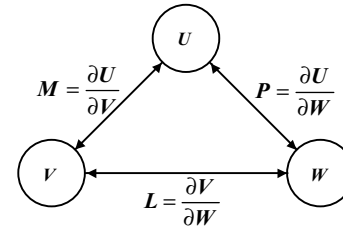

Figure 6.2.1 Relation between conservation variable $\mathbf{U}$, primitive variable $\mathbf{V}$, and characteristic variables $\mathbf{W}$.

6.2.1.3 Characteristic Variables

The existence of characteristic variables postulated in (6.2.19) and (6.2.21) may now be examined for one-dimensional flow.

For the eigenvalues determined from (6.2.15), the three left eigenvectors of $\mathbf{K}$ are given by

$$\begin{bmatrix} \ell^{(1)} \\ \ell^{(2)} \\ \ell^{(3)} \end{bmatrix} = \begin{bmatrix} \alpha & 0 & -\dfrac{\alpha}{a^2} \\ 0 & \beta & \dfrac{\beta}{\rho a} \\ 0 & \delta & \dfrac{-\delta}{\rho a} \end{bmatrix} \tag{6.2.22}$$

where α, β, δ are the three normalization coefficients for the eigenvalues, $\lambda_1 = u$, $\lambda_2 = u + a$, $\lambda_3 = u - a$. With $\alpha = \beta = \delta = 1$, the diagonalization matrices are

$$\mathbf{L}^{-1} = \begin{bmatrix} 1 & 0 & -\dfrac{1}{a^2} \\ 0 & 1 & \dfrac{1}{\rho a} \\ 0 & 1 & \dfrac{-1}{\rho a} \end{bmatrix}, \quad \mathbf{L} = \begin{bmatrix} 1 & \dfrac{\rho}{2a} & -\dfrac{\rho}{2a} \\ 0 & \dfrac{1}{2} & \dfrac{1}{2} \\ 0 & \dfrac{\rho a}{2} & -\dfrac{\rho a}{2} \end{bmatrix} \tag{6.2.23}$$

where $\mathbf{L}^{-1}$ and $\mathbf{L}$ denote left and right eigenvector of $\mathbf{K}$, respectively.

Similarly, transformation matrices $\mathbf{P}^{-1}$ and $\mathbf{P}$ can be derived.

$$\mathbf{P}^{-1} = \mathbf{L}^{-1}\mathbf{M}^{-1} = \begin{bmatrix} 1 - \dfrac{\gamma-1}{2}\dfrac{u^2}{a^2} & (\gamma-1)\dfrac{u}{a} & \dfrac{-(\gamma-1)}{a^2} \\ \left(\dfrac{\gamma-1}{2}u^2 - ua\right)\dfrac{1}{\rho a} & \dfrac{1}{\rho a}[a - (\gamma-1)u] & \dfrac{-(\gamma-1)}{\rho a} \\ -\left(\dfrac{\gamma-1}{2}u^2 + ua\right)\dfrac{1}{\rho a} & \dfrac{1}{\rho a}[a + (\gamma-1)u] & \dfrac{-(\gamma-1)}{\rho a} \end{bmatrix} \tag{6.2.24a}$$

$$\mathbf{P} = \mathbf{M}\mathbf{L} = \begin{bmatrix} 1 & \dfrac{\rho}{2a} & -\dfrac{\rho}{2a} \\ u & \dfrac{\rho}{2a}(u+a) & -\dfrac{\rho}{2a}(u-a) \\ \dfrac{u^2}{2} & \dfrac{\rho}{2a}\left(\dfrac{u^2}{2} + ua + \dfrac{a^2}{\gamma-1}\right) & -\dfrac{\rho}{2a}\left(\dfrac{u^2}{2} - ua + \dfrac{a^2}{\gamma-1}\right) \end{bmatrix} \tag{6.2.24b}$$

where $\mathbf{P}^{-1}$ and $\mathbf{P}$ denote left and right eigenvectors of $\mathbf{a}_i$, respectively.

Rewriting (6.2.16) in one dimension,

$$\mathbf{L}^{-1}\frac{\partial \mathbf{V}}{\partial t} + \mathbf{L}^{-1}\mathbf{A}\mathbf{L}\mathbf{L}^{-1}\frac{\partial \mathbf{V}}{\partial x} = 0 \tag{6.2.25a}$$

or

$$\mathbf{L}^{-1}\frac{\partial \mathbf{V}}{\partial t} + \mathbf{\Lambda}\mathbf{L}^{-1}\frac{\partial \mathbf{V}}{\partial x} = 0 \tag{6.2.25b}$$

where

$$\mathbf{\Lambda} = \begin{bmatrix} u & & \\ & u+a & \\ & & u-a \end{bmatrix} \tag{6.2.26}$$

Expanding (6.2.25b) results in the continuity and momentum equations written in the form

$$\frac{\partial \rho}{\partial t} - \frac{1}{a^2}\frac{\partial p}{\partial t} + u\frac{\partial \rho}{\partial x} - \frac{u}{a^2}\frac{\partial p}{\partial x} = 0 \tag{6.2.27a}$$

$$\frac{\partial u}{\partial t} + \frac{1}{\rho a}\frac{\partial p}{\partial t} + (u+a)\left(\frac{\partial u}{\partial x} + \frac{1}{\rho a}\frac{\partial p}{\partial x}\right) = 0 \tag{6.2.27b}$$

$$\frac{\partial u}{\partial t} - \frac{1}{\rho a}\frac{\partial p}{\partial t} + (u-a)\left(\frac{\partial u}{\partial x} - \frac{1}{\rho a}\frac{\partial p}{\partial x}\right) = 0 \tag{6.2.27c}$$

which are known as compatibility equations. It follows from (6.2.19) or (6.2.27), by introducing an arbitrary variation δ, that

$$\delta W_1 = \delta\rho - \frac{1}{a^2}\delta p = 0 \tag{6.2.28a}$$

$$\delta W_2 = \delta u + \frac{1}{\rho a}\delta p = 0 \tag{6.2.28b}$$

$$\delta W_3 = \delta u - \frac{1}{\rho a}\delta p = 0 \tag{6.2.28c}$$

and subsequently from (6.2.20) or (6.2.28) that

$$\frac{\partial}{\partial t}\begin{bmatrix} W_1 \\ W_2 \\ W_3 \end{bmatrix} + \begin{bmatrix} u & & \\ & u+a & \\ & & u-a \end{bmatrix}\frac{\partial}{\partial x}\begin{bmatrix} W_1 \\ W_2 \\ W_3 \end{bmatrix} = 0 \tag{6.2.29}$$

If the characteristic variables W_1, W_2, W_3 remain constant, they are known as Riemann variables, Riemann invariants, or Riemann solution, defined as follows:

$$W_1 = \rho - \int \frac{dp}{a^2} = \text{constant along the } C_0 \text{ characteristic, stream line}$$

$$W_2 = u + \int \frac{dp}{\rho a} = \text{constant along the } C_+ \text{ characteristic}$$

$$W_3 = u - \int \frac{dp}{\rho a} = \text{constant along the } C_- \text{ characteristic}$$

These characteristic lines are schematically shown in Figure 6.2.2, and propagation of flow lines associated with characteristic lines are shown in Figure 6.2.3.

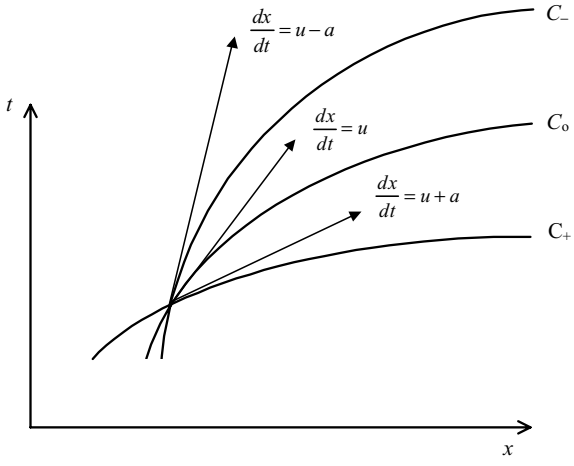

Figure 6.2.2 Characteristic lines for one-dimensional flow.

For isentropic flow it can be shown that

$$W_1 = \frac{p}{\rho^{\gamma}} \tag{6.2.30a}$$

$$W_2 = u + \frac{2a}{\gamma - 1} = J_+ \tag{6.2.30b}$$

$$W_3 = u - \frac{2a}{\gamma - 1} = J_- \tag{6.2.30c}$$

or

$$a = \frac{\gamma - 1}{4}(J_+ - J_-) \tag{6.2.31a}$$

$$u = \frac{1}{2}(J_+ J_-) \tag{6.2.31b}$$

If the values of J_+ and J_- are known at a given point in the x–t plane , then (6.2.31a,b) immediately give the local values of u and a at that point.

The propagation of flow lines associated with characteristic lines as related to expansion wave and shock waves are shown in Figure 6.2.3. The number of boundary conditions to be specified at inflow and outflow boundaries is determined by the eigenvalue spectrum of the Jacobian matrices (6.2.6) in terms of the primitive variables associated with the normal to the boundaries. Details for boundary conditions will be presented in Section 6.7.

6.2.2 CENTRAL SCHEMES WITH COMBINED SPACE-TIME DISCRETIZATION

Central finite differences may be formulated using combined space-time discretization (often known as Lax-Wendroff scheme). An alternative is to use independent space-time discretization which is discussed in Section 6.2.3. In this section, we shall examine the combined space-time discretization schemes.

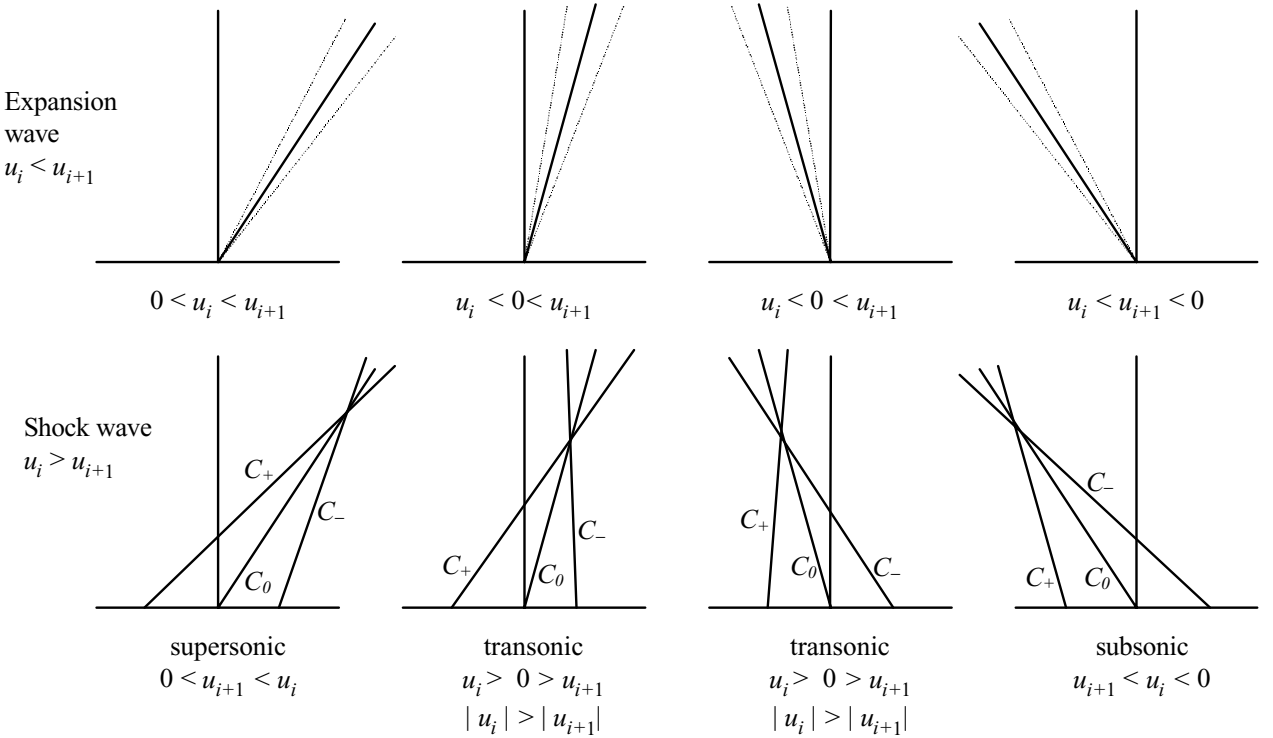

Figure 6.2.3 Propagation of flow quantities.

6.2.2.1 Lax-Friedrichs First Order Scheme

Consider the two-dimensional system of Euler equations in the form

$$\frac{\partial \mathbf{U}}{\partial t} + \frac{\partial \mathbf{f}}{\partial x} + \frac{\partial \mathbf{g}}{\partial y} = 0 \tag{6.2.32}$$

This may be discretized by forward differencing $\mathbf{U}$ in time and central differencing $\mathbf{f}$ and $\mathbf{g}$ in space.

$$\mathbf{U}_{i,j}^{n+1} = \frac{1}{4}\left(\mathbf{U}_{i+1,j}^{n} + \mathbf{U}_{i-1,j}^{n} + \mathbf{U}_{i,j+1}^{n} + \mathbf{U}_{i,j-1}^{n}\right) - \frac{\tau_x}{2}\left(\mathbf{f}_{i+1,j}^{n} - \mathbf{f}_{i-1,j}^{n}\right) - \frac{\tau_y}{2}\left(\mathbf{g}_{i,j+1}^{n} - \mathbf{g}_{i,j-1}^{n}\right) \tag{6.2.33}$$

with

$$\tau_x = \frac{\Delta t}{\Delta x}, \quad \tau_y = \frac{\Delta t}{\Delta y} \tag{6.2.34}$$

It can be shown that the von Neumann analysis leads to the stability condition,

$$J_x^2 + J_y^2 \leq \frac{1}{2} \tag{6.2.35}$$

or

$$\tau_x^2(u+a)^2 + \tau_y^2(\mathrm{v}+a)^2 \leq \frac{1}{2} \tag{6.2.36}$$

where J_x and J_y represent a circle with the radius equal to $\sqrt{\frac{1}{2}}$.

6.2.2.2 Lax-Wendroff Second Order Scheme

We rewrite (6.2.32) in the form

$$\mathbf{U}^{n+1} = \mathbf{U}^{n} + \Delta t\,\mathbf{U}_t + \frac{\Delta t^2}{2}\mathbf{U}_{tt} + \mathbf{O}(\Delta t^3) \tag{6.2.37}$$

and combining (6.2.33) and (6.2.37), we obtain the one-step algorithm,

$$\begin{aligned}\mathbf{U}_{i,j}^{n+1} = {} & \mathbf{U}_{i,j}^{n} - \tau_x \overline{\delta}_x \mathbf{f}_{i,j}^{n} - \tau_y \overline{\delta}_y \mathbf{g}_{i,j}^{n} + \frac{\tau_x^2}{2}\delta_x(\mathbf{a}_{i,j}\delta_x \mathbf{f}_{i,j}) + \frac{\tau_y^2}{2}\delta_y(\mathbf{b}_{i,j}\delta_y \mathbf{g}_{i,j}) \\ & + \frac{\tau_x \tau_y}{2}[\overline{\delta}_x(\mathbf{a}_{i,j}\overline{\delta}_y \mathbf{g}_{i,j}) + \overline{\delta}_y(\mathbf{b}_{i,j}\overline{\delta}_x \mathbf{f}_{i,j})]\end{aligned} \tag{6.2.38}$$

where

$$\overline{\delta}_x \mathbf{f}_{i,j} = \frac{1}{2}(\mathbf{f}_{i+1,j} - \mathbf{f}_{i-1,j}), \qquad \overline{\delta}_y \mathbf{g}_{i,j} = \frac{1}{2}(\mathbf{g}_{i,j+1} - \mathbf{g}_{i,j-1}) \tag{6.2.39}$$

$$\delta_x \mathbf{f}_{i,j} = \mathbf{f}_{i+1,j} - \mathbf{f}_{i-1,j}, \qquad \delta_y \mathbf{g}_{i,j} = \mathbf{g}_{i,j+1} - \mathbf{g}_{i,j-1} \tag{6.2.40}$$

etc.

Determination of Jacobians in (6.2.38) is cumbersome. To avoid this, it is preferable to employ a two-step scheme [Lerat and Peyret, 1974].

Step 1

$$\mathbf{U}_{i,j}^{n+\frac{1}{2}} = \frac{1}{4}\left(\mathbf{U}_{i+1,j}^{n} + \mathbf{U}_{i-1,j}^{n} + \mathbf{U}_{i,j+1}^{n} + \mathbf{U}_{i,j-1}^{n}\right) - \frac{\tau_x}{2}\left(\mathbf{f}_{i+1,j}^{n} - \mathbf{f}_{i-1,j}^{n}\right) - \frac{\tau_y}{2}\left(\mathbf{g}_{i,j+1}^{n} - \mathbf{g}_{i,j-1}^{n}\right) \tag{6.2.41}$$

Step 2

$$\mathbf{U}_{i,j}^{n+1} = \mathbf{U}_{i,j}^{n} - \tau_x\left(\mathbf{f}_{i+1,j}^{n+\frac{1}{2}} - \mathbf{f}_{i-1,j}^{n+\frac{1}{2}}\right) - \tau_y\left(\mathbf{g}_{i,j+1}^{n+\frac{1}{2}} - \mathbf{g}_{i,j-1}^{n+\frac{1}{2}}\right) \tag{6.2.42}$$

The stability condition is shown to be, for $\Delta x = \Delta y$

$$\frac{\Delta t}{\Delta x}(|\mathbf{v}| + a) \leq \frac{1}{\sqrt{2}}$$

The following two-step scheme was introduced by MacCormack and Paullay [1972]:

$$\overline{\mathbf{U}}_{i,j} = \mathbf{U}_{i,j}^{n} - \tau_x\left(\mathbf{f}_{i+1,j}^{n} - \mathbf{f}_{i,j}^{n}\right) - \tau_y\left(\mathbf{g}_{i,j+1}^{n} - \mathbf{g}_{i,j}^{n}\right) \tag{6.2.43}$$

$$\overline{\overline{\mathbf{U}}}_{i,j} = \mathbf{U}_{i,j}^{n} - \tau_x\left(\overline{\mathbf{f}}_{i,j} - \overline{\mathbf{f}}_{i-1,j}\right) - \tau_y\left(\overline{\mathbf{g}}_{i,j} - \overline{\mathbf{g}}_{i,j-1}\right) \tag{6.2.44}$$

$$\mathbf{U}^{n+1} = \frac{1}{2}\left(\overline{\mathbf{U}}_{i,j} + \overline{\overline{\mathbf{U}}}_{i,j}\right) \tag{6.2.45}$$

The corresponding stability condition is

$$\Delta t \leq \left[\frac{|\lambda(A)|\max}{\Delta x} + \frac{|\lambda(B)|\max}{\Delta y}\right]^{-1} \tag{6.2.46}$$

or

$$\Delta t \leq \frac{1}{(|u| + a)/\Delta x + (|\mathrm{v}| + a)/\Delta y} \leq \frac{\Delta x \Delta y}{|u|\Delta y + |\mathrm{v}|\Delta x + a\sqrt{(\Delta x)^2 + (\Delta y)^2}} \tag{6.2.47}$$

6.2.2.3 Lax-Wendroff Method with Artificial Viscosity

The Lax-Wendroff approaches with three-point central schemes lead to oscillations around sharp discontinuities. For one dimension,

$$\mathbf{U}_i^{n+1} - \mathbf{U}_i^{n} = -\tau\left(\mathbf{f}_{i+\frac{1}{2}} - \mathbf{f}_{i-\frac{1}{2}}\right) \tag{6.2.48}$$

where $\mathbf{f}_{i+\frac{1}{2}}$ and $\mathbf{f}_{i-\frac{1}{2}}$, called the numerical flux, are equal at steady state

$$\mathbf{f}_{i+\frac{1}{2}} = \frac{\mathbf{f}_{i+1} + \mathbf{f}_i}{2} - \frac{\tau}{2}a_{i+\frac{1}{2}}(\mathbf{f}_{i+1} - \mathbf{f}_i) \tag{6.2.49a}$$

$$\mathbf{f}_{i-\frac{1}{2}} = \frac{\mathbf{f}_i + \mathbf{f}_{i-1}}{2} - \frac{\tau}{2}a_{i-\frac{1}{2}}(\mathbf{f}_i - \mathbf{f}_{i-1}) \tag{6.2.49b}$$

Now with the artificial viscosity added to (6.2.49), we write

$$\mathbf{f}_{i+\frac{1}{2}} = \frac{\mathbf{f}_{i+1} + \mathbf{f}_i}{2} - \frac{1}{2}\tau a_{i+\frac{1}{2}}(\mathbf{f}_{i+1} - \mathbf{f}_i) + \mathbf{D}_{i+\frac{1}{2}}(\mathbf{U}_{i+1} - \mathbf{U}_i) \tag{6.2.50}$$

where $\mathbf{D}$ is any positive function of $\mathbf{U}_{i+1} - \mathbf{U}_i$ which vanishes at least linearly with $\mathbf{U}_{i+1} - \mathbf{U}_i$.

Substituting (6.2.50) into (6.2.48) leads to

$$\mathbf{U}_i^{n+1} - \mathbf{U}_i^n = -\tau\left(\mathbf{f}_{i+\frac{1}{2}} - \mathbf{f}_{i-\frac{1}{2}}\right)_{LW} + \tau\left[\mathbf{D}_{i+\frac{1}{2}}(\mathbf{U}_{i+1} - \mathbf{U}_i) - \mathbf{D}_{i-\frac{1}{2}}(\mathbf{U}_i - \mathbf{U}_{i-1})\right]$$

where it is seen that the artificial viscosity terms are those discretized as

$$\Delta x \frac{\partial}{\partial x}\left(\mathbf{D}\frac{\partial \mathbf{U}}{\partial x}\right)$$

Hence, the addition of an artificial viscosity term can be seen as

$$\mathbf{f}^{(AV)} = \mathbf{f} - \Delta x \mathbf{D}\frac{\partial \mathbf{U}}{\partial x}$$

or

$$\mathbf{f}_{i+\frac{1}{2}}^{(AV)} = \mathbf{f}_{i+\frac{1}{2}}^{(LW)} - \mathbf{D}_{i+\frac{1}{2}}(\mathbf{U}_{i+1} - \mathbf{U}_i)$$

6.2.2.4 Explicit MacCormack Method

Let us consider a quasi–one-dimensional problem such as occurs in a nozzle with a variable cross-sectional area S.

$$\frac{\partial S\mathbf{U}}{\partial t} + \frac{\partial S\mathbf{F}}{\partial x} - \frac{dS}{dx}\mathbf{B} = 0, \quad S = \hat{S}(x) \tag{6.2.51}$$

with

$$\mathbf{U} = \begin{bmatrix} \rho \\ \rho u \\ \rho E \end{bmatrix}, \quad \mathbf{F} = \begin{bmatrix} \rho u \\ \rho u^2 + p \\ (\rho E + p)u \end{bmatrix}, \quad \mathbf{B} = \begin{bmatrix} 0 \\ p \\ 0 \end{bmatrix}$$

An explicit MacCormack predictor-corrector scheme is formulated as follows:

Predictor

$$\frac{S\mathbf{U}_i^* - S\mathbf{U}_i^n}{\Delta t} + \frac{S\mathbf{F}_{i+1}^n - S\mathbf{F}_i^n}{\Delta x} - \left.\frac{dS}{dx}\right|_i \mathbf{B}_i^n = 0 \tag{6.2.52}$$

or

$$S\mathbf{U}_i^* = S\mathbf{U}_i^n - \frac{\Delta t}{\Delta x}\left(S\mathbf{F}_{i+1}^n - S\mathbf{F}_i^n\right) + \Delta t\left(\frac{dS}{dx}\right)_i \mathbf{B}_i^n + \mathbf{D}_i(\mathbf{U}) \tag{6.2.53}$$

where the artificial viscosity term $\mathbf{D}_j$ may be given by

$$\mathbf{D}_i(U) = \frac{\omega}{8}\left[S\mathbf{U}_{i+2}^n - 4S\mathbf{U}_{i+1}^n + 6S\mathbf{U}_i^n - 4S\mathbf{U}_{i-1} + S\mathbf{U}_{i-2}^n\right] \tag{6.2.54}$$

with $0 \le \omega \le 2$, $\Delta t = C\Delta x/u + a$.

Corrector

$$S\mathbf{U}_i^{n+1} = \frac{1}{2}\left\{ S\mathbf{U}_i^n + S\mathbf{U}_i^* - \frac{\Delta t}{\Delta x}(S\mathbf{F}_i^* - S\mathbf{F}_{i-1}^*) + \Delta t\left(\frac{dS}{dx}\right)_i \mathbf{B}_i^* + \mathbf{D}_i^*(\mathbf{U}) \right\} \tag{6.2.55}$$

Numerical applications for this case are demonstrated in Section 6.8.1.

6.2.3 CENTRAL SCHEMES WITH INDEPENDENT SPACE-TIME DISCRETIZATION

Instead of using combined space-time discretization, we may employ independent time discretization while maintaining central differences for space [Briley and McDonald, 1975; Beam and Warming, 1976, 1978]. We begin with the general form

$$\frac{d\mathbf{U}_{i,j}}{dt} = -\frac{1}{2}\left[\frac{\mathbf{f}_{i+1,j} - \mathbf{f}_{i-1,j}}{\Delta x} + \frac{\mathbf{g}_{i,j+1} - \mathbf{g}_{i,j-1}}{\Delta y} \right]$$

where various finite difference schemes of the time derivative term may be applied. The two level time integration of (6.2.51) leads to

$$(1+\xi)\Delta\mathbf{U}^{n+1} - \xi\Delta\mathbf{U}^n = \Delta t\theta\left[\left(\frac{\partial \mathbf{f}}{\partial x} + \frac{\partial \mathbf{g}}{\partial y} \right)^{n+1} - \left(\frac{\partial \mathbf{f}}{\partial x} + \frac{\partial \mathbf{g}}{\partial y} \right)^{n} \right]$$

with $\xi > -1/2$, $\theta \geq 1/2(\xi + 1)$ for linear stability.

The two-level integration scheme takes the form

$$(1+\xi)\Delta\mathbf{U}^{n+1} + \Delta t\theta\left(\frac{\partial \mathbf{f}}{\partial x} + \frac{\partial \mathbf{g}}{\partial y} \right)^{n+1} = -\Delta t\left(\frac{\partial \mathbf{f}}{\partial x} + \frac{\partial \mathbf{g}}{\partial y} \right)^{n} + \xi\Delta\mathbf{U}^n$$

or

$$\left[(1+\xi) + \Delta t\theta\left(\frac{\partial \mathbf{a}}{\partial x} + \frac{\partial \mathbf{b}}{\partial y} \right) \right]\Delta\mathbf{U}^{n+1} = -\Delta t\left(\frac{\partial \mathbf{f}}{\partial x} + \frac{\partial \mathbf{g}}{\partial y} \right)^{n} + \xi\Delta\mathbf{U}^n$$

Introducing a central discretization, we obtain

$$[(1+\xi) + \theta(\tau_x\overline{\delta}_x\mathbf{a} + \tau_y\overline{\delta}_y\mathbf{b})]\Delta\mathbf{U}_{i,j}^{n+1} = -\tau_x\overline{\delta}_x\mathbf{f}_{i,j}^n + \tau_y\overline{\delta}_y\mathbf{g}_{i,j}^n + \xi\Delta\mathbf{U}_{i,j}^n \tag{6.2.56}$$

or

$$\begin{aligned}
&(1+\xi)\Delta\mathbf{U}_{i,j}^{n+1} + \theta\frac{\Delta t}{2\Delta x}(\mathbf{a}_{i+1,j}\Delta\mathbf{U}_{i+1,j} - \mathbf{a}_{i-1,j}\Delta\mathbf{U}_{i-1,j})^{n+1} \\
&\quad + \theta\frac{\Delta t}{2\Delta y}(\mathbf{b}_{i,j+1}\Delta\mathbf{U}_{i,j+1} - \mathbf{b}_{i,j-1}\Delta\mathbf{U}_{i,j-1})^{n+1} \\
&\quad = -\Delta t\left(\frac{\mathbf{f}_{i+1,j}^n - \mathbf{f}_{i-1,j}^n}{2\Delta x} + \frac{\mathbf{g}_{i,j+1}^n - \mathbf{g}_{i,j-1}^n}{2\Delta y} \right) + \xi\Delta\mathbf{U}_{i,j}^n
\end{aligned} \tag{6.2.57}$$

and with an ADI factorization, for $\xi = 0$

$$(1 + \theta\tau_x\overline{\delta}_x)(1 + \theta\tau_y\overline{\delta}_y\mathbf{b}^n)\Delta\overline{\mathbf{U}}_{i,j} = -\left(\tau_x\overline{\delta}_x\mathbf{f}_{i,j}^n + \tau_y\overline{\delta}_y\mathbf{g}_{i,j}^n\right) \tag{6.2.58a}$$

$$(1 + \theta\tau_y\overline{\delta}_y\mathbf{b}^n)\Delta\mathbf{U}_{i,j}^{n+1} = \Delta\overline{\mathbf{U}}_{i,j} \tag{6.2.58b}$$

Notice that each step is a tridiagonal system along the x lines for $\Delta\overline{\mathbf{U}}$ and along the y lines for $\Delta\mathbf{U}^{n+1}$.

6.2.4 FIRST ORDER UPWIND SCHEMES

In general, the central schemes tend to provide excessive damping with shock discontinuities not well resolveld. To compensate for this trend, first order upwind schemes can be used. However, overshoots and undershoots may occur at discontinuities. A remedy for this difficulty can be provided by low- or high-resolution second order upwind schemes. In this section, we discuss the first order upwind schemes, followed by the second order upwind schemes in Section 6.2.5. High-resolution second order upwind schemes will be discussed in Section 6.2.6. The first order upwind schemes are divided into two groups: flux vector splitting schemes and Godunov schemes. These and other topics are presented below.

6.2.4.1 Flux Vector Splitting Method

The basic strategy here is to split the flux and eigenvalues into positive and negative components and apply the one-dimensional splitting to each flux component separately according to the sign of the associated eigenvalues. This method is known as the flux vector splitting method.

Consider the two-dimensional flow in the form

$$\frac{\partial \mathbf{U}}{\partial t} + \frac{\partial \mathbf{f}}{\partial x} + \frac{\partial \mathbf{g}}{\partial y} = 0 \tag{6.2.59a}$$

or

$$\frac{\partial \mathbf{U}}{\partial t} + \mathbf{A}\frac{\partial \mathbf{U}}{\partial x} + \mathbf{B}\frac{\partial \mathbf{U}}{\partial y} = 0 \tag{6.2.59b}$$

with the convection Jacobians $\mathbf{A}$ and $\mathbf{B}$ as related by diagonalized eigenvalue matrices,

$$\Lambda_1 = \mathbf{P}_1^{-1}\mathbf{A}\mathbf{P}_1 = \begin{bmatrix} u & & & \\ & u & & \\ & & u+a & \\ & & & u-a \end{bmatrix} \tag{6.2.60a}$$

$$\Lambda_2 = \mathbf{P}_2^{-1}\mathbf{B}\mathbf{P}_2 = \begin{bmatrix} \mathrm{v} & & & \\ & \mathrm{v} & & \\ & & \mathrm{v}+a & \\ & & & \mathrm{v}-a \end{bmatrix} \tag{6.2.60b}$$

For the one-dimensional problem, we have

$\mathbf{f}^+ = \mathbf{f}, \quad \mathbf{f}^- = \mathbf{0}$ for supersonic flow

$\mathbf{f}^+ = \mathbf{0}, \quad \mathbf{f}^- = \mathbf{f}$ for subsonic flow

and

$$\Lambda_1^+ = \begin{bmatrix} u & & & \\ & u & & \\ & & u+a & \\ & & & 0 \end{bmatrix}, \quad \Lambda_1^- = \begin{bmatrix} 0 & & & \\ & 0 & & \\ & & 0 & \\ & & & u-a \end{bmatrix}$$

with

$$\mathbf{A}^{+} = \mathbf{P}_1 \Lambda_1^{+} \mathbf{P}_1^{-1}, \quad \mathbf{A}^{-} = \mathbf{P}_1 \Lambda_1^{-} \mathbf{P}_1^{-1}$$

and similarly for $\mathbf{B}$. The split fluxes are defined by

$$\mathbf{f}^{\pm} = \mathbf{A}^{\pm}\mathbf{U} \quad \mathbf{g}^{\pm} = \mathbf{B}^{\pm}\mathbf{U}$$

The general eigenvalue matrix may written as given by Steger and Warming [1980]

$$\Lambda = \begin{bmatrix} \lambda_1 & & & \\ & \lambda_2 & & \\ & & \lambda_3 & \\ & & & \lambda_4 \end{bmatrix} \tag{6.2.61}$$

which will allow the split flux components to be written as follows:

$$f = \frac{\rho}{2\gamma} \begin{bmatrix} \eta \\ \eta u + a(\lambda_2 - \lambda_3) \\ \eta \mathrm{v} \\ \eta \dfrac{u^2 + \mathrm{v}^2}{2} + ua(\lambda_2 - \lambda_3) + a^2 \dfrac{\lambda_2 + \lambda_3}{\gamma - 1} \end{bmatrix} \tag{6.2.62a}$$

$$g = \frac{\rho}{2\gamma} \begin{bmatrix} \eta \\ \eta u \\ \eta \mathrm{v} + a(\lambda_2 - \lambda_3) \\ \eta \dfrac{u^2 + \mathrm{v}^2}{2} + \mathrm{v}a(\lambda_2 - \lambda_3) + a^2 \dfrac{\lambda_2 + \lambda_3}{\gamma - 1} \end{bmatrix} \tag{6.2.62b}$$

with

$$\eta = 2(\gamma - 1)\lambda_1 + \lambda_2 + \lambda_3$$

Rewriting (6.2.59a) in a discrete form for a variable cross section $S(x)$:

$$\mathbf{U}_{i,j}^{n+1} - \mathbf{U}_{i,j}^{n} = -\frac{\Delta t}{\Delta x}\left(\mathbf{f}^{*}_{i+\frac{1}{2},j} - \mathbf{f}^{*}_{i-\frac{1}{2},j}\right) - \frac{\Delta t}{\Delta y}\left(\mathbf{g}^{*}_{i,j+\frac{1}{2}} - \mathbf{g}^{*}_{i,j-\frac{1}{2}}\right) \tag{6.2.63}$$

with

$$\mathbf{f}^{*}_{i+\frac{1}{2},j} = \mathbf{f}^{-}_{i+1,j} + \mathbf{f}^{+}_{i,j}, \qquad \mathbf{g}^{*}_{i,j+\frac{1}{2}} = \mathbf{g}^{-}_{i,j+1} + \mathbf{g}^{+}_{i,j} \tag{6.2.64}$$

For quasi–one-dimensional problems such as a nozzle with variable cross-section area considered in (6.2.51), the solution procedure using the flux vector splitting is presented below.

$$\frac{\partial S\mathbf{U}}{\partial t} + \frac{\partial S\mathbf{F}}{\partial x} - \frac{dS}{dx}\mathbf{B} = 0 \tag{6.2.65}$$

Linearizing the above,

$$\mathbf{F}^{n+1} = \mathbf{F}^{n} + \frac{\partial \mathbf{F}^{n}}{\partial t}\Delta t = \mathbf{F}^{n} + \frac{\partial \mathbf{F}^{n}}{\partial \mathbf{U}}\Delta \mathbf{U} = \mathbf{F}^{n} + \mathbf{a}\Delta \mathbf{U}$$

$$\mathbf{B}^{n+1} = \mathbf{B}^{n} + \frac{\partial \mathbf{B}^{n}}{\partial t}\Delta t = \mathbf{B}^{n} + \frac{\partial \mathbf{B}^{n}}{\partial \mathbf{U}}\Delta \mathbf{U} = \mathbf{B}^{n} + \mathbf{b}\Delta \mathbf{U}$$

where

$$F_1 = \rho u = U_2$$

$$F_2 = \rho u^2 + p = \frac{\rho^2 u^2}{\rho} + (\gamma - 1)\left(\rho E - \frac{\rho^2 u^2}{2\rho}\right) = \frac{U_2^2}{U_2} + (\gamma - 1)\left(U_3 - \frac{U_2^2}{2U_1}\right)$$

$$= \frac{3 - \gamma}{2}\left(\frac{U_2^2}{U_1}\right) + (\gamma - 1)U_3$$

$$F_3 = (\rho E + p)u = \frac{\gamma U_3 U_2}{U_1} - (\gamma - 1)\frac{U_2^2}{2U_1^2}$$

The flux vector $\mathbf{F}$ can be split into subvectors such that each is associated with either positive or negative eigenvalues of $\mathbf{a}$.

$$\mathbf{a} = \mathbf{a}^+ + \mathbf{a}^- = \mathbf{P}\boldsymbol{\Lambda}^+\mathbf{P}^{-1} + \mathbf{P}\boldsymbol{\Lambda}^-\mathbf{P}^{-1}$$

$$\Lambda = \Lambda^+ + \Lambda^- = \begin{bmatrix} u & 0 & 0 \\ 0 & u+a & 0 \\ 0 & 0 & 0 \end{bmatrix} + \begin{bmatrix} 0 & 0 & 0 \\ 0 & 0 & 0 \\ 0 & 0 & u-a \end{bmatrix}$$

$$\mathbf{F}^+ = \mathbf{a}^+\mathbf{U}, \quad \mathbf{F}^- = \mathbf{a}^-\mathbf{U}, \quad \mathbf{a}^+ = \mathbf{P}\boldsymbol{\Lambda}^+\mathbf{P}^{-1}, \quad \mathbf{a}^- = \mathbf{P}\boldsymbol{\Lambda}^-\mathbf{P}^{-1}$$

For $M < 1\,(u < a)$

$$\left.\begin{array}{l} u > 0 \\ u + a > 0 \\ u - a < 0 \end{array}\right\} \quad a^+ = 0, \quad a^- = a$$

For $M > 1\,(u > a)$

$$\left.\begin{array}{l} u > 0 \\ u + a > 0 \\ u - a > 0 \end{array}\right\}, \quad a^+ = a, \quad a^- = 0$$

The above criteria require that backward differencing (upwinding) be used for terms associated with positive eigenvalues, whereas forward differencing should be used for terms involved in negative eigenvalues. Furthermore, the number of boundary conditions to apply are also dictated by the eigenvalues, compatibility relations, and characteristic variables as discussed in Sections 6.2.1 and 6.7.

In order to write the finite difference equations, we return to the governing equation (6.2.65) and obtain the discretized form

$$S\frac{\Delta \mathbf{U}}{\Delta t} + \frac{\partial}{\partial x}\left[S\left(\mathbf{F} + \frac{\partial \mathbf{F}}{\partial \mathbf{U}}\Delta \mathbf{U}\right)\right] - \frac{dS}{dx}\left[\mathbf{B} + \frac{\partial \mathbf{B}}{\partial \mathbf{U}}\Delta \mathbf{U}\right] = 0$$

In terms of the Jacobians,

$$S\frac{\Delta \mathbf{U}}{\Delta t} + \frac{\partial}{\partial x}(S\mathbf{a}\Delta \mathbf{U}) - \frac{dS}{dx}(\mathbf{b}\Delta \mathbf{U}) = -\frac{\partial S\mathbf{F}}{\partial x} + \frac{dS}{dx}\mathbf{B}$$

or

$$\left[S\mathbf{I} + \Delta t\frac{\partial}{\partial x}S\mathbf{a} - \Delta t\frac{dS}{dx}\mathbf{b}\right]\Delta \mathbf{U} = -\Delta t\left[\frac{\partial S\mathbf{F}}{\partial x} - \frac{dS}{dx}\mathbf{B}\right]$$

Introducing the flux vector splitting, we write

$$\left\{S\mathbf{I}+\Delta t\left[\frac{\partial}{\partial x}(S\mathbf{a}^{+}+S\mathbf{a}^{-})-\frac{dS}{dx}\mathbf{b}\right]\right\}\Delta\mathbf{U}=-\Delta t\left[\frac{\partial}{\partial x}(S\mathbf{F}^{+}+S\mathbf{F}^{-})-\frac{dS}{dx}\mathbf{B}\right]$$

A backward (upwind) differencing is used for $\mathbf{a}^{+}$ and $\mathbf{F}^{+}$ as follows:

$$\left\{S\mathbf{I}+\frac{\Delta t}{\Delta x}[(S\mathbf{a}_j^{-}-S\mathbf{a}_{j-1}^{+})+(S\mathbf{a}_{j+1}^{-}-S\mathbf{a}_j^{-})]-\Delta t\frac{dS}{dx}\mathbf{b}_j\right\}\Delta\mathbf{U}$$
$$=-\frac{\Delta t}{\Delta x}[(S\mathbf{F}_j^{+}-S\mathbf{F}_{j-1}^{+})+(S\mathbf{F}_{j+1}^{-}-S\mathbf{F}_j^{-})]+\Delta t\frac{dS}{dx}\mathbf{B}_j$$

The above results may be rearranged in the form:

$$\alpha\Delta\mathbf{U}_{j+1}+\beta\Delta\mathbf{U}_j+\gamma\Delta\mathbf{U}_{j-1}=\delta \tag{6.2.66}$$

where

$$\alpha=\frac{\Delta t}{\Delta x}S_{j+1}\mathbf{a}_{j+1}^{-}$$

$$\beta=S\mathbf{I}+\frac{\Delta t}{\Delta x}(S_j\mathbf{a}_j^{+}-S_j\mathbf{a}_j^{-})-\Delta t\left.\frac{dS}{dx}\right|_j\mathbf{b}_j$$

$$\gamma=-\frac{\Delta t}{\Delta x}S_{j-1}\mathbf{a}_{j-1}^{+}$$

$$\delta=-\frac{\Delta t}{\Delta x}(S_j\mathbf{F}_j^{+}-S_{j-1}\mathbf{F}_{j-1}^{+}+S_{j+1}\mathbf{F}_{j+1}^{-}-S_j\mathbf{F}_j^{-})+\Delta t\left.\frac{dS}{dx}\right|_j\mathbf{B}_j$$

with

$$\Delta\mathbf{U}=\mathbf{U}^{n+1}-\mathbf{U}^{n}$$

Here it is seen that for supersonic flow, $\mathbf{a}^{-}=0$, making the scheme upwinded with the diagonal term β being maximum. For subsonic flow, the diagonal term β is still large with the eigenvalue Λ^{-} or $\mathbf{a}^{-}$ being negative. The scheme provides a stable solution. A numerical example for this problem is demonstrated in Section 6.8.1.

The flux vector splitting has been applied to many first and second order upwind schemes such as in MUSCL (monotone upstream centered schemes for conservation laws) and TVD (total variation diminishing). For example, in the construction of the second order schemes, MUSCL approach has been used to extrapolate the primitive variables to the cell interface rather than the fluxes. Similar approaches and various other versions of flux vector splitting were used for TVD. These and other topics on the flux vector splitting will be discussed in Section 6.2.5.

6.2.4.2 Godunov Methods

The basic idea of a Godunov scheme is to use the finite volume structure of spatial discretization (Figure 6.2.4a) and a piecewise constant distribution of the variable u with the shock discontinuities occurring at each cell interface in order to obtain the

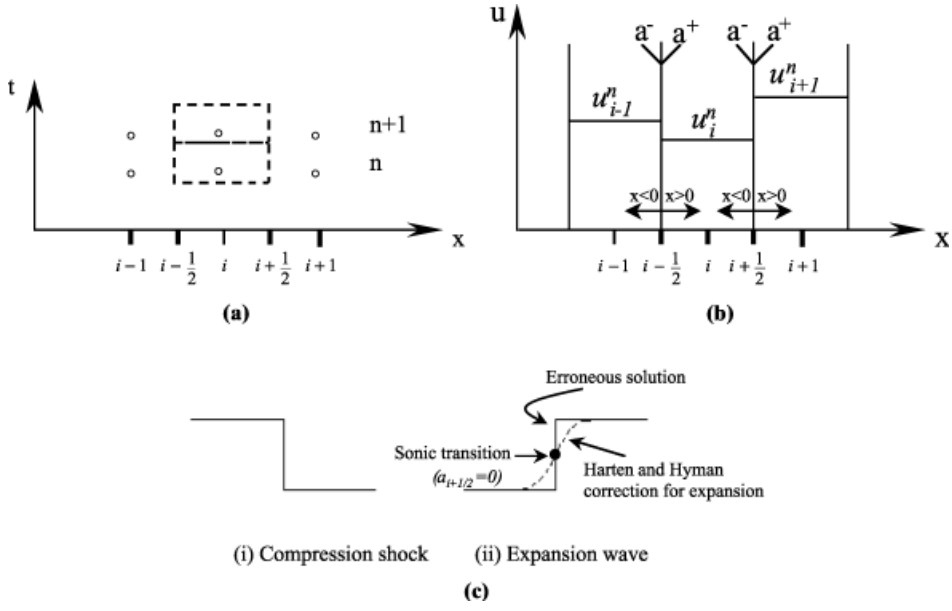

Figure 6.2.4 Control volume and piecewise constant distribution of u. **(a)** Control volume for Godunov method. **(b)** Piecewise constant distribution of u at $t = n\Delta t$. **(c)** Compression shock and expansion wave.

exact Riemann solution (Figure 6.2.4b). Here, the dependent variable u may be written as

$$u_i^{n+1} = u_i^n - \frac{\Delta t}{\Delta x}\left[f(u_{i+1/2}) - f(u_{i-1/2})\right] \tag{6.2.67a}$$

with the value of u over the volume element given by the average value u_i,

$$u_i = \frac{1}{\Delta x}\int_{x-\Delta x/2}^{x+\Delta x/2} u(x,t)\,dx$$

and the flux time-averaged at the control volume surface:

$$f = \frac{1}{\Delta t}\int_t^{t+\Delta t} f\,dt$$

As an exact Riemann solution, we note that (6.2.67a) can be reduced to

$$u_i^{n+1} = u_i^n - \frac{a\Delta t}{\Delta x}\left[u_i^n - u_{i-1}^n\right] \quad \text{for } a > 0 \tag{6.2.67b}$$

$$u_i^{n+1} = u_i^n - \frac{a\Delta t}{\Delta x}\left[u_{i+1}^n - u_i^n\right] \quad \text{for } a < 0 \tag{6.2.67c}$$

with $|a_{\max}|\Delta t/\Delta x \le 1/2$ for stability. This is because the wave can travel at almost half the cell.

Godunov's idea has been extended for improvements by various investigators including Roe [1981] and Enquist and Osher [1980] among others. One of the most widely used schemes is the Roe's approximate Riemann solver. This scheme is described below.

Roe's Approximate Riemann Solver

The original Godunov scheme (6.2.67) may be *approximated* by splitting the Jacobian a into positive and negative components as

$$a_{i-1/2} = a^+_{i-1/2} - a^-_{1-1/2}, \qquad a_{i+1/2} = a^+_{i+1/2} - a^-_{1+1/2}$$

For $a > 0$, the upwinding scheme is given by

$$u_i^{n+1} = u_i^n - \frac{\Delta t}{\Delta x}(f_i - f_{i-1})$$

with the flux terms split in terms of positive and negative Jacobians,

$$\begin{aligned} f_{i-1/2} - f_{i-1} &= a^-_{i-1/2}(u_i - u_{i-1}) \\ f_i - f_{i-1/2} &= a^+_{i-1/2}(u_i - u_{i-1}) \end{aligned} \tag{6.2.68a,b}$$

Subtracting (6.2.68b) from (6.2.68a) leads to

$$f_{i-1/2} = \frac{f_i + f_{i-1}}{2} - \frac{1}{2}|a_{i-1/2}|(u_i - u_{i-1}) = f^*_{i-1/2} \tag{6.2.69a}$$

with the symbol * representing the first order upwind numerical flux at $i - 1/2$.

Similarly, for $a < 0$, the upwinding scheme is written as

$$u_i^{n+1} = u_i^n - \frac{\Delta t}{\Delta x}(f_{i+1} - f_i)$$

with

$$\begin{aligned} f_{i+1/2} - f_i &= a^-_{i+1/2}(u_{i+1} - u_i) \\ f_{i+1} - f_{i+1/2} &= a^+_{i+1/2}(u_{i+1} - u_i) \end{aligned}$$

from which we obtain

$$f_{i+1/2} = \frac{f_{i+1} + f_i}{2} - \frac{1}{2}|a_{i+1/2}|(u_{i+1} - u_i) = f^*_{i+1/2} \tag{6.2.69b}$$

with * denoting the first order upwind numerical flux at $i + 1/2$.

Unfortunately, the scheme given by (6.2.68b) above does not recognize the possible occurrence of expansion wave at a sonic transition identified by

$$|a_{i+1/2}| = a^+_{i+1/2} - a^-_{i+1/2} = 0$$

at which the scheme computes as a shock discontinuity that represents a nonphysical behavior, violating the entropy condition. A remedy for this situation can be found in Harten and Hyman [1983] in which the following modification is made to (6.2.69b):

$$|a_{i+1/2}| = \begin{cases} |a_{i+1/2}| & \text{for } |a_{i+1/2}| \geq \varepsilon \\ \varepsilon & \text{for } |a_{i+1/2}| < \varepsilon \end{cases}, \qquad \varepsilon = \max\left(0, \left|\frac{a_{i+1} - a_i}{2}\right|\right) \tag{6.2.70}$$

Note that for expansion we have $\varepsilon = (u_{i+1} - u_i)/2$ and this requires a modification. On the other hand, for compression ($\varepsilon = 0$), no modification is needed. This accommodation will allow a correct expansion wave to develop instead of the nonphysical discontinuity as shown in Figure 6.2.4c(ii).

The expressions given by (6.2.69a,b) can be substituted into (6.2.67a) in the form of finite volume discretization. This process can easily be formulated in terms of diagonalized Jacobians with eigenvalues and eignevectors for multidimensional Euler equations as shown in Section 6.2.1. Thus, the first order upwind scheme for the solution of Euler equations is of the form:

$$u_i^{n+1} = u_i^n - \frac{\Delta t}{\Delta x}\left[f^*_{i+1/2} - f^*_{i-1/2}\right] \tag{6.2.71}$$

with the numerical fluxes determined from (6.2.69a,b).

6.2.5 SECOND ORDER UPWIND SCHEMES WITH LOW RESOLUTION

There are two approaches for the second order upwind schemes with low resolution: (1) variable extrapolation and (2) flux extrapolation. In each of these approaches, an additional predictor step may or may not be included. In these schemes it is intended that the second order upwind approaches lead to greater accuracy.

(1) Variable Extrapolation – MUSCL Approach

In this approach, known as Monotone Upstream-Centered Schemes for Conservation Laws (MUSCL) [Van Leer, 1979], the variables are extrapolated instead of the flux terms.

$$\mathbf{f}^{**}_{i+\frac{1}{2}} = \frac{1}{2}\left[\mathbf{f}\left(\mathbf{U}^L_{i+\frac{1}{2}}\right) + \mathbf{f}\left(\mathbf{U}^R_{i+\frac{1}{2}}\right) - |\mathbf{a}|_{i+\frac{1}{2}}\left(\mathbf{U}^R_{1+\frac{1}{2}} - \mathbf{U}^L_{i+\frac{1}{2}}\right)\right] \tag{6.2.72}$$

with ** representing the second order scheme and

$$\mathbf{U}^L_{i+\frac{1}{2}} = \mathbf{U}_i + \frac{1}{4}[(1-\kappa)(\mathbf{U}_i - \mathbf{U}_{i-1}) + (1+\kappa)(\mathbf{U}_{i+1} - \mathbf{U}_i)]$$

$$\mathbf{U}^R_{i+\frac{1}{2}} = \mathbf{U}_{i+1} - \frac{1}{4}[(1+\kappa)(\mathbf{U}_{i+1} - \mathbf{U}_i) + (1-\kappa)(\mathbf{U}_{i+2} - \mathbf{U}_{i+1})]$$

where the superscripts L and R refer to the left and right sides at the considered boundary and κ denotes a weight ($\kappa = -1, 0, 1$) leading to various extrapolation schemes Figure 6.2.5a,b).

The final solution is obtained as

$$\mathbf{U}_i^{n+1} = \mathbf{U}_i^n - \tau\left(\mathbf{f}^{**}_{i+\frac{1}{2}} - \mathbf{f}^{**}_{i-\frac{1}{2}}\right) \tag{6.2.73}$$

Second order upwind schemes in space and time are obtained with an additional predictor step

$$\mathbf{U}^{L^*}_{i+\frac{1}{2}} = \overline{\mathbf{U}}_i + \frac{1}{4}[(1-\kappa)(\mathbf{U}_i - \mathbf{U}_{i-1}) + (1+\kappa)(\mathbf{U}_{i+1} - \mathbf{U}_i)] \tag{6.2.74}$$

$$\overline{\mathbf{U}}_i = \mathbf{U}_i^n - \frac{\Delta t}{2\Delta x}\left(\mathbf{f}^*_{i+\frac{1}{2}} - \mathbf{f}^*_{i-\frac{1}{2}}\right) \tag{6.2.75a}$$

$$\mathbf{U}^{R^*}_{i+\frac{1}{2}} = \overline{\mathbf{U}}_{i+1} - \frac{1}{4}[(1+\kappa)(\mathbf{U}_{i+1} - \mathbf{U}_i) + (1-\kappa)(\mathbf{U}_{i+2} - \mathbf{U}_{i+1})] \tag{6.2.75b}$$

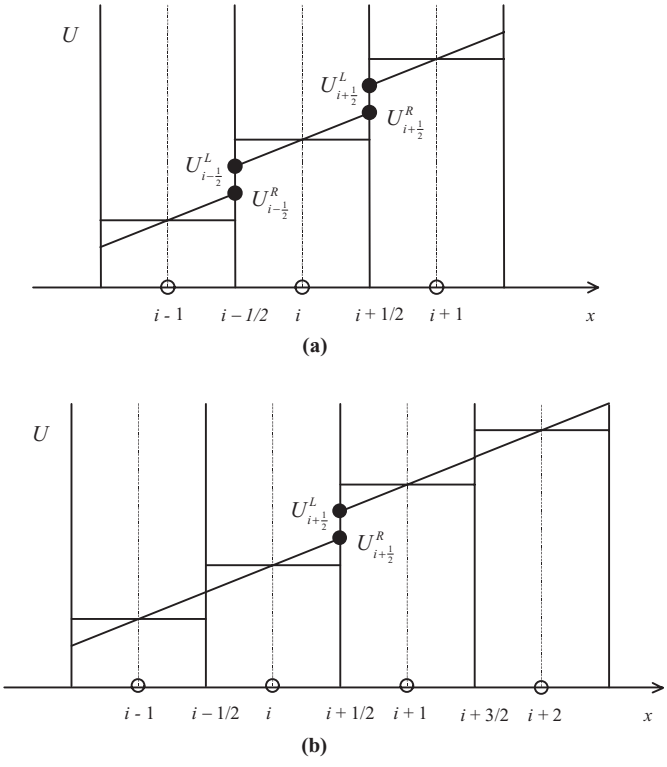

Figure 6.2.5 Variable extrapolation. **(a)** Piecewise linear representation within cells. **(b)** Linear one-sided extrapolation of interface values for $\kappa = -1$.

with * indicating the first order approximation. Thus, (6.2.72) may be replaced by

$$\overline{\mathbf{f}^{**}_{i+\frac{1}{2}}} = \frac{1}{2}\left[\mathbf{f}^*\left(\mathbf{U}^{L^*}_{i+\frac{1}{2}}\right) + \mathbf{f}^*\left(\mathbf{U}^{R^*}_{i+\frac{1}{2}}\right) - |\mathbf{a}|_{i+\frac{1}{2}}\left(\mathbf{U}^{R^*}_{i+\frac{1}{2}} - \mathbf{U}^{L^*}_{i+\frac{1}{2}}\right)\right]$$

Finally, we obtain

$$\mathbf{U}^{n+1}_i = \mathbf{U}^n_i - \tau\left(\overline{\mathbf{f}^{**}_{i+\frac{1}{2}}} - \overline{\mathbf{f}^{**}_{i-\frac{1}{2}}}\right) \tag{6.2.76}$$

This is one of the most widely used schemes for capturing discontinuities in capturing shock discontinuities in compressible flows.

(2) Flux Extrapolation Approach

In the previous approach, the state variables are directly extrapolated to the cell interfaces. The fluxes at the cell boundaries are then calculated from these values. In the flux extrapolation approach, the fluxes in the cell are directly extrapolated to the boundaries.

The extrapolation formulas for the fluxes are the same as the formulas applied to the variables. A general backward extrapolation of the positive flux is given by

$$\mathbf{f}^{+b}_{i+\frac{1}{2}} = \mathbf{f}^+_i + \frac{1}{4}\left[(1-\kappa)\left(\mathbf{f}_i - \mathbf{f}^*_{i-\frac{1}{2}}\right) + (1+\kappa)\left(\mathbf{f}_{i+1} - \mathbf{f}^*_{i+\frac{1}{2}}\right)\right] \tag{6.2.77a}$$

whereas a forward extrapolation is applied to the negative part of the flux,

$$\mathbf{f}^{-f}_{i+\frac{1}{2}} = \mathbf{f}^{-}_{i+1} - \frac{1}{4}\left[(1+\kappa)\left(\mathbf{f}^{*}_{i+\frac{1}{2}} - \mathbf{f}_i\right) + (1-\kappa)\left(\mathbf{f}^{*}_{i+\frac{3}{2}} - \mathbf{f}_{i+1}\right)\right] \tag{6.2.77b}$$

Thus, the second order upwind scheme based on flux extrapolation becomes

$$\mathbf{f}^{**}_{i+\frac{1}{2}} = \mathbf{f}^{+b}_{i+\frac{1}{2}} + \mathbf{f}^{-f}_{i+\frac{1}{2}} \tag{6.2.78}$$

Similarly, as in the variable extrapolation, we obtain the second order accuracy in time by adding a first integration step over $\Delta t/2$ with the associated first order scheme (6.2.74). Defining

$$\overline{\mathbf{f}^{*}_{i+\frac{1}{2}}} = \mathbf{f}^{*}(\overline{\mathbf{U}}_i, \overline{\mathbf{U}}_{i+1}) \tag{6.2.79}$$

we obtain the numerical flux as

$$\begin{aligned}\overline{\mathbf{f}^{**}_{i+\frac{1}{2}}} = \overline{\mathbf{f}^{*}_{i+\frac{1}{2}}} &+ \frac{1}{2}\left[\frac{(1-\kappa)}{2}\left(\mathbf{f}_i - \mathbf{f}^{*}_{i-\frac{1}{2}}\right) + \frac{(1+\kappa)}{2}\left(\mathbf{f}_{i+1} - \mathbf{f}^{*}_{i+\frac{1}{2}}\right)\right] \\ &+ \frac{1}{2}\left[\frac{(1+\kappa)}{2}\left(\mathbf{f}_i - \mathbf{f}^{*}_{i+\frac{1}{2}}\right) + \frac{(1-\kappa)}{2}\left(\mathbf{f}_{i+1} - \mathbf{f}^{*}_{i+\frac{1}{2}}\right)\right]\end{aligned} \tag{6.2.80}$$

Finally,

$$\mathbf{U}^{n+1}_i = \mathbf{U}^{n}_i - \tau\left(\overline{\mathbf{f}^{**}_{i+\frac{1}{2}}} - \overline{\mathbf{f}^{**}_{i-\frac{1}{2}}}\right) \tag{6.2.81}$$

Unfortunately, the above schemes have had some difficulty; they are unable to control overshoots and undershoots at shock discontinuities. A remedy is found in second order upwind schemes with high resolution, discussed in the following subsection.

6.2.6 SECOND ORDER UPWIND SCHEMES WITH HIGH RESOLUTION (TVD SCHEMES)

The most important development in computational fluid dynamics may be the second order upwind schemes with high resolution, known as the total variation diminishing (TVD) schemes, pioneered by Godunov [1959], VanLeer [1973, 1979], Harten and Lax [1981], Harten [1983, 1984], Osher [1984], Osher and Chakravarthy [1984] as reviewed by Hirsch [1990], which are based on the following physical properties:

- *Entropy condition* – A decrease of entropy associated with expansion shocks must not be admitted.
- *Monotonicity condition* – This condition must be enforced to prevent oscillatory behavior in the numerical scheme.
- *Total Variation Diminishing (TVD)* – The total variation of any physically admissible solution must not be allowed to increase in time.

In general, undesirable gradients, undershoots, overshoots which may occur in second order upwind schemes with low resolution may be controlled by providing nonlinear corrections, called limiters, which satisfy the above properties: entropy condition, monotonicity condition, and total variation diminishing.

(1) Definition of High Resolution Schemes

(a) Entropy Condition. The solution of the Euler equations may contain discontinuities of variable gradients involving an entropy increase (or compression shocks) and, unfortunately, an unrealistic entropy decrease (or expansion shocks) which violate the second law of thermodynamics. In order to eliminate such undesirable (numerically generated) entropy decrease or expansion shocks, we must guarantee that

$$a_R < a < a_L \tag{6.2.82}$$

where a is the speed of propagation of the discontinuity satisfying the Rankine-Hugoniot relations and

$$a_R = \frac{df_R}{du}, \quad a_L = \frac{df_L}{du} \tag{6.2.83}$$

with R and L being the right and left sides of the discontinuity. The requirement (6.2.82) is schematically shown in Figure 6.2.6, implying that a_R and a_L must intersect along the surface of discontinuity, resulting in a compression shock. In terms of eigenvalues, the entropy condition is given by

$$\lambda_k(U_R) < a < \lambda_k(U_L) \tag{6.2.84}$$

Another treatment of the entropy condition may be given by the smooth and positive entropy function $S(u_i)$ such that

$$\frac{\partial^2 S}{\partial u_i \partial u_j} > 0 \tag{6.2.85}$$

as proposed by Lax [1973]. This is equivalent to the existence of a system of equations with an artificial viscosity ν such that

$$U_t + aU_x = \nu U_{xx} \tag{6.2.86}$$

the solution of which confirms the entropy condition given by (6.2.85) in the limit as the

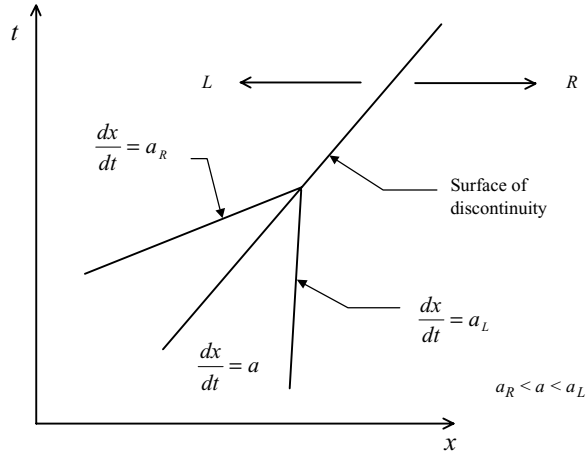

Figure 6.2.6 Intersection of two characteristics a_L and a_R leading to compression shock discontinuity.

artificial viscosity vanishes. In general, however, the satisfaction of entropy conditions alone may lead to oscillatory motions (overshoots and undershoots) along the discontinuities. Remedies can be found in the concepts of monotonicity and total variation diminishing, which are described below.

(b) Monotonicity Condition. A monotonicity condition refers to the nonoscillatory behavior of the numerical solution. Consider the solution of Euler equation to be in the form

$$u_i^{n+1} = H\left(u_{i-k}^n, u_{i-k+1}^n, \ldots, u_{i+k}^n\right) \tag{6.2.87}$$

This scheme is monotone if H is a monotonically increasing function such that

$$\frac{\partial H}{\partial u_j}(u_{i-k}, u_{i-k+1}, \ldots, u_{i+k}) \geq 0 \tag{6.2.88}$$

for all $i - k \leq j \leq i + k$, with

$$u_i^{n+1} = u_i^n - \tau\left(f_{i+\frac{1}{2}}^* - f_{i-\frac{1}{2}}^*\right) \tag{6.2.89}$$

$$f_{i+\frac{1}{2}}^* = f^*\left(u_{i-k+1}^n, u_{i-k+2}^n, \ldots, u_{i+k}^n\right) \tag{6.2.90}$$

The condition for monotonicity is given by

$$\frac{\partial f_{i+\frac{1}{2}}^*}{\partial u_{i-k+1}} \geq 0, \quad \frac{\partial f_{i+\frac{1}{2}}^*}{\partial u_{i+k}} \leq 0 \tag{6.2.91}$$

This represents a severe limitation, resulting in a scheme that is too diffusive. A compromise is the total variation diminishing concept, described next.

(c) Total Variation Diminishing (TVD) Schemes. As we have seen that the satisfaction of entropy and monotonicity conditions may still be restricted with oscillatory motions and excessive damping, respectively, our air now is to look to the concept of total variation diminishing to resolve these problems. To this end, we define the total variation [Lax, 1973] as

$$TV = \int \left|\frac{\partial u}{\partial x}\right| dx \tag{6.2.92}$$

A numerical scheme is said to be total variation diminishing (TVD) if

$$TV(u^{n+1}) \leq TV(u^n) \tag{6.2.93}$$

Let us consider the semi-discretized system

$$\frac{du_i}{dt} = -\frac{1}{\Delta x}\left(f_{i+\frac{1}{2}}^* - f_{i-\frac{1}{2}}^*\right) \tag{6.2.94}$$

or

$$\frac{du_i}{dt} = -\frac{1}{\Delta x}\left(C_{i+\frac{1}{2}}^- \delta u_{i+\frac{1}{2}} + C_{i-\frac{1}{2}}^+ \delta u_{i-\frac{1}{2}}\right) \tag{6.2.95}$$

with

$$C^-_{i+\frac{1}{2}}\delta u_{i+\frac{1}{2}} = f^*_{i+\frac{1}{2}} - f_i = a^-_{i+\frac{1}{2}}(u_{i+1} - u_i) \tag{6.2.96a}$$

$$C^+_{i-\frac{1}{2}}\delta u_{i-\frac{1}{2}} = f_i - f^*_{i-\frac{1}{2}} = a^+_{i-\frac{1}{2}}(u_i - u_{i-1}) \tag{6.2.96b}$$

and

$$C^+_{i+\frac{1}{2}} + C^-_{i+\frac{1}{2}} = \frac{f_{i+1} - f_i}{u_{i+1} - u_i} = \frac{\delta f_{i+\frac{1}{2}}}{\delta u_{i+\frac{1}{2}}} \equiv a_{i+\frac{1}{2}} \tag{6.2.97}$$

To compare the results above with the central scheme, we consider

$$f^*_{i+\frac{1}{2}} = \frac{1}{2}(f_i + f_{i+1}) - \frac{1}{2}\overline{D}_{i+\frac{1}{2}}\delta u_{i+\frac{1}{2}} \tag{6.2.98}$$

where $\overline{D}$ denotes the numerical viscosity coefficient. Combining (6.2.96) and (6.2.98), we obtain the wave speeds $C^-_{i+\frac{1}{2}}$ and $C^+_{i+\frac{1}{2}}$ in the form

$$C^-_{i+\frac{1}{2}} = \frac{1}{2}\left(a_{i+\frac{1}{2}} - \overline{D}_{i+\frac{1}{2}}\right) \tag{6.2.99}$$

$$C^+_{i+\frac{1}{2}} = \frac{1}{2}\left(a_{i+\frac{1}{2}} + \overline{D}_{i+\frac{1}{2}}\right) \tag{6.2.100}$$

from which the numerical viscosity coefficient becomes

$$\overline{D}_{i+\frac{1}{2}} = C^+_{i+\frac{1}{2}} - C^-_{i+\frac{1}{2}} \tag{6.2.101}$$

Thus the viscosity is expected to be proportional to the difference between the positive and negative wave speeds.

It follows from (6.2.101) that the semi-discrete system (6.2.95) is TVD if and only if

$$C^-_{i+\frac{1}{2}} \geq 0 \quad \text{and} \quad C^+_{i+\frac{1}{2}} \leq 0 \tag{6.2.102}$$

Once again from (6.2.95) we obtain, using the sign function $s_{i+\frac{1}{2}} = \text{sign}(\delta u_{i-\frac{1}{2}})$,

$$\begin{aligned}\frac{d}{dt}[TV(u)] &= \sum_i s_{i+\frac{1}{2}}\frac{d}{dt}(u_{i+1} - u_i) = \frac{1}{\Delta x}\sum_i s_{i+\frac{1}{2}}\Big[(C^- - C^+)_{i+\frac{1}{2}}\delta u_{i+\frac{1}{2}} \\ &\quad - C^-_{i+\frac{3}{2}}\delta u_{i+\frac{3}{2}} + C^+_{i-\frac{1}{2}}\delta u_{i-\frac{1}{2}}\Big] \\ &= \frac{1}{\Delta x}\sum_i \left[s_{i+\frac{1}{2}}\left(C^-_{i+\frac{1}{2}} - C^+_{i+\frac{1}{2}}\right) - s_{i-\frac{1}{2}}C^-_{i+\frac{1}{2}} + s_{i+\frac{3}{2}}C^+_{i+\frac{1}{2}}\right]\delta u_{i+\frac{1}{2}}\end{aligned} \tag{6.2.103}$$

The TVD condition requires that the right-hand side of (6.2.103) be nonpositive to ensure (6.2.102). This condition is satisfied for $\delta u_{i+\frac{1}{2}} = 1$ and $\delta u_{i+\frac{3}{2}} = \delta u_{i-\frac{1}{2}} = 0$. Thus, from (6.2.95) with an explicit Euler method

$$u^{n+1}_i = u^n_i - \frac{\Delta t}{\Delta x}\left(C^-_{i+\frac{1}{2}}\delta u_{i+\frac{1}{2}} + C^-_{i-\frac{1}{2}}\delta u_{i-\frac{1}{2}}\right)^n \tag{6.2.104}$$

with the CFL-like condition

$$\tau\left(C^+_{i+\frac{1}{2}} - C^-_{i+\frac{1}{2}}\right) \leq 1 \tag{6.2.105}$$

Integrating (6.2.95) and (6.2.103) and combining the results, together with (6.2.102), we obtain [Harten, 1983],

$$TV(u^{n+1}) \le \sum_i \left\{ \left[1 - \tau (C^+ - C^-)_{i+\frac{1}{2}}\right] \left|\delta u_{i+\frac{1}{2}}\right| - \tau C^-_{i+\frac{1}{2}} \left|\delta u_{i+\frac{1}{2}}\right| + \tau C^+_{i+\frac{1}{2}} \left|\delta u_{i+\frac{1}{2}}\right| \right\}$$
$$= \sum_i \left|\delta u_{i+\frac{1}{2}}\right| = TV(u^n) \tag{6.2.106}$$

This is the basic requirement for the total variation diminishing.

Note that the second order upwind scheme (6.2.77a,b) with $\kappa = -1$ can be written as

$$\frac{du_i}{dt} = -\frac{1}{2\Delta x}(3 f_i^+ - 4 f_{i-1}^+ + f_{i-2}^+) - \frac{1}{2\Delta x}(-3 f_i^- + 4 f_{i+1}^- - f_{i+2}^-)$$
$$= -\frac{a^+}{2\Delta x}[3(u_i - u_{i-1}) - (u_{i-1} - u_{i-2})] - \frac{a^-}{2\Delta x}[3(u_{i+1} - u_i) - (u_{i+2} - u_{i+1})] \tag{6.2.107}$$

in which oscillations along discontinuities may still prevail. In what follows, we shall discuss the TVD schemes with limiters to achieve accuracy and stability based on (6.2.107).

(2) TVD Schemes with Limiters

The TVD scheme described above may have over- and under-shoots which can be treated with the concept of limiters [Roe, 1984; Sweby, 1984]. To this end, rewrite (6.2.107) in the form,

$$\frac{du_i}{dt} = -\frac{a^+}{\Delta x}\left[(u_i - u_{i-1}) + \frac{1}{2}(u_i - u_{i-1}) - \frac{1}{2}(u_{i-1} - u_{i-2})\right]$$
$$-\frac{a^-}{\Delta x}\left[(u_{i+1} - u_i) + \frac{1}{2}(u_{i+1} - u_i) - \frac{1}{2}(u_{i+2} - u_{i+1})\right] \tag{6.2.108}$$

Here, the variations in the second and third terms within the square brackets will be limited as follows:

$$\frac{du_i}{dt} = -\frac{a^+}{\Delta x}\left[(u_i - u_{i-1}) + \frac{1}{2}\Psi^+_{i-\frac{1}{2}}(u_i - u_{i-1}) - \frac{1}{2}\Psi^+_{i-\frac{3}{2}}(u_{i-1} - u_{i-2})\right]$$
$$-\frac{a^-}{\Delta x}\left[(u_{i+1} - u_i) + \frac{1}{2}\Psi^-_{i+\frac{1}{2}}(u_{i+1} - u_i) - \frac{1}{2}\Psi^-_{i+\frac{3}{2}}(u_{i+2} - u_{i+1})\right] \tag{6.2.109}$$

Now the TVD conditions are obtained by rewriting (6.2.109) in the form similar to (6.2.95),

$$\frac{du_i}{dt} = -\frac{a^+}{\Delta x}\left[1 + \frac{1}{2}\Psi^+_{i-\frac{1}{2}} - \frac{1}{2}\frac{\Psi_{i-\frac{3}{2}}}{r^+_{i-\frac{3}{2}}}\right](u_i - u_{i-1})$$
$$-\frac{a^-}{\Delta x}\left[1 + \frac{1}{2}\Psi^-_{i+\frac{1}{2}} - \frac{1}{2}\frac{\Psi^-_{i+\frac{3}{2}}}{r^-_{i+\frac{3}{2}}}\right](u_{i+1} - u_i) \tag{6.2.110}$$

with

$$\begin{aligned} r^+_{i+\frac{1}{2}} &= \frac{u_{i+2}-u_{i+1}}{u_{i+1}-u_i}, & r^-_{i+\frac{1}{2}} &= \frac{u_i-u_{i-1}}{u_{i+1}-u_i} \\ r^+_{i-\frac{1}{2}} &= \frac{u_{i+1}-u_i}{u_i-u_{i-1}}, & r^-_{i-\frac{1}{2}} &= \frac{u_{i-1}-u_{i-2}}{u_i-u_{i-1}} \\ r^+_{i-\frac{3}{2}} &= \frac{u_i-u_{i-1}}{u_{i-1}-u_{i-2}}, & r^-_{i-\frac{3}{2}} &= \frac{u_{i-2}-u_{i-3}}{u_{i-1}-u_{i-2}} \\ r^-_{i+\frac{3}{2}} &= \frac{u_{i+3}-u_{i+2}}{u_{i+2}-u_{i+1}}, & r^-_{i+\frac{3}{2}} &= \frac{u_{i+1}-u_i}{u_{i+2}-u_{i+1}} \end{aligned} \tag{6.2.111}$$

$$\Psi^+_{i-\frac{1}{2}} = \Psi\left(r^+_{i-\frac{1}{2}}, r^+_{i+\frac{3}{2}}\right), \qquad \Psi^-_{i+\frac{1}{2}} = \Psi\left(r^-_{i+\frac{1}{2}}, r^-_{i+\frac{3}{2}}\right) \tag{6.2.112}$$

Thus, the TVD conditions are

$$\Psi^+ = 1 + \frac{1}{2}\Psi^+_{i-\frac{1}{2}} - \frac{1}{2}\frac{\Psi^+_{i-\frac{3}{2}}}{r^+_{i-\frac{3}{2}}} \geq 0 \tag{6.2.113a}$$

$$\Psi^- = 1 + \frac{1}{2}\Psi^-_{i+\frac{1}{2}} - \frac{1}{2}\frac{\Psi^-_{i+\frac{3}{2}}}{r^-_{i+\frac{3}{2}}} \geq 0 \tag{6.2.113b}$$

It is interesting to note that the basic Godunov's scheme (6.2.67b) is recovered for $\Psi^+ = \Psi^- = 1$. With more restricted definitions for the limiter,

$$\begin{aligned} \Psi^+_{i-\frac{1}{2}} &= \Psi\left(r^+_{i-\frac{1}{2}}\right), & \Psi^+_{i-\frac{3}{2}} &= \Psi\left(r^+_{i-\frac{3}{2}}\right) \\ \Psi^-_{i+\frac{1}{2}} &= \Psi\left(r^-_{i+\frac{1}{2}}\right), & \Psi^-_{i+\frac{3}{2}} &= \Psi\left(r^-_{i+\frac{3}{2}}\right) \end{aligned} \tag{6.2.114}$$

the TVD conditions (6.2.113a,b) may be written in the form [Roe, 1984, 1985; Swevy, 1984] as

$$\frac{\Psi\left(r^+_{i-\frac{3}{2}}\right)}{r^+_{i-\frac{3}{2}}} - \Psi\left(r^+_{i-\frac{1}{2}}\right) \leq 2 \tag{6.2.115a}$$

$$\frac{\Psi\left(r^-_{i+\frac{3}{2}}\right)}{r^-_{i+\frac{3}{2}}} - \Psi\left(r^-_{i+\frac{1}{2}}\right) \leq 2 \tag{6.2.115b}$$

which may be generalized in the following form for all values of r and s:

$$\frac{\Psi(r)}{r} - \Psi(s) \leq 2 \tag{6.2.116}$$

with the following constraints:

$$\Psi(r) \geq 0 \quad \text{for } r \geq 0 \tag{6.2.117a}$$

$$\Psi(r) = 0 \quad \text{for } r < 0 \tag{6.2.117b}$$

where (6.2.117b) is designed to avoid nonmonotone behavior. Thus, the sufficient

condition becomes

$$0 \leq \Psi(r) \leq 2r \tag{6.2.118}$$

Let us examine the above condition with another scheme such as the explicit second order Warming and Beam scheme:

$$u_i^{n+1} - u_i^n = -\sigma(u_i - u_{i-1})^n - \frac{\sigma}{2}(1-\sigma)(u_i - 2u_{i-1} + u_{i-2})^n \tag{6.2.119}$$

which may be rewritten as

$$u_i^{n+1} = u_i^n - \sigma(u_i - u_{i-1})^n - \frac{\sigma}{2}(1-\sigma)\delta^- \left[\Psi\left(r^+_{i-\frac{1}{2}}\right)(u_i - u_{i-1})^n\right] \tag{6.2.120}$$

Using the conditions (6.2.107) and (6.2.120), we obtain

$$0 \leq \tau\ C^+_{i-\frac{1}{2}} = \sigma\left\{1 + \frac{1}{2}(1-\sigma)\left[\Psi\left(r^+_{i-\frac{1}{2}}\right) - \frac{1}{2}\frac{\Psi\left(r^+_{i-\frac{3}{2}}\right)}{r^+_{i-\frac{3}{2}}}\right]\right\} \leq 1 \tag{6.2.121a}$$

$$C^-_{i-1/2} = 0 \tag{6.2.121b}$$

This requires, for arbitrary values of r and s,

$$\frac{\Psi(r)}{r} - \Psi(s) \leq \frac{2}{1-\sigma} \tag{6.2.122a}$$

and

$$\Psi(s) - \frac{\Psi(r)}{r} \leq \frac{2}{\sigma} \tag{6.2.122b}$$

Combining (6.2.118) and (6.2.122), the second order upwind scheme is TVD for

$$0 \leq \Psi(r) \leq \min(2r, 2) \tag{6.2.123}$$

with $\Psi = 1$ for the Warming and Beam Scheme and $\Psi(r) = r$ for the Lax-Wendroff scheme.

Various limiters for second order schemes are summarized below:

(a) TVD regions for $\Psi(r)$ in general

(b) Van Leer's limiter $\Psi = \dfrac{r + |r|}{1 + r}$ (6.2.124)

(c) Minimum modulus (minmod) $\Psi(r) = \begin{cases} \min(r, 1) & \text{if } r > 0 \\ 0 & \text{if } r \leq 0 \end{cases}$ (6.2.125a)

$$\text{minmod}(x, y) = \begin{cases} x & \text{if } |x| < |y|, \quad xy > 0 \\ y & \text{if } |x| > |y|, \quad xy > 0 \\ 0 & \text{if } xy < 0 \end{cases} \tag{6.2.125b}$$

(d) Roe's Superbee limiter $\Psi(r) = \max[0, \min(2r, 1), \min(r, 2)]$ (6.2.126)

(e) General β-limiters $\Psi = \max[0, \min(\beta r, 1), \min(r, \beta)]$, $1 \leq \beta \leq 2$ (6.2.127)

(f) Chakravarthy and Osher limiter $\Psi(r) = \max[0, \min(r, \beta)]$, $1 \leq \beta \leq 2$ (6.2.128)

In these limiters, we observe the following features:

(i) For $r < 1$ or

$$\frac{u_{i+1} - u_i}{\Delta x} < \frac{u_i - u_{i-1}}{\Delta x}$$

Then set $\Psi(r) = r$ and the contribution $u_i^n - u_{i-1}^n$ to u_i^{n+1} is replaced by the smaller quantity $(u_{i+1}^n - u_i^n)$.

(ii) If $r > 1$, the contribution $(u_i - u_{i-1})$ remains unchanged.

(iii) If the slopes of consecutive intervals change sign, then the updated point i receives no contribution from the upstream interval.

The limiters as defined above may be applied to numerical fluxes in the form

$$\begin{aligned}\frac{du_i}{dt} = &-\frac{1}{\Delta x}\left[1 + \frac{1}{2}\Psi\left(r^+_{i-\frac{1}{2}}\right) - \frac{1}{2}\frac{\Psi\left(r^+_{i-\frac{3}{2}}\right)}{r^+_{i-\frac{3}{2}}}\right]\left(f_i - f^*_{i-\frac{1}{2}}\right)\\ &-\frac{1}{\Delta x}\left[1 + \frac{1}{2}\Psi\left(r^-_{i+\frac{1}{2}}\right) - \frac{1}{2}\frac{\Psi\left(r^-_{i+\frac{3}{2}}\right)}{r^-_{i+\frac{3}{2}}}\right]\left(f^*_{i+\frac{1}{2}} - f_i\right)\end{aligned} \tag{6.2.129}$$

with

$$r^+_{i-\frac{3}{2}} = \frac{f_i - f^*_{i-\frac{1}{2}}}{f^+_i - f^*_{i-1}}, \quad r^-_{i+\frac{3}{2}} = \frac{f^*_{i+\frac{1}{2}} - f_i}{f^-_{i-1} - f^-_i} \tag{6.2.130}$$

and equivalently,

$$\begin{aligned}\frac{du_i}{dt} = &-\frac{1}{\Delta x}\left[1 + \frac{1}{2}\Psi\left(r^+_{i-\frac{1}{2}}\right) - \frac{1}{2}\frac{\Psi\left(r^+_{i-\frac{3}{2}}\right)}{r^+_{i-\frac{3}{2}}}\right]a^+_{i-\frac{1}{2}}(u_i - u_{i-1})\\ &-\frac{1}{\Delta x}\left[1 + \frac{1}{2}\Psi\left(r^-_{i+\frac{1}{2}}\right) - \frac{1}{2}\frac{\Psi\left(r^-_{i+\frac{3}{2}}\right)}{r^-_{i+\frac{3}{2}}}\right]a^-_{i+\frac{1}{2}}(u_{i+1} - u_i)\end{aligned} \tag{6.2.131}$$

Here it is seen that with redefinition of slope ratios (6.2.130), the limiters are generalized to nonlinear scalar conservation equations from (6.2.113).

(3) Time Integration Methods for TVD Schemes

So far we have been concerned with the second order space-accurate TVD schemes only. We are now prepared to discuss integration of the time dependent term.

Recall that there are two types of time integration methods: (1) the combined space time methods (Section 6.2.2) and (2) separate space-time methods (Section 6.2.3). The former is more suitable for time dependent problems (time accurate), whereas the latter are more suitable for steady-state problems (not time accurate).

(a) Explicit TVD Schemes of First Order Accuracy in Time. Consider the first order time integration of (6.2.128) in the form

$$\frac{du_i}{dt} = -\frac{1}{\Delta x}\left[1 + \frac{1}{2}\Psi\left(r^+_{i-\frac{1}{2}}\right) - \frac{1}{2}\frac{\Psi\left(r^+_{i-\frac{3}{2}}\right)}{r^+_{i-\frac{3}{2}}}\right]\left(f_i - f^*_{i-\frac{1}{2}}\right)^n$$
$$-\frac{1}{\Delta x}\left[1 + \frac{1}{2}\Psi\left(r^-_{i+\frac{1}{2}}\right) - \frac{1}{2}\frac{\Psi\left(r^-_{i+\frac{3}{2}}\right)}{r^-_{i+\frac{3}{2}}}\right]\left(f^*_{i+\frac{1}{2}} - f_i\right)^n \tag{6.2.132}$$

This scheme without the limiter ($\Psi = 1$) is unstable, whereas the nonlinear TVD version with $\Psi > 1$ is conditionally stable, as seen from (6.2.107).

Define the local, positive, and negative CFL numbers,

$$\sigma^+_{i+\frac{1}{2}} = \tau\frac{f_{i+1} - f^*_{i+\frac{1}{2}}}{u_{i+1} - u_i} = \tau\frac{f^+_{i+1} - f^+_i}{u_{i+1} - u_i} \tag{6.2.133a}$$

$$\sigma^-_{i+\frac{1}{2}} = \tau\frac{f^*_{i+\frac{1}{2}} - f_i}{u_{i+1} - u_i} = \tau\frac{f^-_{i+1} - f^-_i}{u_{i+1} - u_i} \tag{6.2.133b}$$

with

$$\sigma_{i+\frac{1}{2}} = \sigma^+_{i+\frac{1}{2}} + \sigma^-_{i+\frac{1}{2}} = \tau\frac{f_{i+1} - f_i}{u_{i+1} - u_i} = \tau a_{i+\frac{1}{2}} \tag{6.2.134}$$

$$|\sigma|_{i+\frac{1}{2}} = \sigma^+_{i+\frac{1}{2}} - \sigma^-_{i+\frac{1}{2}} = \tau\left|\frac{f_{i+1} - f_i}{u_{i+1} - u_i}\right| = \tau|a|_{i+\frac{1}{2}} \tag{6.2.135}$$

and

$$\tau C^+_{i-\frac{1}{2}} = \sigma^+_{i-\frac{1}{2}}\left[1 + \frac{1}{2}\Psi\left(r^+_{i-\frac{1}{2}}\right) - \frac{1}{2}\frac{\Psi\left(r^+_{i-\frac{3}{2}}\right)}{r^+_{i-\frac{3}{2}}}\right] \tag{6.2.136a}$$

$$\tau C^-_{i+\frac{1}{2}} = \sigma^-_{i+\frac{1}{2}}\left[1 + \frac{1}{2}\Psi\left(r^-_{i+\frac{1}{2}}\right) - \frac{1}{2}\frac{\Psi\left(r^-_{i+\frac{3}{2}}\right)}{r^-_{i+\frac{3}{2}}}\right] \tag{6.2.136b}$$

Thus, the TVD condition (6.2.107) with (6.2.115) is given by

$$\tau\left(C^+_{i+\frac{1}{2}} - C^-_{i+\frac{1}{2}}\right) \le \tau|a|_{i+\frac{1}{2}}\left(\frac{1+\alpha}{2}\right) \le 1 \tag{6.2.137}$$

where

$$\left|\Psi(s) - \frac{\Psi(r)}{r}\right| \le \alpha$$

with $0 < \alpha \le 2$. The CFL condition for this case is

$$|\sigma| \le \frac{2}{2+\alpha} \tag{6.2.138}$$

The stability conditions for various limiters are

minmod limiter: $|\sigma| < \frac{2}{3}$

superbee limiter: $|\sigma| < \frac{1}{2}$

and so on.

(b) Implicit TVD Schemes. An implicit multistep method for the second order TVD scheme may be written as

$$\Delta u_i^n + \tau\theta\left(f_{i+\frac{1}{2}}^{*n+1} - f_{i-\frac{1}{2}}^{*n+1}\right) = -\tau(1-\theta)\left(f_{i+\frac{1}{2}}^{*n} - f_{i-\frac{1}{2}}^{*n}\right) \tag{6.2.139}$$

Using (6.2.104), we may rewrite (6.2.139) as

$$\left[1 + \tau\theta\left(C_{i+\frac{1}{2}}^{-}\delta^{+} + C_{i-\frac{1}{2}}^{+}\delta^{-}\right)\right]^n \Delta u_i^n = -\tau\left(f_{i+\frac{1}{2}}^{*} - f_{i-\frac{1}{2}}^{*}\right)^n \tag{6.2.140}$$

or

$$[1 + \tau\theta(C^{+} - C^{-})]\Delta u_i + \tau\theta C^{-}\Delta u_{i+1} - \tau\theta C^{+} = -\tau\left(f_{i+\frac{1}{2}}^{*} - f_{1-\frac{1}{2}}^{*}\right) \tag{6.2.141}$$

It is now seen from (6.2.105) that the left-hand side of (6.2.141) is diagonally dominant. The CFL-like condition is given as

$$\tau(1-\theta)\left(C_{i+\frac{1}{2}}^{-} - C_{i-\frac{1}{2}}^{+}\right) \le 1 \tag{6.2.142}$$

(c) Explicit Second Order TVD Schemes. Consider (6.2.74) with $\kappa = -1$ in (6.2.80),

$$\overline{u}_i = u_i^n - \frac{\tau}{2}\delta^{-} f_{i+\frac{1}{2}}^{*} \tag{6.2.143a}$$

$$\overline{f}_{i+\frac{1}{2}}^{*} = f^{*}(\overline{u}_i, \overline{u}_{i+1}) \tag{6.2.143b}$$

$$u_i^{n+1} = u_i^n - \tau\delta^{-1}\left[\overline{f}_{i+\frac{1}{2}}^{*} + \frac{1}{2}\Psi_{i-\frac{1}{2}}^{+}\left(f_i^n - f_{i-\frac{1}{2}}^{*}\right) + \Psi_{i+\frac{3}{2}}^{-}\left(f_{i+1}^n - f_{i+\frac{3}{2}}^{*}\right)\right] \tag{6.2.143c}$$

Applying (6.2.143c) to the linear convection equation, we obtain

$$u_i^{n+1} = u_i^n - \sigma\left[1 + \frac{1}{2}\left(\Psi_{i-\frac{1}{2}}^{+} - \sigma\right) - \frac{1}{2}\frac{\left(\Psi_{i-\frac{3}{2}}^{+} - \sigma\right)}{r_{i-\frac{3}{2}}^{+}}\right](u_i^n - u_{i-1}^n) \tag{6.2.144}$$

with the TVD conditions,

$$0 \le \sigma\left[2 + \Psi(s) - \sigma - \frac{\Psi(r) - \sigma}{r}\right] \le 2 \tag{6.2.145}$$

where

$$s = r_{i-\frac{1}{2}}^{+}, \quad r = r_{i-\frac{3}{2}}^{+}$$

and

$$0 \le \Psi(r) \le (2-\sigma)r + \sigma \tag{6.2.146a}$$

$$0 \le \Psi(r) \le \frac{2}{\sigma} \tag{6.2.146b}$$

These conditions lead to, for $0 < \sigma \le 1$,

$$\Psi(r) \le \min(2, 2r) \tag{6.2.147}$$

It is interesting to recognize that the limited terms in (6.2.143c) represent the difference (prior to limiting) between the second and the first order numerical fluxes, $f^{**} - f^{*}$, and that this is the antidiffusive flux of the Flux Corrected Transport (FCT) [Boris and Book, 1973].

Various second order TVD schemes are identified as follows:

(i) Explicit Second-Order Schemes with Variable Extrapolation (MUSCL) Approach. Once again, from (6.2.74), (6.2.80), and (6.2.72a,b), we obtain

$$u_i = u_i^n - \frac{\Delta t}{2\Delta x}\left(f^*_{i+\frac{1}{2}} - f^*_{i-\frac{1}{2}}\right) \tag{6.2.148a}$$

$$\tilde{u}^L_{i+\frac{1}{2}} = \overline{u}_i + \frac{1}{2}\hat{\Psi}^L(u_i - u_{i-1}) \tag{6.2.148b}$$

$$\tilde{u}^R_{i+\frac{1}{2}} = \overline{u}_{i+1} - \frac{1}{2}\hat{\Psi}^R(U_{i+1} - u_i) \tag{6.2.148c}$$

with the tilde indicating monotonicity conditions, leading to

$$u_i^{n+1} - u_i^n = -\tau\left(\overline{f}^{**}_{i+\frac{1}{2}} - \overline{f}^{**}_{i-\frac{1}{2}}\right) \tag{6.2.149}$$

where

$$\overline{f}^{**}_{i+\frac{1}{2}} = f^*\left(\tilde{u}^L_{i+\frac{1}{2}}, \tilde{u}^R_{i+\frac{1}{2}}\right) \tag{6.2.150}$$

(ii) Lax-Wendroff TVD Scheme. This is an application of TVD to the Lax-Wendroff Scheme [Davis, 1984; Roe, 1984]. Here, the Lax-Wendroff numerical flux,

$$f_{i+\frac{1}{2}} = \frac{1}{2}(f_i + f_{i+1})$$

is transformed into an equivalent flux split form by decomposing the fluxes and the Jacobians into their positive and negative parts,

$$f^{*(LW)}_{i+\frac{1}{2}}\Big|_{TVD} = f_i^+ + f_{i+1}^- + \frac{1}{2}\left(1 + \tau A^+_{i+\frac{1}{2}}\right)\delta f^+_{i+\frac{1}{2}} - \frac{1}{2}\left(1 + \tau A^-_{i+\frac{1}{2}}\right)\delta f^-_{i+\frac{1}{2}} \tag{6.2.151}$$

Thus, the TVD Lax-Wendroff scheme becomes

$$f^{*(LW)}_{i+\frac{1}{2}}\big|_{TVD} = f^+_i + f^-_{i+1} + \frac{1}{2}\Psi\left(\frac{1}{r^+_{i-\frac{1}{2}}}\right)\left(1-\sigma^+_{i+\frac{1}{2}}\right)\delta f^+_{i+\frac{1}{2}} - \frac{1}{2}\Psi\left(\frac{1}{r^-_{i+\frac{3}{2}}}\right)\left(1+\sigma^-_{i+\frac{1}{2}}\right)\delta f^-_{i+\frac{1}{2}} \tag{6.2.152}$$

where the symmetry property

$$\frac{\Psi(r)}{r} = \Psi\left(\frac{1}{r}\right)$$

is utilized. Note that the presence of the functional dependence on $r_{i+3/2}$ is required, leading to a five-point scheme to satisfy the TVD and second order accuracy conditions.

(iii) Harten's Modified Flux Method. The first order upwind scheme has a truncation error h_x such that

$$u_t + f_x + h_x = 0 \tag{6.2.153}$$

with

$$h = \Delta t\beta(u)u_x \tag{6.2.154}$$

Equation (6.2.153) represents a second order approximation to $u_t + f_x = 0$. For the first order upwind scheme,

$$f^*_{i+\frac{1}{2}} = \frac{1}{2}(f_i + f_{i+1}) - \frac{1}{2}|a|_{i+\frac{1}{2}}(u_{i+1} - u_i) \tag{6.2.155}$$

the truncation error becomes

$$h = \frac{\Delta x}{2}|a|(1-\tau|a|)u_x + O(\Delta x^2) = \frac{\Delta x}{2\tau}|\sigma|(1-|\sigma|)u_x + O(\Delta x^2) \tag{6.2.156}$$

Thus, the numerical flux for (6.2.153) assumes the second order form,

$$f^{**}_{i+\frac{1}{2}} = \frac{1}{2}(f_i + f_{i+1}) + \frac{1}{2}(h_i + h_{i+1}) - \frac{1}{2}|a+b|_{i+\frac{1}{2}}(u_{i+1} - u_i) \tag{6.2.157}$$

with

$$h_{i+\frac{1}{2}} = |a|_{i+\frac{1}{2}}\left(1-|\sigma|_{i+\frac{1}{2}}\right)\frac{u_{i+1}-u_i}{2} = \frac{h_{i+1}+h_i}{2} \tag{6.2.158a}$$

$$b_{i+\frac{1}{2}} = \frac{h_{i+1}-h_i}{u_{i+1}-u_i} \tag{6.2.158b}$$

This scheme is TVD with

$$\tau|a+b|_{i+\frac{1}{2}} \le 1 \tag{6.2.159}$$

and

$$h_i = \min\text{mod}\left(h_{i-\frac{1}{2}}, h_{i+\frac{1}{2}}\right) \tag{6.2.160}$$

(d) Artificial Dissipation and TVD Schemes. Let us rearrange (6.2.152) in the form

$$f^{*(LW)}_{i+\frac{1}{2}}\big|_{TVD} = \frac{1}{2}(f_i + f_{i+1}) - \frac{1}{2}|a|_{i+\frac{1}{2}}(u_{i+1} - u_i) + \frac{1}{2}[\Psi^+(1-\sigma^+)a^+ - \Psi^-(1-\sigma^-)a^-]_{i+\frac{1}{2}}(u_{i+1} - u_i) \tag{6.2.161}$$

where

$$\begin{aligned} &\Psi^+ a^- = 0 \quad \text{or} \quad \Psi^+ f^- = 0 \\ &\Psi^- a^+ = 0 \quad \text{or} \quad \Psi^- f^+ = 0 \end{aligned} \tag{6.2.162}$$

Thus

$$f^{*(LW)}_{i+\frac{1}{2}}\big|_{TVD} = \frac{1}{2}(f_i + f_{i+1}) - \frac{1}{2}|a|_{i+\frac{1}{2}}(u_{i+1} - u_i) + \frac{1}{2}(\Psi^+ + \Psi^-)[(1-\sigma^+)a^+ - (1+\sigma^-)a^-]_{i+\frac{1}{2}}(u_{i+1} - u_i) \tag{6.2.163a}$$

or

$$f^{*(LW)}_{i+\frac{1}{2}}\big|_{TVD} = \frac{1}{2}(f_i + f_{i+1}) - \frac{1}{2}|a|_{i+\frac{1}{2}}(u_{i+1} - u_i) + \frac{1}{2}(\Psi^+ + \Psi^-)[|a|(1-|\sigma|)]_{i+\frac{1}{2}}(u_{i+1} - u_i) \tag{6.2.163b}$$

Written alternatively,

$$f^{*(LW)}_{i+\frac{1}{2}}\big|_{TVD} = \frac{1}{2}(f_i + f_{i+1}) - \frac{1}{2}\tau a^2_{i+\frac{1}{2}}(u_{i+1} - u_i) + \frac{1}{2}(\Psi^+ + \Psi^- - 1)[|a|(1-|\sigma|)]_{i+\frac{1}{2}}(u_{i+1} - u_i) \tag{6.2.164}$$

Comparing with (6.2.50), $\Psi^{\pm}$ are identified as

$$D_{i+\frac{1}{2}} = \frac{1}{2}(1 - \Psi^+ - \Psi^-)[|a|(1-|\sigma|)]_{i+\frac{1}{2}} \tag{6.2.165}$$

Similarly, a TVD MacCormack scheme is given by

$$\begin{aligned} &\overline{u}_i = u_i^n - \tau(f_{i+1} - f_i)^n \\ &\overline{\overline{u}} = u_i^n - \tau(\overline{f}_i - \overline{f}_{i-1}) \\ &u_i^{n+1} = \frac{1}{2}(\overline{u}_i + \overline{\overline{u}}_i) + \tau\Big[D_{i+\frac{1}{2}}(u_{i+1} - u_i) - D_{i-\frac{1}{2}}(u_i - u_{i-1})\Big] \end{aligned} \tag{6.2.166}$$

Although the artificial viscosity of the central schemes is analogous to the TVD schemes, accuracy and efficiency of the TVD schemes have proven to be superior.

In summary, the TVD schemes, although capable of resolving shock waves, are not uniformly high order accurate. They are reduced to first order accurate at local extrema of the solutions, while maintaining second order accuracy in other smooth regions. To circumvent this difficulty, the essentially nonoscillatory (ENO) schemes have been introduced. This is the subject of the next section.

6.2.7 ESSENTIALLY NONOSCILLATORY SCHEME

In the previous sections, we have studied low- and high-resolution schemes of Godunov, MUSCL, and TVD. In this section we examine a generalization and extension of these schemes, leading to a uniformly high order accurate essentially nonoscillatory scheme (ENO) as advanced by Harten and Osher [1987], and subsequently by Shu and Osher [1988, 1989], among others.

In the ENO scheme, high-order accuracy is obtained, whenever the solution is smoothed by means of a piecewise polynomial reconstruction procedure, yielding high order pointwise information from the cell averages of the solution. When applied to piecewise smooth initial data, this reconstruction enables a flux computation which is of high order accuracy, whenever the function is smooth, and avoids nonconvergence.

Initially, ENO schemes were developed in terms of cell averages conducive to FVM applications, followed by numerical fluxes for FDM applications with TVD Runge-Kutta discretization. These two types of ENO schemes were compared and evaluated by Casper, Shu, and Atkins [1994]. Recently, the ENO scheme has been extended to the Navier-Stokes system of equations [Zhong, 1994] and to unstructured triangular grids [Abgrall,1994; Suresh and Jorgenson, 1995; Stanescu and Habashi, 1998], among others. The basic theory of ENO is briefly summarized below.

The purpose of ENO is to achieve uniformly high order accuracy by avoiding the growth of spurious oscillations at shock discontinuities known as Gibb's phenomena. To this end, we employ piecewise polynomial reconstruction in the numerical solution based on an adaptive stencil. Such stencil is chosen according to the local smoothness of the flow variable.

Although ENO schemes have been applied to multidimensional Euler and Navier-Stokes system of equations, we illustrate the procedure using one-dimensional hyperbolic conservation law,

$$\frac{\partial \mathbf{U}}{\partial t} + \frac{\partial \mathbf{F}}{\partial x} = 0 \tag{6.2.167}$$

For simplicity, we consider a one-dimensional scalar function and reconstruct the point values $u(x)$ of a piecewise smooth function u from its known values of cell average $\overline{u}_i$.

$$\overline{u}_i = \int_{x_i-1/2}^{x_i+1/2} u(\xi)d\xi \tag{6.2.168}$$

with $h_i = x_{i+1/2} - x_{i-1/2}$. Let us now reconstruct $u(x)$ from $\overline{u}_i$ by interpolating the primitive function $U(x)$,

$$U(x) = \int_{x_0}^{x} u(\xi)d\xi \tag{6.2.169}$$

The point value of the primitive function at $x = x_{i+1/2}$ is given by

$$U_{i+1/2} = \sum_{i=i_0}^{i} \overline{u}_i h_i \tag{6.2.170}$$

Table 6.2.2 Illustration of Divided Difference

x^k	Δ^0	Δ^1 (1st divided difference)	Δ^2 (2nd divided difference)	Δ^3 (3rd divided difference)
p_0 x_0	U_0	$\frac{U_1-U_0}{x_1-x_0}=\Delta U_0$		
			$\frac{\Delta U_1-\Delta U_0}{x_2-x_0}=\Delta^2 U_0$	
p_1 x_1	U_1	$\frac{U_2-U_1}{x_2-x_1}=\Delta U_1$		$\frac{\Delta^2 U_1-\Delta^2 U_0}{x_3-x_0}=\Delta^3 U_0$
			$\frac{\Delta U_2-\Delta U_1}{x_3-x_1}=\Delta^2 U_1$	
p_2 x_2	U_2	$\frac{U_3-U_2}{x_3-x_2}=\Delta U_2$		
p_3 x_3	U_3			

Since we have

$$u(x) = \frac{d}{dx}U(x) \tag{6.2.171}$$

it is now possible to obtain a piecewise polynomial interpolation function $H_m(x, U)$ of degree m by interpolating the point values of $U_{i+1/2}$ from (6.2.170) and arrive at the reconstruction polynomial of the form

$$R(x, \overline{u}) = \frac{d}{dx}H_m(x, U) \tag{6.2.172}$$

where, for cell $x_{i-1/2}$ and $x_{i+1/2}$, $H_m(x, U)$ represents the mth degree polynomial that interpolates the values of $U_{i+1/2}$ at $m+1$ successive points $x_{j+1/2}(j_m \le j \le j_m + m)$ including $x_{i-1/2}$ and $x_{i+1/2}$. Thus, our objective is to choose a stencil with $H_m(x, U)$ being the smoothest. This can be extracted from a table of divided differences of $U(x)$ such as shown in Table 6.2.2.

The one-dimensional ENO reconstruction described above has been extended to two dimensions via primitive function [Casper, 1992]. The cell average can be carried out as follows:

$$U_{ij} = \frac{1}{\Delta x_i}\int_{x_i-1/2}^{x_i+1/2} \overline{U}_j(x)dx \tag{6.2.173}$$

with

$$\overline{U}_j(x) = \frac{1}{\Delta y_j}\int_{y_i-1/2}^{y_i+1/2} \overline{U}(x, y)dy \tag{6.2.174}$$

Recently, applications of ENO to the Euler equations in unstructured triangular grids have been reported by Abgrall [1994], Suresh and Jorgenson [1995], and Stanescu and Habashi [1998]. The reconstruction via extrapolation allows the selection in one step of all of the cells in the required stencil for each cell. For an rth order-of-accuracy,

the approximation polynomials of degree $m = r - 1$ are written as

$$R_i[U, r] = \sum_{p=0}^{m} \sum_{j+k=p} a_{jk} X^j Y^k \tag{6.2.175}$$

Here, we have $M = (m+1)(m+2)/2$ unknowns, requiring a stencil of M cells to build the interpolation polynomial.

The ENO reconstruction such as given by (6.2.175) can be used to compute fluxes so that the solution procedure of any scheme presented in the previous subsections will be followed.

6.2.8 FLUX-CORRECTED TRANSPORT SCHEMES

The flux-corrected transport (FCT) scheme was originally developed by Boris and Book [1973] and subsequently generalized by Zalesak [1979] in which monotonicity is assured in multidimensional problems. The basic idea is to combine a high order scheme with a low order scheme in such a way that the high order scheme is employed in smooth regions of the flow, whereas the low order scheme is used near discontinuities in an attempt to obtain a monotonic solution. The following six steps are used for the solution.

(1) Compute $F^L_{i+1/2}$, the transportive flux given by some low order method guaranteed to give monotonic results.
(2) Compute $F^H_{i+1/2}$, the transportive flux given by some high order method. This flux is mathematically more accurate, but can lead to physically unacceptable ripples in the solution.
(3) Compute the updated low order, transported and diffused solution,

$$U_i^{TD} = U_i^o - \frac{\Delta t}{\Delta x_i}\left(F^L_{i+1/2} - F^L_{i-1/2}\right) \tag{6.2.176}$$

(4) Define the antidiffusive flux which becomes the amount of the monotone transportive flux that we would like to limit before correcting the transported and diffused conservation variables of step (3).

$$F^{AD}_{i+1/2} = F^H_{i+1/2} - F^L_{i+1/2} \tag{6.2.177}$$

Limit the antidiffusive fluxes $F^A_{i+1/2}$ so that U^n as computed in step (4) is free of the overshoots and undershoots which also do not appear in U_i^{TD}.

$$F^C_{i+1/2} = C_{i+1/2} F^{AD}_{i+1/2} \quad 0 \le C_{i+1/2} \le 1 \tag{6.2.178}$$

Apply the limited antidiffusive fluxes to get the new values U_i^n,

$$U_i^n = U_i^{TD} - \frac{\Delta t}{\Delta x}\left(F^C_{i+1/2} - F^C_{i-1/2}\right) \tag{6.2.179}$$

Note that if $F^C_{i+1/2} = F^{AD}_{i+1/2}$ for $C_{i+1/2} = 1$, the U_i^n reduces to the time-advanced higher order method without the required monotonicity correction.

The procedure described above can be generalized to the two-dimensional case,

$$U^n_{i,j} = U^o_{i,j} - \frac{\Delta t}{A_{i,j}}[(F_x)_{i+1/2,j} - (F_x)_{i-1/2,j} + (F_y)_{i,j+1/2} - (F_y)_{i,j-1/2}] \tag{6.2.180}$$

where $A_{i,j}$ is the two-dimensional area element centered on grid point (i, j). Here, two sets of transportive fluxes F_x and F_y are treated as follows:

a. Compute $(F_x)^L_{i+1/2,j}$ and $(F_y)^L_{i,j+1/2}$ by a lower order method.
b. Compute $(F_x)^H_{i+1/2,j}$ and $(F_y)^H_{i,j+1/2}$ by a higher order method.
c. Compute the previously updated low order, transported and diffused solution.

$$U^{TD}_{i,j} = U^n_{i,j} - \frac{\Delta t}{A_{i,j}}\left[(F_x)^L_{i+1/2,j} - (F_x)^L_{i-1/2,j} + (F_y)^L_{i,j+1/2} - (F_y)^L_{i,j-1/2}\right] \tag{6.2.181}$$

d. Define the vector components of the antidiffusive fluxes

$$\begin{aligned} F^{AD}_{i+1/2,j} &= (F_x)^H_{i+1/2,j} - F^L_{i+1/2,j} \\ F^{AD}_{i,j+1/2,} &= (F_y)^H_{i+1/2,j} - F^L_{i,j+1/2} \end{aligned} \tag{6.2.182}$$

e. Limit the antidiffusive fluxes so that there are no overshoots or undershoots in $U^n_{i,j}$ of step (f) below that do not appear in $U^n_{i,j}$ of step (c).

$$\begin{aligned} F^C_{i+1/2,j} &= C_{i+1/2,j} F^{AT}_{i+1/2,j} \quad 0 \le C_{i+1/2,j} \le 1 \\ F^C_{i,j+1/2,} &= C_{i+1/2,j} F^{AT}_{i,j+1/2} \quad 0 \le C_{i,j+1/2,j} \le 1 \end{aligned} \tag{6.2.183}$$

f. Apply the limited antidiffusive fluxes to get the new values $U^n_{i,j}$

$$U^n_{i,j} = U^{TD}_{i,j} - \frac{\Delta t}{A_{i,j}}\left[F^C_{i+1/2,j} - F^C_{i-1/2,j} + F^C_{i,j+1/2} - F^C_{i,j-1/2}\right] \tag{6.2.184}$$

Here, it is important to limit the antidiffusive fluxes $F^{AT}_{i+1/2,j}$ and $F^{AT}_{i,j+1/2}$ by choosing the cell-interface flux-correcting factors $C_{i+1,j}$ and $C_{i,j+1}$ such that the combination of four fluxes acting together, through (6.2.184), does not allow $U^n_{i,j}$ to exceed some maximum value $U^{\max}_{i,j}$ or to fall below some minimum value $U^{\min}_{i,j}$. It should be noted that determination of suitable values of flux-correcting factors $C_{i+1,j}$ and $C_{i,j+1}$ is analogous to the TVD limiters. There are many possible ways to determine these limiters, as suggested in Zalesak [1979].

6.3 NAVIER-STOKES SYSTEM OF EQUATIONS

Diffusion processes due to viscosity and thermal conductivity are characterized by the Navier-Stokes system of equations. As the Reynolds number increases, boundary layers are formed and the laminar flow undergoes a transition toward turbulence. In high Reynolds number and high Mach number flows, shock waves and turbulent boundary layer interactions are most likely to occur. Furthermore, diffusivity due to chemical reactions also adds to the complexity of governing equations and computations. In general, such physical properties make the length and time scales of the variables widely disparate, thus causing the resulting algebraic finite difference equations to become "stiff." The subjects of turbulence and chemical reactions will not be discussed until Part Five.

Although implicit schemes are used predominantly in dealing with stiff equations for compressible viscous flows, explicit schemes have also been used in relatively low

Reynolds number flows. In this section, some of the prominent explicit and implicit schemes are discussed, followed by PISO.

6.3.1 EXPLICIT SCHEMES

The compressible viscous flow in its most general form was presented in Chapter 2. An expanded form in 3-D is shown below, but without source terms.

$$\frac{\partial \mathbf{U}}{\partial t}+\frac{\partial \mathbf{A}}{\partial x}+\frac{\partial \mathbf{B}}{\partial y}+\frac{\partial \mathbf{C}}{\partial z}=0 \tag{6.3.1}$$

with

$$\mathbf{U}=\begin{bmatrix}\rho\\ \rho u\\ \rho \mathrm{v}\\ \rho \mathrm{w}\\ \rho E\end{bmatrix} \qquad \mathbf{A}=\begin{bmatrix}\rho u\\ \rho u^2+p-\tau_{xx}\\ \rho u\mathrm{v}-\tau_{xy}\\ \rho u\mathrm{w}-\tau_{xz}\\ (\rho E+p)u-u\tau_{xx}-\mathrm{v}\tau_{xy}-w\tau_{xz}+q_x\end{bmatrix}$$

$$\mathbf{B}=\begin{bmatrix}\rho \mathrm{v}\\ \rho \mathrm{v}u-\tau_{yx}\\ \rho \mathrm{v}^2+p-\tau_{yy}\\ \rho \mathrm{v}w-\tau_{yz}\\ (\rho E+p)\mathrm{v}-u\tau_{yx}-\mathrm{v}\tau_{yy}-w\tau_{yz}+q_y\end{bmatrix}$$

$$\mathbf{C}=\begin{bmatrix}\rho w\\ \rho wu-\tau_{zx}\\ \rho \mathrm{v}w-\tau_{zy}\\ \rho w^2+p-\tau_{zz}\\ (\rho E+p)w-u\tau_{zx}-\mathrm{v}\tau_{zy}-w\tau_{zz}+q_z\end{bmatrix}$$

$$\tau_{xx}=\frac{2}{3}\mu\left(2\frac{\partial u}{\partial x}-\frac{\partial \mathrm{v}}{\partial y}-\frac{\partial w}{\partial z}\right), \qquad \tau_{yy}=\frac{2}{3}\mu\left(2\frac{\partial \mathrm{v}}{\partial y}-\frac{\partial u}{\partial x}-\frac{\partial w}{\partial z}\right),$$

$$\tau_{zz}=\frac{2}{3}\mu\left(2\frac{\partial w}{\partial z}-\frac{\partial u}{\partial x}-\frac{\partial \mathrm{v}}{\partial y}\right)$$

$$\tau_{xy}=\mu\left(\frac{\partial u}{\partial y}+\frac{\partial \mathrm{v}}{\partial x}\right)=\tau_{yx}, \qquad \tau_{xz}=\mu\left(\frac{\partial u}{\partial z}+\frac{\partial w}{\partial x}\right)=\tau_{zx}, \qquad \tau_{yz}=\mu\left(\frac{\partial w}{\partial y}+\frac{\partial \mathrm{v}}{\partial z}\right)=\tau_{zy}$$

$$q_x=-k\frac{\partial T}{\partial x}, \qquad q_y=-k\frac{\partial T}{\partial y}, \qquad q_z=-k\frac{\partial T}{\partial z}$$

In terms of a curvilinear coordinate system (ξ, η, ζ) (see Section 4.6), equations (6.3.1) are transformed to

$$\frac{\partial}{\partial t}\left(\frac{\mathbf{U}}{J}\right)+\frac{\partial}{\partial \xi}\left[\frac{1}{J}(\xi_x\mathbf{A}+\xi_y\mathbf{B}+\xi_z\mathbf{C})\right]+\frac{\partial}{\partial \eta}\left[\frac{1}{J}(\eta_x\mathbf{A}+\eta_y\mathbf{B}+\eta_z\mathbf{C})\right]$$
$$+\frac{\partial}{\partial \zeta}\left[\frac{1}{J}(\zeta_x\mathbf{A}+\zeta_y\mathbf{B}+\zeta_z\mathbf{C})\right]=0 \tag{6.3.2}$$

with

$$J = [x_\xi(y_\eta z_\zeta - y_\zeta z_\eta) - x_\eta(y_\xi z_\zeta - y_\zeta z_\xi) - x_\zeta(y_\xi z_\eta - y_\eta z_\xi)]^{-1}$$

$$\xi_x = J(y_\eta z_\zeta - y_\zeta z_\eta), \qquad \xi_y = -J(x_\eta z_\zeta - x_\zeta z_\eta), \qquad \xi_z = J(x_\eta y_\zeta - x_\zeta y_\eta),$$

$$\eta_x = -J(y_\xi z_\zeta - y_\zeta z_\xi), \qquad \eta_y = J(x_\xi z_\zeta - x_\zeta z_\xi), \qquad \eta_z = -J(x_\xi y_\zeta - x_\zeta y_\xi),$$

$$\zeta_x = J(y_\xi z_\eta - y_\eta z_\xi), \qquad \zeta_y = -J(x_\xi z_\eta - x_\eta z_\xi), \qquad \zeta_z = J(x_\xi y_\eta - x_\eta y_\xi)$$

$$\tau_{xx} = \frac{2}{3}\mu[2(\xi_x u_\xi + \eta_x u_\eta + \zeta_x u_\zeta) - (\xi_y v_\xi + \eta_y v_\eta + \zeta_y v_\zeta) - (\xi_z w_\xi + \eta_z w_\eta + \zeta_z w_\zeta)]$$

$$\tau_{yy} = \frac{2}{3}\mu[2(\xi_y v_\xi + \eta_y v_\eta + \zeta_y v_\zeta) - (\xi_x u_\xi + \eta_x u_\eta + \zeta_x u_\zeta) - (\xi_z w_\xi + \eta_z w_\eta + \zeta_z w_\zeta)]$$

$$\tau_{zz} = \frac{2}{3}\mu[2(\xi_z w_\xi + \eta_z w_\eta + \zeta_z w_\zeta) - (\xi_x u_\xi + \eta_x u_\eta + \zeta_x u_\zeta) - (\xi_y v_\xi + \eta_y v_\eta + \zeta_y v_\zeta)]$$

$$\tau_{xy} = \mu(\xi_x u_\xi + \eta_y u_\eta + \zeta_y u_\zeta + \xi_x v_\xi + \eta_x v_\eta + \zeta_x v_\zeta)$$

$$\tau_{xz} = \mu(\xi_z u_\xi + \eta_z u_\eta + \zeta_z u_\zeta + \xi_x w_\xi + \eta_x w_\eta + \zeta_x w_\zeta)$$

$$\tau_{yz} = \mu(\xi_z v_\xi + \eta_y v_\eta + \zeta_y v_\zeta + \xi_y w_\xi + \eta_y w_\eta + \zeta_y w_\zeta)$$

$$q_x = -k(\xi_x T_\xi + \eta_x T_\eta + \zeta_x T_\zeta), \qquad q_x = -k(\xi_x T_\xi + \eta_x T_\eta + \zeta_x T_\zeta),$$

$$q_x = -k(\xi_x T_\xi + \eta_x T_\eta + \zeta_x T_\zeta)$$

Equations (6.3.1) and (6.3.2) are mixed sets of hyperbolic and parabolic equations in time. If the unsteady terms are dropped, then a mixed set of hyperbolic-elliptic system results. As a consequence, the compressible Navier-Stokes system of equations are normally solved in their unsteady form using the time dependent approach, in which the equations are integrated forward in time until either the desired time is reached or a steady-state solution is obtained asymptotically after a sufficient number of time steps. If only the steady-state solution is desired, an implicit finite difference scheme can be used, where fewer iterations are necessary. If time accuracy is required, then a second order accurate explicit scheme may be used with small time increments.

Explicit schemes include the leapfrog/DuFort-Frankel method, Lax-Wendroff method, Runge-Kutta method, MacCormack method, among others. Highlights of the explicit MacCormack scheme [MacCormack, 1969] with predictor and corrector steps are presented below.

Predictor

$$\overline{U_{i,j,k}^{n+1}} = \mathbf{U}_{i,j,k}^n - \frac{\Delta t}{\Delta x}(\mathbf{A}_{i+1,j,k}^n - \mathbf{A}_{i,j,k}^n) - \frac{\Delta t}{\Delta y}(\mathbf{B}_{i,j+1,k}^n - \mathbf{B}_{i,j,k}^n) - \frac{\Delta t}{\Delta z}(\mathbf{C}_{i,j,k+1}^n - \mathbf{C}_{i,j,k}^n) \tag{6.3.3}$$

Corrector

$$\mathbf{U}_{i,j,k}^{n+1} = \frac{1}{2}\Big[\mathbf{U}_{i,j,k}^n + \overline{U_{i,j,k}^{n+1}} - \frac{\Delta t}{\Delta x}(\overline{\mathbf{A}_{i+1,j,k}^{n+1}} - \overline{\mathbf{A}_{i,j,k}^{n+1}}) - \frac{\Delta t}{\Delta y}(\overline{\mathbf{B}_{i,j+1,k}^{n+1}} - \overline{\mathbf{B}_{i,j,k}^{n+1}}) - \frac{\Delta t}{\Delta z}(\overline{\mathbf{C}_{i,j,k+1}^{n+1}} - \overline{\mathbf{C}_{i,j,k}^{n+1}})\Big] \tag{6.3.4}$$

with $x = i\Delta x$, $y = j\Delta y$, $z = k\Delta z$. This explicit scheme is second order accurate in both space and time, and useful for time accurate calculations or problems with low to moderate Reynolds numbers. Although forward differences are used for all spatial derivatives in the predictor step while backward differences are used in the correction step, the forward and backward differencing can be alternated between predictor and corrector steps as well as between the three spatial derivatives in order to eliminate any bias.

Unfortunately, no analytical stability analysis is available to determine limiting time step requirements because of the nonlinear nature of the governing equations, but the following empirical formula [Tannehill, Hoist, and Rakich, 1975] is proposed.

$$\Delta t \leq \frac{\sigma(\Delta t)_{\mathrm{CFL}}}{1 + 2/\mathrm{Re}_{\Delta}} \tag{6.3.5}$$

with $\sigma \cong 0.7 - 0.9$

$$(\Delta t)_{\mathrm{CFL}} \leq \left[\frac{|u|}{\Delta x} + \frac{|v|}{\Delta y} + \frac{|w|}{\Delta z} + a\sqrt{\frac{1}{\Delta x^2} + \frac{1}{\Delta y^2} + \frac{1}{\Delta z^2}} \right]^{-1}$$

$$\mathrm{Re}_{\Delta} = \min(\mathrm{Re}_{\Delta x}, \mathrm{Re}_{\Delta y}, \mathrm{Re}_{\Delta z}) \geq 0$$

$$\mathrm{Re}_{\Delta x} = \frac{\rho|u|\Delta x}{\mu}, \qquad \mathrm{Re}_{\Delta y} = \frac{\rho|v|\Delta y}{\mu}, \qquad \mathrm{Re}_{\Delta z} = \frac{\rho|w|\Delta z}{\mu}$$

It is often necessary to add artificial viscosity using the fourth order derivatives of the form,

$$-\varepsilon(\Delta x_i \Delta x_j \Delta x_k \Delta x_m)\frac{\partial^4 \mathbf{U}}{\partial x_i \partial x_j \partial x_k \partial x_m} \tag{6.3.6}$$

where ε is an experimentally determined parameter.

For high Reynolds number flows (thin viscous layers), the mesh must be refined (small time steps), leading to long computer times. To circumvent this difficulty, implicit methods may be used. We discuss this subject in the following section.

6.3.2 IMPLICIT SCHEMES

Earlier developments of implicit schemes for the Navier-Stokes system of equations include Briley and McDonald [1975], Beam and Warming [1978], and MacCormack [1981], among others. First, let us consider the Navier-Stokes system of equations in the general form

$$\frac{\partial \mathbf{U}}{\partial t} + \frac{\partial \mathbf{F}_i}{\partial x_i} + \frac{\partial \mathbf{G}_i}{\partial x_i} = 0 \tag{6.3.7}$$

Here, it is assumed that the convection and diffusion fluxes are functions of the conservation flow variables $\mathbf{U}$. In addition, the diffusion flux is assumed to be a function of the gradient of conservation flow variables. These functional relations are characterized by the convection Jacobian $\mathbf{a}_i$, diffusion Jacobian $\mathbf{b}_i$, and diffusion gradient Jacobian $\mathbf{c}_{ij}$.

$$\mathbf{a}_i = \frac{\partial \mathbf{F}_i}{\partial \mathbf{U}}, \qquad \mathbf{b}_i = \frac{\partial \mathbf{G}_i}{\partial \mathbf{U}}, \qquad \mathbf{c}_{ij} = \frac{\partial \mathbf{G}_i}{\partial \mathbf{U}_{,j}} \tag{6.3.8}$$

To evaluate the Jacobians, we set new variables $\ell = \rho u$, $m = \rho \mathrm{v}$, $e = \rho E$, and $\mu_R = \lambda + 2\mu$ for two-dimensional flows,

$$\mathbf{U} = \begin{bmatrix} U_1 \\ U_2 \\ U_3 \\ U_4 \end{bmatrix} = \begin{bmatrix} \rho \\ \rho u \\ \rho \mathrm{v} \\ \rho E \end{bmatrix} = \begin{bmatrix} \rho \\ \ell \\ m \\ e \end{bmatrix}$$

$$\mathbf{F}_1 = \begin{bmatrix} F_1^1 \\ F_1^2 \\ F_1^3 \\ F_1^4 \end{bmatrix} = \begin{bmatrix} \rho u \\ p + \rho u^2 \\ \rho u \mathrm{v} \\ \rho E u + p u \end{bmatrix} = \begin{bmatrix} \ell \\ p + \ell^2/\rho \\ \ell m/\rho \\ (p+e)\dfrac{\ell}{\rho} \end{bmatrix}$$

$$\mathbf{F}_2 = \begin{bmatrix} F_2^1 \\ F_2^2 \\ F_2^3 \\ F_2^4 \end{bmatrix} = \begin{bmatrix} \rho \mathrm{v} \\ \rho \mathrm{v} u \\ p + \rho \mathrm{v}^2 \\ \rho E \mathrm{v} + p \mathrm{v} \end{bmatrix} = \begin{bmatrix} m \\ \ell m/\rho \\ p + m^2/\rho \\ (p+e)\dfrac{m}{\rho} \end{bmatrix}$$

where

$$p = (\gamma - 1)\rho\left(E - \frac{1}{2}\mathrm{v}_j \mathrm{v}_j\right) = (\gamma - 1)\rho\left[E - \frac{1}{2}(u^2 + \mathrm{v}^2)\right] = (\gamma - 1)\left[e - \frac{1}{2\rho}(\ell^2 + m^2)\right]$$

$$T = \frac{1}{c_v}\left(E - \frac{1}{2}\mathrm{v}_j \mathrm{v}_j\right) = \frac{1}{c_v}\left[E - \frac{1}{2}(u^2 + \mathrm{v}^2)\right] = \frac{1}{\rho c_v}\left[e - \frac{1}{2\rho}(\ell^2 + m^2)\right]$$

The convective Jacobian $\mathbf{a}_i$ can be evaluated as

$$\mathbf{a}_1 = \frac{\partial \mathbf{F}_1}{\partial \mathbf{U}} = \begin{bmatrix} \dfrac{\partial F_1^1}{\partial U_1} & \dfrac{\partial F_1^1}{\partial U_2} & \dfrac{\partial F_1^1}{\partial U_3} & \dfrac{\partial F_1^1}{\partial U_4} \\ \dfrac{\partial F_1^2}{\partial U_1} & \dfrac{\partial F_1^2}{\partial U_2} & \dfrac{\partial F_1^2}{\partial U_3} & \dfrac{\partial F_1^2}{\partial U_4} \\ \dfrac{\partial F_1^3}{\partial U_1} & \dfrac{\partial F_1^3}{\partial U_2} & \dfrac{\partial F_1^3}{\partial U_3} & \dfrac{\partial F_1^3}{\partial U_4} \\ \dfrac{\partial F_1^4}{\partial U_1} & \dfrac{\partial F_1^4}{\partial U_2} & \dfrac{\partial F_1^4}{\partial U_3} & \dfrac{\partial F_1^4}{\partial U_4} \end{bmatrix}$$

$$\mathbf{a}_1 = \frac{\partial \mathbf{F}_1}{\partial \mathbf{U}} = \begin{bmatrix} 0 & 1 & 0 & 0 \\ \dfrac{\gamma - 3}{2}u^2 + \dfrac{\gamma - 1}{2}\mathrm{v}^2 & (3 - \gamma)u & -(\gamma - 1)\mathrm{v} & \gamma - 1 \\ -u\mathrm{v} & \mathrm{v} & u & 0 \\ -\dfrac{\gamma e u}{\rho} + (\gamma - 1)u(u^2 + \mathrm{v}^2) & \dfrac{\gamma e}{\rho} + \dfrac{1 - \gamma}{2}(3u^2 + \mathrm{v}^2) & (1 - \gamma)u\mathrm{v} & \gamma u \end{bmatrix}$$

$$\mathbf{a}_2 = \frac{\partial \mathbf{F}_2}{\partial \mathbf{U}} = \begin{bmatrix} 0 & 0 & 1 & 0 \\ -u\mathrm{v} & \mathrm{v} & u & 0 \\ \frac{\gamma-3}{2}\mathrm{v}^2 + \frac{\gamma-1}{2}u^2 & -(\gamma-1)u & (3-\gamma)\mathrm{v} & \gamma-1 \\ -\frac{\gamma e \mathrm{v}}{\rho} + (\gamma-1)\mathrm{v}(u^2+\mathrm{v}^2) & (1-\gamma)u\mathrm{v} & \frac{\gamma e}{\rho} + \frac{1-\gamma}{2}(3\mathrm{v}^2+u^2) & \gamma\mathrm{v} \end{bmatrix} \tag{6.3.9a}$$

Similarly, the diffusion terms with their Jacobians are of the form

$$\mathbf{G}_1 = \begin{bmatrix} G_1^1 \\ G_1^2 \\ G_1^3 \\ G_1^4 \end{bmatrix} = -\begin{bmatrix} 0 \\ \tau_{11} \\ \tau_{12} \\ \tau_{11}u + \tau_{12}\mathrm{v} - q_1 \end{bmatrix} \quad \mathbf{G}_2 = \begin{bmatrix} G_2^1 \\ G_2^2 \\ G_2^3 \\ G_2^4 \end{bmatrix} = -\begin{bmatrix} 0 \\ \tau_{21} \\ \tau_{22} \\ \tau_{21}u + \tau_{22}\mathrm{v} - q_2 \end{bmatrix}$$

$$\mathbf{b}^1 = \frac{\partial \mathbf{G}_1}{\partial \mathbf{U}} = \begin{bmatrix} 0 & 0 & 0 & 0 \\ b_{21}^1 & b_{22}^1 & b_{23}^1 & 0 \\ b_{31}^1 & b_{32}^1 & b_{33}^1 & 0 \\ b_{41}^1 & b_{42}^1 & b_{43}^1 & b_{44}^1 \end{bmatrix} \quad \mathbf{b}_2 = \frac{\partial \mathbf{G}_2}{\partial \mathbf{U}} = \begin{bmatrix} 0 & 0 & 0 & 0 \\ b_{21}^2 & b_{22}^2 & b_{23}^2 & 0 \\ b_{31}^2 & b_{32}^2 & b_{33}^2 & 0 \\ b_{41}^2 & b_{42}^2 & b_{43}^2 & b_{44}^2 \end{bmatrix} \tag{6.3.9b}$$

with $m_1 = \rho u, m_2 = \rho \mathrm{v}$

$$b_{21}^1 = -\frac{1}{\rho^2}\left(-\mu_R m_{1,1} - \lambda m_{2,2} + 2\mu_R \frac{m_1 \rho_{,1}}{\rho} + 2\lambda \frac{m_2 \rho_{,2}}{\rho}\right) \quad b_{22}^1 = \frac{\mu_R}{\rho^2}\rho_{,1} \quad b_{23}^1 = \frac{\lambda}{\rho^2}\rho_{,2}$$

$$b_{31}^1 = -\frac{\mu}{\rho^2}\left(-m_{2,1} - m_{1,2} + 2\frac{m_1 \rho_{,2}}{\rho} + 2\frac{m_2 \rho_{,1}}{\rho}\right) \qquad b_{32}^1 = \frac{\mu}{\rho^2}\rho_{,2} \quad b_{33}^1 = \frac{\mu}{\rho^2}\rho_{,1}$$

$$b_{41}^1 = u b_{21}^1 + \mathrm{v} b_{31}^1 - \frac{1}{\rho^2}(m_1\tau_{11} + m_2\tau_{12}) + \frac{k}{\rho^2 c_v}[-(\rho E)_{,1} + 2u m_{1,1} + 2\mathrm{v} m_{2,1} + (2E - 3u^2 - 3\mathrm{v}^2)\rho_{,1}]$$

$$b_{42}^1 = -\frac{\tau_{11}}{\rho} + u b_{22}^1 + \mathrm{v} b_{32}^1 + \frac{k}{\rho^2 c_v}[-m_{1,1} + 2u\rho_{,1}]$$

$$b_{43}^1 = -\frac{\tau_{12}}{\rho} + u b_{23}^1 + \mathrm{v} b_{33}^1 - \frac{k}{\rho^2 c_v}[-m_{2,1} + 2\mathrm{v}\rho_{,1}] b_{44}^1 - \frac{k}{\rho^2 c_v}\rho_{,1}$$

$$b_{21}^2 = b_{31}^1, \quad b_{22}^2 = b_{32}^1, \quad b_{23}^2 = b_{33}^1, \quad b_{31}^2 = \frac{1}{\rho^2}(\lambda m_{1,1} + \mu_R m_{2,2} + \mu_R u\rho_{,1} - \mu_R \mathrm{v}\rho_{,2}),$$

$$b_{32}^2 = \frac{\lambda}{\rho^2}\rho_{,1}, \quad b_{33}^2 = \frac{\mu_R}{\rho^2}\rho_{,2}$$

$$b_{41}^2 = u b_{21}^2 + \mathrm{v} b_{31}^2 + \frac{1}{\rho^2}(m_1\tau_{12} + m_2\tau_{22}) - \frac{k}{\rho^2 c_v}[-(\rho E)_{,2} + 2u m_{1,2} + 2\mathrm{v} m_{2,2} + (2E - 3u^2 - 3\mathrm{v}^2)\rho_{,2}],$$

$$b_{42}^2 = -\frac{\tau_{12}}{\rho} + ub_{22}^2 - \mathrm{v}b_{32}^2 + \frac{k}{\rho^2 c_v}[-m_{1,2} + 2u\rho_{,2}],$$
$$b_{43}^2 = -\frac{\tau_{22}}{\rho} + ub_{23}^2 + \mathrm{v}b_{33}^2 - \frac{k}{\rho^2 c_v}[-m_{2,2} + 2\mathrm{v}\rho_{,2}], \quad b_{44}^2 = \frac{k}{\rho^2 c_v}\rho_{,2}$$

The diffusion gradient Jacobians are evaluated as

$$\mathbf{c}_{11} = \frac{\partial \mathbf{G}_1}{\partial \mathbf{U}_{,1}} = -\begin{bmatrix} 0 & 0 & 0 & 0 \\ c_{21}^{11} & c_{22}^{11} & 0 & 0 \\ c_{31}^{11} & 0 & c_{33}^{11} & 0 \\ c_{41}^{11} & c_{42}^{11} & c_{43}^{11} & c_{44}^{11} \end{bmatrix} \qquad \mathbf{c}_{12} = \frac{\partial \mathbf{G}_1}{\partial \mathbf{U}_{,2}} = -\begin{bmatrix} 0 & 0 & 0 & 0 \\ c_{21}^{12} & 0 & c_{23}^{12} & 0 \\ c_{31}^{13} & c_{32}^{12} & 0 & 0 \\ c_{41}^{12} & c_{42}^{12} & c_{43}^{12} & 0 \end{bmatrix}$$
$$\mathbf{c}_{21} = \frac{\partial \mathbf{G}_2}{\partial \mathbf{U}_{,1}} = -\begin{bmatrix} 0 & 0 & 0 & 0 \\ c_{21}^{21} & 0 & c_{23}^{21} & 0 \\ c_{31}^{21} & c_{32}^{21} & 0 & 0 \\ c_{41}^{21} & c_{42}^{21} & c_{43}^{21} & 0 \end{bmatrix} \qquad \mathbf{c}_{22} = \frac{\partial \mathbf{G}_2}{\partial \mathbf{U}_{,2}} = -\begin{bmatrix} 0 & 0 & 0 & 0 \\ c_{22}^{22} & c_{22}^{22} & 0 & 0 \\ c_{31}^{22} & 0 & c_{33}^{22} & 0 \\ c_{41}^{22} & c_{42}^{22} & c_{43}^{22} & c_{44}^{22} \end{bmatrix} \tag{6.3.9c}$$

with

$$c_{21}^{11} = -(2\mu + \lambda)\frac{m_1}{\rho^2}, \quad c_{22}^{11} = (2\mu + \lambda)\frac{1}{\rho}, \quad c_{31}^{11} = -\mu\frac{m_2}{\rho^2}, \quad c_{33}^{11} = \frac{\mu}{\rho},$$
$$c_{41}^{11} = -(2\mu + \lambda)\frac{m_1^2}{\rho^3} - \mu\frac{m_2^2}{\rho^3} + \frac{k}{c_v}\left(-\frac{e}{\rho^2} + \frac{m_1^2 + m_2^2}{\rho^3}\right),$$
$$c_{42}^{11} = \left(2\mu + \lambda - \frac{k}{c_v}\right)\frac{m_1}{\rho^2}, \quad c_{43}^{11} = \left(\mu - \frac{k}{c_v}\right)\frac{m_2}{\rho^2}, \quad c_{44}^{11} = \frac{k}{c_v}\frac{1}{\rho},$$
$$c_{21}^{12} = -\lambda\frac{m_2}{\rho^2}, \quad c_{23}^{12} = \frac{\lambda}{\rho}, \quad c_{31}^{12} = -\mu\frac{m_1}{\rho^2}, \quad c_{32}^{12} = \frac{\mu}{\rho},$$
$$c_{41}^{12} = -(\mu + \lambda)\frac{m_1 m_2}{\rho^3}, \quad c_{42}^{12} = \mu\frac{m_2}{\rho^2}, \quad c_{43}^{12} = \lambda\frac{m_1}{\rho^2},$$
$$c_{21}^{21} = -\mu\frac{m_2}{\rho^2}, \quad c_{23}^{21} = \frac{\mu}{\rho}, \quad c_{31}^{21} = -\lambda\frac{m_1}{\rho^2}, \quad c_{32}^{21} = \frac{\lambda}{\rho}$$
$$c_{41}^{21} = -(\mu + \lambda)\frac{m_1 m_2}{\rho^3}, \quad c_{42}^{21} = \lambda\frac{m_2}{\rho^2}, \quad c_{43}^{21} = \mu\frac{m_1}{\rho^2},$$
$$c_{21}^{22} = -\mu\frac{m_1}{\rho^2}, \quad c_{22}^{22} = \frac{\mu}{\rho}, \quad c_{31}^{22} = -(2\mu + \lambda)\frac{m_2}{\rho^2}, \quad c_{33}^{22} = (2\mu + \lambda)\frac{1}{\rho},$$
$$c_{41}^{22} = -(2\mu + \lambda)\frac{m_2^2}{\rho^3} - \mu\frac{m_1^2}{\rho^3} + \frac{k}{c_v}\left(-\frac{e}{\rho^2} + \frac{m_1^2 + m_2^2}{\rho^3}\right),$$
$$c_{42}^{22} = \left(\mu - \frac{k}{c_v}\right)\frac{m_1}{\rho^2}, \quad c_{43}^{22} = \left(2\mu + \lambda - \frac{k}{c_v}\right)\frac{m_2}{\rho^2}, \quad c_{44}^{22} = \frac{k}{c_v}\frac{1}{\rho}$$

An extension to three-dimensional flux Jacobians follows the similar procedure. The 3-D convection, diffusion, and diffusion gradient flux Jacobians are presented in Appendix A.

A typical implicit scheme may be constructed by linearizing the convection flux, diffusion flux, and diffusion gradient as follows:

$$\mathbf{F}_i^{n+1} = \mathbf{F}_i^n + \frac{\partial \mathbf{F}_i^n}{\partial \mathbf{U}} \Delta \mathbf{U}^{n+1} = \mathbf{F}_i^n + \mathbf{a}_i^n \Delta \mathbf{U}^{n+1} \tag{6.3.10a}$$

$$\mathbf{G}_i^{n+1} = \mathbf{G}_i^n + \frac{\partial \mathbf{G}_i^n}{\partial \mathbf{U}} \Delta \mathbf{U}^{n+1} + \frac{\partial \mathbf{G}_i^n}{\partial \mathbf{U}_{,j}} \Delta \mathbf{U}_{,j}^{n+1} = \mathbf{G}_i^n + \mathbf{b}_i^n \Delta \mathbf{U}^{n+1} + \mathbf{c}_{ij}^n \Delta \mathbf{U}_{,j}^{n+1} \tag{6.3.10b}$$

An unsteady implicit scheme for (6.3.7) can be represented as an average of the flowfield between the current and previous time steps,

$$\frac{\Delta \mathbf{U}^{n+1}}{\Delta t} = -\frac{1}{2}\left[\left(\frac{\partial \mathbf{F}_i}{\partial x_i} + \frac{\partial \mathbf{G}_i}{\partial x_i}\right)^n + \left(\frac{\partial \mathbf{F}_i}{\partial x_i} + \frac{\partial \mathbf{G}_i}{\partial x_i}\right)^{n+1}\right] \tag{6.3.11}$$

Substituting (6.3.10) into (6.3.11) and using the relation,

$$\mathbf{c}_{ij} \Delta \mathbf{U}_{,j} = (\mathbf{c}_{ij} \Delta \mathbf{U})_{,j} - \mathbf{c}_{ij,j} \Delta \mathbf{U} \tag{6.3.12}$$

it follows that

$$\left\{\mathbf{I} + \frac{\Delta t}{2}\left[\frac{\partial}{\partial x_i}(\mathbf{a}_i + \mathbf{b}_i - \mathbf{c}_{ij,j}) + \frac{\partial^2 \mathbf{c}_{ij}}{\partial x_i \partial x_j}\right]^n\right\} \Delta \mathbf{U}^{n+1} = -\frac{\Delta t}{2}\left(\frac{\partial \mathbf{F}_i}{\partial x_i} + \frac{\partial \mathbf{G}_i}{\partial x_i}\right)^n \tag{6.3.13}$$

Although (6.3.13) can be used for general applications, it may be modified specifically for ADI procedure, leading to the so-called Beam-Warming scheme [Beam and Warming, 1978], described below.

For simplicity of notation, let the Navier-Stokes system of equations be written as

$$\frac{\partial \mathbf{U}}{\partial t} = \mathbf{W}, \qquad \mathbf{W} = -\frac{\partial \mathbf{F}_i}{\partial x_i} - \frac{\partial \mathbf{G}_i}{\partial x_i}$$

The Beam-Warming implicit method begins with an introduction of implicitness parameters ξ and θ such that

$$\frac{1}{\Delta t}\left[(1+\xi)\Delta \mathbf{U}^{n+1} - \xi \Delta \mathbf{U}^n\right] = \theta \mathbf{W}^{n+1} + (1-\theta)\mathbf{W}^n \tag{6.3.14a}$$

with $0 \le (\xi, \theta) \le 1$, $\Delta \mathbf{U}^{n+1} = \mathbf{U}^{n+1} - \mathbf{U}^n$, and $\Delta \mathbf{U}^n = \mathbf{U}^n - \mathbf{U}^{n-1}$. Equivalently, we may write (6.3.14a) in the form,

$$\Delta \mathbf{U}^{n+1} = \frac{\Delta t}{1+\xi}\left[\frac{\partial}{\partial t}(\theta \Delta \mathbf{U}^{n+1} + \mathbf{U}^n) + \xi \frac{\Delta \mathbf{U}^n}{\Delta t}\right] \tag{6.3.14b}$$

Using the linearization procedure of (6.3.10) in (6.3.14), we obtain

$$\begin{aligned}\frac{1}{\Delta t}\left[(1+\xi)\Delta \mathbf{U}^{n+1} - \xi \Delta \mathbf{U}^n\right] = &-\theta\left[\frac{\partial}{\partial x_i}(\mathbf{a}_i \Delta \mathbf{U} + \mathbf{b}_i \Delta \mathbf{U} + \mathbf{c}_{ij} \Delta \mathbf{U}_{,j})\right]^{n+1} \\ &- \left[\frac{\partial}{\partial x_i}(\mathbf{F}_i + \mathbf{G}_i)\right]^n\end{aligned}$$

or

$$\begin{aligned}&\left\{\mathbf{I} + \frac{\theta \Delta t}{1+\xi}\left[\frac{\partial}{\partial x_i}(\mathbf{a}_i + \mathbf{b}_i - \mathbf{c}_{ij,j}) + \frac{\partial^2 \mathbf{c}_{ij}}{\partial x_i \partial x_j}\right]^n\right\} \Delta \mathbf{U}^{n+1} \\ &\quad = \frac{\xi}{1+\xi} \Delta \mathbf{U}^n - \frac{\Delta t}{1+\xi}\left(\frac{\partial \mathbf{F}_i}{\partial x_i} + \frac{\partial \mathbf{G}_i}{\partial x_i}\right)^n\end{aligned} \tag{6.3.15}$$

At this point, we anticipate difficulties handling the cross derivatives of the viscosity terms in the ADI procedure. Therefore, the diffusion flux terms are separated into two parts: normal derivatives and cross derivatives so that the differentiation of the diffusion gradient Jacobians is performed only for normal derivatives, whereas the cross derivative Jacobians on the left-hand side are excluded from the $(n+1)$th step in (6.3.15). Furthermore, the θ terms on the right-hand side are to retain only the cross derivatives (shear stresses) and allowed to lag to the n-1 step explicitly. With these arrangements, (6.3.15) is rewritten as

$$\left\{\mathbf{I}+\frac{\theta\Delta t}{1+\xi}\left[\frac{\partial}{\partial x_i}(\mathbf{a}_i+\mathbf{b}_i-\mathbf{c}_{ij,j})+\frac{\partial^2\mathbf{c}_{ij}}{\partial x_i\partial x_j}\right]^n\right\}\Delta\mathbf{U}^{n+1}$$
$$=\frac{\xi}{1+\xi}\Delta\mathbf{U}^n-\frac{\Delta t}{1+\xi}\left(\frac{\partial\mathbf{F}_i}{\partial x_i}+\frac{\partial\mathbf{G}_i}{\partial x_i}\right)^n+\frac{\Delta t\theta}{1+\xi}\frac{\partial\mathbf{G}_{(i)}^{n-1}}{\partial x_{(j)}} \tag{6.3.16}$$

with $(i)\neq(j)$. Here, it should be noted that in Beam and Warming [1978] the cross derivative terms alone become associated with the implicitness parameter θ at the $(n-1)$ step. This will allow (6.3.16) to be solved in two steps in the spirit of ADI with a block tridiagonal form. In step 1, set $i=1$ and $j=1,2$ in the x-direction with only the normal derivative Jacobians ($\mathbf{c}_{11}$ of $\mathbf{c}_{ij}$) retained on the left-hand side. Step 2 is to set $i=2$ and $j=1,2$ with only $\mathbf{c}_{22}$ being involved in the y-direction on the left-hand side and place the solution obtained in step 1 on the right-hand side to determine the final solution. In this process, the diffusion gradient Jacobian components, $\boldsymbol{c}_{12}$ and $\boldsymbol{c}_{21}$ are never used, contrary to the general case of (6.3.14). Expansion of (6.3.16) as described above leads to the following expressions.

$$\left\{\mathbf{I}+\frac{\theta\Delta t}{1+\xi}\left[\frac{\partial}{\partial x}(\mathbf{a}_1+\mathbf{b}_1-\mathbf{c}_{11.1})+\frac{\partial^2\mathbf{c}_{11}}{\partial x^2}+\frac{\partial}{\partial y}(\mathbf{a}_2+\mathbf{b}_2-\mathbf{c}_{22.2})+\frac{\partial^2\mathbf{c}_{22}}{\partial y^2}\right]^n\right\}\Delta\mathbf{U}^{n+1}$$
$$=\mathrm{RHS} \tag{6.3.17}$$
$$\mathrm{RHS}=\frac{\xi}{1+\xi}\Delta\mathbf{U}^n-\frac{\Delta t}{1+\xi}\mathbf{W}^n+\frac{\theta\Delta t}{1+\xi}\left[\frac{\partial\tau_{xy}}{\partial x}+\frac{\partial\tau_{yx}}{\partial y}\right]^n$$
$$+O\left[\left(\theta-\frac{1}{2}-\xi\right)\Delta t^2,\Delta t^3\right]$$

with

$$\mathbf{b}_1-\mathbf{c}_{11.1}=\frac{1}{\rho}\begin{bmatrix}0 & 0 & 0 & 0\\ -u\left(\frac{4}{3}\mu\right)_x & \left(\frac{4}{3}\mu\right)_x & 0 & 0\\ -\mathrm{v}\mu_x & 0 & \mu_x & 0\\ -u^2\left(\frac{4}{3}\mu\right)_x-\mathrm{v}^2\mu_x & u\left(\frac{4}{3}\mu\right)_x & \mathrm{v}\mu_x & 0\end{bmatrix} \tag{6.3.18a}$$

$$\mathbf{b}_2-\mathbf{c}_{22.2}=\frac{1}{\rho}\begin{bmatrix}0 & 0 & 0 & 0\\ -u\mu_x & \mu_y & 0 & 0\\ -\mathrm{v}\left(\frac{4}{3}\mu\right)_y & 0 & \left(\frac{4}{3}\mu\right)_y & 0\\ -\mathrm{v}^2\left(\frac{4}{3}\mu\right)_y-u^2\mu_y & u\mu_y & \mathrm{v}\frac{4}{3}\mu_y & 0\end{bmatrix} \tag{6.3.18b}$$

The solution of (6.3.17) is carried out in the manner of an ADI scheme as follows:

Step 1

$$\left\{\mathbf{I}+\frac{\theta\Delta t}{1+\xi}\left[\frac{\partial}{\partial x}(\mathbf{a}_1+\mathbf{b}_1-\mathbf{c}_{11.1})+\frac{\partial^2\mathbf{c}_{11}}{\partial x^2}\right]^n\right\}\Delta\mathbf{U}^*=\text{RHS} \tag{6.3.19a}$$

Step 2

$$\left\{\mathbf{I}+\frac{\theta\Delta t}{1+\xi}\left[\frac{\partial}{\partial y}(\mathbf{a}_2+\mathbf{b}_2-\mathbf{c}_{22.2})+\frac{\partial^2\mathbf{c}_{22}}{\partial y^2}\right]^n\right\}\Delta\mathbf{U}^{n+1}=\Delta\mathbf{U}^* \tag{6.3.19b}$$

where it should be noted that the substitution of (6.3.19b) into (6.3.19a) is equivalent to (6.3.17), but with additional higher order terms which may be neglected. This approach is known as the approximate factorization [Beam and Warming, 1978].

For assurance of convergence, an explicit artificial viscosity of fourth order derivatives (6.3.6) may be added to the right-hand side of (6.3.19a). Furthermore, implicit second order derivative artificial viscosities may be added to the left-hand side of both (6.3.19a) and (6.3.19b) in the x- and y-directions, respectively. The stability analysis by Beam and Warming [1978] shows that $\xi \geq 0.385$ and $\theta = 1/2 + \xi$, leading to $0.639 \leq \frac{\theta}{1+\xi} \leq 0.75$.

The Beam-Warming scheme has been used successfully and many improvements have been reported for the last two decades. An important question still remains. That is, dominance of implicitness or excessive artificial dissipation enforced uniformly everywhere in the flow domain must be adjusted according to the actual local flow physics such as inviscid-viscous interactions, transition to turbulence, shock wave boundary layer interactions, etc. This subject will be presented in the flowfield-dependent variation (FDV) methods in Section 6.5.

6.3.3 PISO SCHEME FOR COMPRESSIBLE FLOWS

Recall that in Section 5.3.2 we discussed the PISO scheme for incompressible flows. We demonstrate here that a similar procedure may be followed for compressible flows except that an additional corrector stage must be incorporated because the coupling between the momentum, energy, and pressure (continuity) equations involves the density and temperature [Issa, Gosman, and Watkins, 1986].

We begin with the continuity, momentum, and energy equations using the notations given in Section 5.3.2.

$$\frac{1}{\Delta t}(\rho^{n+1}-\rho^n)+(\rho \mathrm{v}_i)^{n+1}_{,i}=0 \tag{6.3.20a}$$

$$\frac{1}{\Delta t}\left[(\rho \mathrm{v}_j)^{n+1}-(\rho \mathrm{v}_j)^n\right]=-S^{n+1}_{ij,i}-p^{n+1}_{,j} \tag{6.3.20b}$$

$$\frac{1}{\Delta t}\left[(\rho E)^{n+1}-(\rho E)^n\right]+(\rho E \mathrm{v}_i)^{n+1}_{,i}=-(p\mathrm{v}_i)^{n+1}_{,i}-(\tau_{ij}\mathrm{v}_i)^{n+1}_{,j} \tag{6.3.20c}$$

The predictor and corrector steps are as follows:

(a) Momentum Predictor

$$\left(\frac{\delta_{ij}}{\Delta t}+\frac{A_{ji}^{(D)}}{\rho^n}\right)(\rho^n v_i^*)=-S_{ij,i}^{*(N)}-p_{,j}^n+\frac{\rho^n v_j^n}{\Delta t} \tag{6.3.21}$$

(b) Momentum Corrector I

$$\left(\frac{\delta_{ij}}{\Delta t}+\frac{A_{ji}^{(D)}}{\rho^n}\right)(\rho^* v_i^{**})=-S_{ij,i}^{*(N)}-p_{,j}^*+\frac{\rho^n v_j^n}{\Delta t} \tag{6.3.22}$$

Subtracting (6.3.22) from (6.3.21) gives

$$\rho^* v_j^{**}-\rho^n v_j^*=-\left(\frac{\delta_{ij}}{\Delta t}+\frac{A_{ji}^{(D)}}{\rho^n}\right)^{-1}(p^*-p^n)_{,i} \tag{6.3.23}$$

Writing (6.3.20a) in the form

$$(\rho^* v_i^{**})_{,i}=-\frac{1}{\Delta t}(\rho^*-\rho^n) \tag{6.3.24}$$

Differentiating (6.3.23) and using (6.3.24) we obtain

$$\left[\left(\frac{\delta_{ij}}{\Delta t}+\frac{A_{ji}^{(D)}}{\rho^n}\right)^{-1}(p^*-p^n)_{,i}\right]_{,j}=(\rho^n v_j^*)_{,j}+\frac{1}{\Delta t}(\rho^*-\rho^n) \tag{6.3.25}$$

Introducing the equation of state in the form

$$\rho^*=p^*\phi(p^n,T^n) \tag{6.3.26}$$

it is seen that (6.3.25) combined with (6.3.24) leads to

$$\left[\left(\frac{\delta_{ij}}{\Delta t}+\frac{A_{ji}^{(D)}}{\rho^n}\right)^{-1}(p^*-p^n)_{,i}\right]_{,j}-\frac{\phi(p^n,T^n)}{\Delta t}(p^*-p^n)=(\rho^n v_j^*)_{,j} \tag{6.3.27}$$

from which p^*, ρ^*, and v_j^{**} can be solved.

(c) Energy Predictor

$$\left(\frac{1}{\Delta t}+\frac{B^{(D)}}{\rho^*}\right)(\rho^* E^*)=-(\rho E v_i)_{,i}^{*(N)}-(p^* v_i^{**})_{,i}+(\tau_{ij} v_i^{**})_i+\frac{\rho^n E^n}{\Delta t} \tag{6.3.28}$$

with $B^{(D)}$ being the diagonal components of the convective terms.

(d) Momentum Corrector II

$$\left(\frac{\delta_{ij}}{\Delta t}+\frac{A_{ji}^{(D)}}{\rho^*}\right)(\rho^{**} v_i^{***})=-S_{ij,i}^{**(N)}-p_{,j}^{**}+\frac{\rho^n v_j^n}{\Delta t} \tag{6.3.29}$$

$$(\rho^{**} v_i^{***})_{,i}=-\frac{1}{\Delta t}(\rho^{**}-\rho^n) \tag{6.3.30}$$

$$\left[\left(\frac{\delta_{ij}}{\Delta t}+\frac{A_{ji}^{(D)}}{\rho^*}\right)^{-1}(p^{**}-p^*)_{,i}\right]_{,j}-\frac{\phi(p^*,T^*)}{\Delta t}(\rho^{**},v_i^{***})(p^{**}-p^*)$$
$$=\left[\left(\frac{\delta_{ij}}{\Delta t}+\frac{A_{ji}^{(D)}}{\rho^*}\right)^{-1}(S_{ki,k}^{**(N)}-S_{ki,k}^{*(N)})-A_{ji}\left(\frac{\rho^*-\rho^n}{\rho^n}\right)v_i^{**}\right]_{,j}$$
$$+\frac{p^*}{\Delta t}[\phi(p^n,T^n)-\phi(p^n,T^n)] \tag{6.3.31}$$

with

$$\rho^{**}=p^{**}\phi(p^*,T^*) \tag{6.3.32}$$

Now (6.3.31) can be solved for p^{**}, whereas ρ^{**} and v_i^{***} are calculated from Eqs. (6.3.32) and (6.3.30), respectively,

(e) Energy Corrector

The energy equation is updated in the form

$$\left(\frac{1}{\Delta t}+\frac{B^{(D)}}{\rho^{**}}\right)(\rho^{**}E^{**})=-(\rho Ev_i)_{,i}^{**(N)}-(p^{**}v_i^{***})_{,i}+(\tau_{ij}v_j^{***})_{,i}+\frac{\rho^nE^n}{\Delta t} \tag{6.3.33}$$

from which E^{**}, v_i^{***}, and T^{**} are evaluated.

(f) Momentum Corrector III

This is the final step for all variables:

Momentum Equation

$$\left(\frac{\delta_{ij}}{\Delta t}-\frac{A_{ji}^{(D)}}{\rho^{**}}\right)(\rho^{***}v_i^{****})=-S_{ij,i}^{***(N)}-p_{,j}^{***}+\frac{\rho^nv_j^n}{\Delta t} \tag{6.3.34}$$

Continuity Equation

$$(\rho^{***}v_i^{****})=-\frac{1}{\Delta t}(\rho^{***}-\rho^n) \tag{6.3.35}$$

Pressure Equation

$$\left[\left(\frac{\delta_{ij}}{\Delta t}+\frac{A_{ji}^{(D)}}{\rho^{**}}\right)^{-1}(p^{***}-p^{**})_{,i}\right]_{,j}-\frac{\phi(p^{**},T^{**})}{\Delta t}(p^{***}-p^{**})$$
$$=\left[\left(\frac{\delta_{ij}}{\Delta t}+\frac{A_{ji}^{(D)}}{\rho^{**}}\right)^{-1}(S_{ki,k}^{***(N)}-S_{ki,k}^{**(N)})-A_{ji}\left(\frac{\rho^{**}-\rho^n}{\rho^n}\right)v_i^{***}\right]_{,j}$$
$$+\frac{p^{**}}{\Delta t}[\phi(p^{**},T^{**})-\phi(p^n,T^n)] \tag{6.3.36}$$

with

$$\rho^{***}=p^{***}\phi(p^{**},T^{**}) \tag{6.3.37}$$

It is seen that p^{***} can be solved from (6.3.36) with ρ^{***} and v_i^{***} determined from (6.3.37) and (6.3.34).

6.4 PRECONDITIONING PROCESS FOR COMPRESSIBLE AND INCOMPRESSIBLE FLOWS

6.4.1 GENERAL

For the analysis of compressible flows, it is possible that some regions of the flow domain such as in the boundary layers have low speeds and thus are incompressible. As a result, the density-based formulations in terms of conservation variables may suffer extremely slow or nonconvergence of the solution. This is due to an ill-conditioned system of algebraic equations contributed by the stiff eigenvalues of convection terms. The reason for this is that the acoustic speed is so much higher than the flow velocity in incompressible flows. This phenomenon then appears to be numerical, but it is important to realize that actually physical aspects of the fluid flows precipitate such numerical disorder. For example, transitions and interactions between inviscid/viscous flows induce physical disturbances or instabilities, which may then contribute to transitions and interactions between laminar and turbulent flows and/or compressible and incompressible flows. We address the subjects of transitions and interactions between different properties of fluid flows in Section 6.5 on flowfield-dependent variation (FDV) methods. In this section, our discussion will be limited strictly to the numerical aspect of the transition from the compressible flow to incompressible flow or vice versa. Our objective is to begin with the density-based formulation and subsequently by providing the preconditioning matrix to the time-dependent terms we improve the convection eigenvalues for low Mach number or incompressible flows.

The numerical difficulties of the density-based formulation dealing with low Mach number flows or incompressible flows have been addressed by a number of investigators [Peyret and Vivian, 1985; Choi and Merkle, 1993; Pletcher and Chen, 1993; Merkle et al., l998], among others. In this vein, we construct Jacobian matrices transforming the conservation variables into the primitive variables such that

$$\frac{\partial \mathbf{U}}{\partial t} + \frac{\partial \mathbf{F}_i}{\partial x_i} + \frac{\partial \mathbf{G}_i}{\partial x_i} = 0 \tag{6.4.1}$$

$$\mathbf{A}\frac{\partial \mathbf{Q}}{\partial t} + \mathbf{B}_i \frac{\partial \mathbf{Q}}{\partial x_i} + \mathbf{C}_i \frac{\partial \mathbf{Q}}{\partial x_i} + \mathbf{C}_{ij} \frac{\partial^2 \mathbf{Q}}{\partial x_i \partial x_i} = 0 \tag{6.4.2}$$

where $\mathbf{Q}$ is the primitive variables, $\mathbf{Q} = [\rho, u, v, w, T]^T$, and $\mathbf{A}$ is the time Jacobian.

$$\mathbf{A} = \frac{\partial \mathbf{U}}{\partial \mathbf{Q}} = \begin{bmatrix} \rho\beta_T & 0 & 0 & 0 & -\rho\alpha_p \\ \rho\beta_T u & \rho & 0 & 0 & -\rho\alpha_p u \\ \rho\beta_T v & 0 & \rho & 0 & -\rho\alpha_p v \\ \rho\beta_T w & 0 & 0 & \rho & -\rho\alpha_p w \\ e_1^p & \rho u & \rho v & \rho w & e_4^p \end{bmatrix} \tag{6.4.3}$$

with

$$\beta_T = \frac{1}{\rho}\left(\frac{\partial \rho}{\partial p}\right)_T, \qquad \alpha_p = -\frac{1}{\rho}\left(\frac{\partial \rho}{\partial T}\right)_p \tag{6.4.4}$$

$$e_1^p = \rho\beta_T E_1 - \alpha_p T, \qquad e_4^p = -\rho\alpha_p E_1 + \rho c_p \tag{6.4.5}$$

$$E_1 = H + K = c_p T + \frac{1}{2} v_i v_i \tag{6.4.6}$$

Here, the convection eigenvalues can be examined from

$$|\mathbf{A}^{-1}\mathbf{B}_i - \lambda_i \mathbf{I}| = 0 \tag{6.4.7}$$

However, for incompressible limits, the eigenvalues become stiff as the algebraic equations resulting from (6.4.2) are ill-conditioned, with the acoustic speed being infinite.

6.4.2 PRECONDITIONING MATRIX

To improve the eigenvalues of (6.4.7), let us examine the quantities of the first column of the time Jacobian which contain the derivative of density with respect to pressure at the constant temperature.

$$\left(\frac{\partial \rho}{\partial p}\right)_T = \frac{1}{RT} = \frac{\gamma}{a^2} \tag{6.4.8}$$

Note that this derivative vanishes for incompressible flows ($a = \infty$), leading to the stiff eigenvalues in (6.4.7). To circumvent this problem, we may adjust (6.4.8) in the form

$$\rho\beta_T = \left(\frac{\partial \rho}{\partial p}\right)_T = \frac{1}{RT} = \frac{1}{\gamma RT} + \frac{1}{c_p T} = \frac{1}{a^2} + \frac{1}{c_p T} = \frac{1}{V_r^2} + \frac{\alpha_p}{c_p} = \frac{1}{V_r^2} - \frac{1}{c_p \rho}\left(\frac{\partial \rho}{\partial T}\right)_p \tag{6.4.9}$$

where V_r is a reference velocity which may be defined differently for compressible and incompressible flows. A logical choice would be that $V_r = a$ for compressible flows and $V_r = (\mathrm{v}_i \mathrm{v}_i)^{1/2}$ for incompressible flows. Thus, the time Jacobian matrix $\mathbf{A}$ is adjusted to $\hat{\mathbf{A}}$ implying the preconditioning matrix with $\rho\beta_T$ in (6.4.3) given by (6.4.9). For highly viscous flow such as in the boundary layers, it is necessary to choose the reference velocity to be governed by the diffusion velocity such that

$$V_r = \max(V_r, \nu/\Delta x)$$

The adjusted eigenvalues of the preconditioned system are determined from

$$|\hat{\mathbf{A}}^{-1}\mathbf{B}_i - \lambda_i \mathbf{I}| = 0 \tag{6.4.10}$$

$$\Lambda = diag(u, u, u,\ u^* + a^*, u^* - a^*) \tag{6.4.11}$$

with

$$u^* = \frac{1}{2} u \left[1 - \left(\rho\beta_T - \frac{\alpha_p}{c_p}\right) V_r^2\right] \tag{6.4.12a}$$

$$a^* = \frac{1}{2}\left\{\left[1 - \left(\rho\beta_T - \frac{\alpha_p}{c_p}\right) V_r^2\right] u^2 + V_r^2\right\}^{1/2} \tag{6.4.12b}$$

Here, it is seen that, for $V_r \geq a$, the eigenvalues in (6.4.12) become $u \pm a$, whereas if $V_r \cong 0$, all eigenvalues are of the same order as u. This shows that the eigenvalues of the preconditioned system remain well conditioned at all speeds.

To provide efficiency and time-accurate solutions, one may utilize a dual time stepping by introducing a pseudo-time derivative term into (6.4.2) in linearized iteration steps:

$$\hat{\mathbf{A}}\frac{\partial \Delta \mathbf{Q}}{\partial \tau} + \mathbf{A}\frac{\partial \Delta \mathbf{Q}}{\partial t} + \mathbf{B}_i \frac{\partial \Delta \mathbf{Q}}{\partial x_i} + \mathbf{C}_i \frac{\partial \Delta \mathbf{Q}}{\partial x_i} + \mathbf{C}_{ij} \frac{\partial^2 \Delta \mathbf{Q}}{\partial x_i \partial x_j} = -\mathbf{H} \tag{6.4.13}$$

with **H** given by (6.4.1). As the pseudo time τ approaches infinity, the pseudo time term vanishes and we recover (6.4.1) at steady state.

Pletcher and Chen [1993] constructs the time Jacobian matrix in nondimensional quantities with the first column and last row of (6.4.3) in terms of Mach number to obtain the pseudo-time preconditioning matrix by dividing by the Mach number so that the fatal ill-conditioning can be eliminated. Some examples have been presented by Merkle et al. [1998] using the pseudo-time preconditioning of the type given by (6.4.3) with (6.4.9).

6.5 FLOWFIELD-DEPENDENT VARIATION METHODS

So far, the major portions of the historical developments in FDM have been covered and various computational schemes for the various flow properties have also been discussed. In this section we explore a general approach which leads to most of the currently available computational schemes as special cases. Such an approach, called the flowfield-dependent variation (FDV) methods, is examined in this section.

6.5.1 BASIC THEORY

The original idea of FDV methods began from the need to address the physics involved in shock wave turbulent boundary layer interactions [Chung, 1999; Schunk et al., 1999]. In this situation, transitions and interactions of inviscid/viscous, compressible/incompressible, and laminar/turbulent flows constitute not only the physical complexities but also computational difficulties. This is where the very low velocity in the vicinity of the wall ($M \cong 0$, $\mathrm{Re} \cong 0$) and very high velocity far away from the wall (e.g., $M \cong 20$, $\mathrm{Re} \cong 10^9$) coexist within a domain of study. Transitions from one type of flow to another and interactions between two distinctly different flows have been studied for many years, both experimentally and numerically. Incompressible flows were analyzed using the pressure-based formulation with the primitive variables for the implicit solution of the Navier-Stokes system of equations. The precondition process for the time-dependent term intended for all speed flows was also discussed. Compressible flows were analyzed using the density-based formulation with the conservation variables for the solution of the Navier-Stokes system of equations. However, in dealing with the domain which contains all speed flows with various physical properties where the equations of state for compressible and incompressible flows are different, and where the transitions between laminar and turbulent flows are involved in dilatational dissipation due to compressibility, we must provide very special and powerful numerical treatments. The FDV scheme has been devised toward resolving these issues.

For the purpose of the discussion, we shall consider the conservation form of the Navier-Stokes system (2.2.11) without the source terms (see Section 13.6 for the source terms not equal to zero in FEM).

$$\frac{\partial \mathbf{U}}{\partial t} + \frac{\partial \mathbf{F}_i}{\partial x_i} + \frac{\partial \mathbf{G}_i}{\partial x_i} = 0 \tag{6.5.1}$$

In expanding $\mathbf{U}^{n+1}$ in a special form of Taylor series about $\mathbf{U}^n$, we introduce the parameters s_a and s_b for the first and second order derivatives of **U** with respect to

time, respectively,

$$\mathbf{U}^{n+1} = \mathbf{U}^n + \Delta t \frac{\partial \mathbf{U}^{n+s_a}}{\partial t} + \frac{\Delta t^2}{2} \frac{\partial^2 \mathbf{U}^{n+s_b}}{\partial t^2} + \mathrm{O}(\Delta t^3) \tag{6.5.2}$$

where

$$\frac{\partial \mathbf{U}^{n+s_a}}{\partial t} = \frac{\partial \mathbf{U}^n}{\partial t} + s_a \frac{\partial \Delta \mathbf{U}^{n+1}}{\partial t} \quad 0 \le s_a \le 1 \tag{6.5.3a}$$

$$\frac{\partial^2 \mathbf{U}^{n+s_b}}{\partial t^2} = \frac{\partial^2 \mathbf{U}^n}{\partial t^2} + s_b \frac{\partial^2 \Delta \mathbf{U}^{n+1}}{\partial t^2} \quad 0 \le s_b \le 1 \tag{6.5.3b}$$

with $\Delta \mathbf{U}^{n+1} = \mathbf{U}^{n+1} - \mathbf{U}^n$. Substituting (6.5.3) into (6.5.2) yields

$$\mathbf{U}^{n+1} = \mathbf{U}^n + \Delta t \left(\frac{\partial \mathbf{U}^n}{\partial t} + s_a \frac{\partial \Delta \mathbf{U}^{n+1}}{\partial t} \right) + \frac{\Delta t^2}{2} \left(\frac{\partial^2 \mathbf{U}^n}{\partial t^2} + s_b \frac{\partial^2 \Delta \mathbf{U}^{n+1}}{\partial t^2} \right) + \mathrm{O}(\Delta t^3) \tag{6.5.4}$$

Introducing the Jacobians of convection, diffusion, and diffusion gradients, we write the first and second derivatives of the conservation variables in the form,

$$\frac{\partial \mathbf{U}}{\partial t} = -\frac{\partial \mathbf{F}_i}{\partial x_i} - \frac{\partial \mathbf{G}_i}{\partial x_i} \tag{6.5.5}$$

$$\frac{\partial^2 \mathbf{U}}{\partial t^2} = -\frac{\partial}{\partial x_i} \left(\mathbf{a}_i \frac{\partial \mathbf{U}}{\partial t} \right) - \frac{\partial}{\partial x_i} \left(\mathbf{b}_i \frac{\partial \mathbf{U}}{\partial t} \right) - \frac{\partial^2}{\partial x_i \partial x_j} \left(\mathbf{c}_{ij} \frac{\partial \mathbf{U}}{\partial t} \right) \tag{6.5.6a}$$

in which the convection Jacobian $\mathbf{a}_i$, the diffusion Jacobian $\mathbf{b}_i$, and the diffusion gradient Jacobian $\mathbf{c}_{ij}$ are defined as in (6.3.9) for 2-D and Appendix A for 3-D. Combining (6.5.5) and (6.5.6a) leads to

$$\frac{\partial^2 \mathbf{U}}{\partial t^2} = \frac{\partial}{\partial x_i} (\mathbf{a}_i + \mathbf{b}_i) \left(\frac{\partial \mathbf{F}_j}{\partial x_j} + \frac{\partial \mathbf{G}_j}{\partial x_j} \right) + \frac{\partial^2}{\partial x_i \partial x_k} \mathbf{c}_{ik} \left(\frac{\partial \mathbf{F}_j}{\partial x_j} + \frac{\partial \mathbf{G}_j}{\partial x_j} \right) \tag{6.5.6b}$$

Substituting (6.5.5) and (6.5.6b) into (6.5.4), and assuming the product of the diffusion gradient Jacobian with third order spatial derivatives to be negligible, we have

$$\begin{aligned} \Delta \mathbf{U}^{n+1} = \Delta t & \left[-\frac{\partial \mathbf{F}_i^n}{\partial x_i} - \frac{\partial \mathbf{G}_i^n}{\partial x_i} + s_a \left(-\frac{\partial \Delta \mathbf{F}_i^{n+1}}{\partial x_i} - \frac{\partial \Delta \mathbf{G}_i^{n+1}}{\partial x_i} \right) \right] \\ & + \frac{\Delta t^2}{2} \left\{ \frac{\partial}{\partial x_i} (\mathbf{a}_i + \mathbf{b}_i) \left(\frac{\partial \mathbf{F}_j^n}{\partial x_j} + \frac{\partial \mathbf{G}_j^n}{\partial x_j} \right) \right. \\ & \left. + s_b \left[\frac{\partial}{\partial x_i} (\mathbf{a}_i + \mathbf{b}_i) \left(\frac{\partial \Delta \mathbf{F}_j^{n+1}}{\partial x_j} + \frac{\partial \Delta \mathbf{G}_j^{n+1}}{\partial x_j} \right) \right] \right\} + \mathrm{O}(\Delta t^3) \end{aligned} \tag{6.5.7}$$

The parameters s_a and s_b which appear in (6.5.7) above may be given appropriate physical roles by calculating them from the flowfield-dependent quantities. For example, if s_a is associated with the temporal changes (fluctuations) of convection, it may be calculated from the changes of Mach number between adjacent nodal points so that $s_a = 0$ would imply no changes in convection fluctuations. The functional dependency

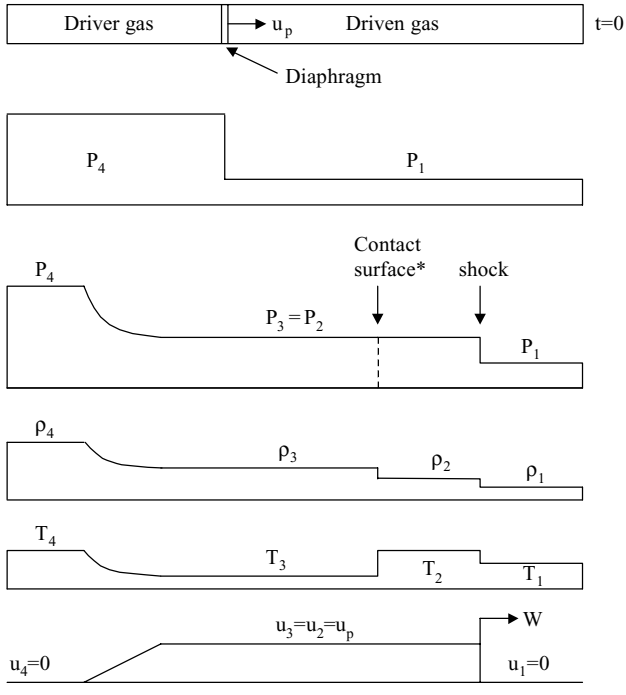

*Analogous to sliplines ($P_3=P_2$, $T_3 \neq T_2$, $\rho_3 \neq \rho_2$, $u_3=u_2$) leading to entropy discontinuity at the contact surface.

Figure 6.5.1 Mechanism of shock wave discontinuities as related to s_1 in terms of the changes of Mach number with respect to the velocity and square root of pressure, density, or temperature, $s_a = f(u/\sqrt{p/\rho}) = f(u/\sqrt{RT}) = f(M)$.

of s_a on Mach number is illustrated from the shock tube physics as shown in Figure 6.5.1. Here it is seen that discontinuities of pressure, density, and temperature are related as a function of Mach number,

$$s_a = f(u/\sqrt{p/\rho}) = f(u/\sqrt{RT}) = f(M)$$

Similarly, if s_a is associated with the changes (fluctuations) of diffusion, such as in boundary layers, then it may be calculated from the changes of Reynolds number or Peclet number between adjacent nodal points such that $s_a = 0$ would signify no changes in diffusion fluctuations. Therefore, the role of s_a for diffusion is different from that of convection. For example, we may define the fluctuation quantities associated with s_a as

$$s_a\left(\frac{\partial \Delta \mathbf{F}_i^{n+1}}{\partial x_i} + \frac{\partial \Delta \mathbf{G}_i^{n+1}}{\partial x_i}\right) \Rightarrow s_1 \frac{\partial \Delta \mathbf{F}_i^{n+1}}{\partial x_i} + s_3 \frac{\partial \Delta \mathbf{G}_i^{n+1}}{\partial x_i}$$
$$= \frac{\sqrt{M_{\max}^2 - M_{\min}^2}}{M_{\min}} \frac{\partial \Delta \mathbf{F}_i^{n+1}}{\partial x_i} + \frac{\sqrt{Re_{\max}^2 - Re_{\min}^2}}{Re_{\min}} \frac{\partial \Delta \mathbf{G}_i^{n+1}}{\partial x_i} \tag{6.5.8}$$

where it is seen that the parameter s_a originally adopted as a single mathematical or

numerical parameter has now turned into multiple physical parameters such as the changes of Mach numbers and Reynolds numbers (or Peclet numbers) between adjacent nodal points. The magnitudes of fluctuations of convection, diffusion, and source terms are dictated by the current flowfield situations in space and time. Similar assessments can be applied to the parameter s_b as associated with its corresponding fluctuation terms of convection and diffusion. Thus, in order to provide variations to the changes of convection and diffusion differently in accordance with the current flowfield situations, we reassign s_a and s_b associated with convection and diffusion as follows:

$$s_a\Delta\mathbf{F}_i \Rightarrow s_1\Delta\mathbf{F}_i, \quad s_a\Delta\mathbf{G}_i \Rightarrow s_3\Delta\mathbf{G}_i$$
$$s_b\Delta\mathbf{F}_i \Rightarrow s_2\Delta\mathbf{F}_i, \quad s_b\Delta\mathbf{G}_i \Rightarrow s_4\Delta\mathbf{G}_i$$

with the various parameters, called the flowfield-dependent variation (FDV) parameters or simply variation parameters, defined as follows:

s_1 = first order convection FDV parameter

s_2 = second order convection FDV parameter

s_3 = first order diffusion FDV parameter

s_4 = second order diffusion FDV parameter

The first order FDV parameters s_1 and s_3 are flowfield-dependent, whereas the second order FDV parameters s_2 and s_4 are exponentially proportional to the first order FDV parameters, and mainly act as artificial viscosity. Details of these FDV parameters are given below.

6.5.2 FLOWFIELD-DEPENDENT VARIATION PARAMETERS

As has been pointed out, the success of FDV methods depends on accurate calculations of the flowfield-dependent variation parameters. Specifically, the convection FDV parameters s_1 and s_2 and diffusion FDV parameters s_3 and s_4 are dependent on Mach numbers and Reynolds numbers or Peclet numbers, respectively. The first order FDV parameters s_1 and s_3 dictate the flowfield solution accuracy, whereas the second order FDV parameters s_2 and s_4 maintain the solution stability.

Convection FDV Parameters

$$s_1 = \begin{cases} \min(r, 1), & r > \alpha \\ 0 & r < \alpha,\ M_{\min} \neq 0 \\ 1 & M_{\min} = 0 \end{cases} \tag{6.5.9a}$$

$$s_2 = \frac{1}{2}\left(1 + s_1^{\eta}\right), \quad 0.05 < \eta < 0.2 \tag{6.5.9b}$$

with

$$r = \sqrt{M_{\max}^2 - M_{\min}^2}\,/\,M_{\min} \tag{6.5.10}$$

where the maximum and minimum Mach numbers are calculated between the local

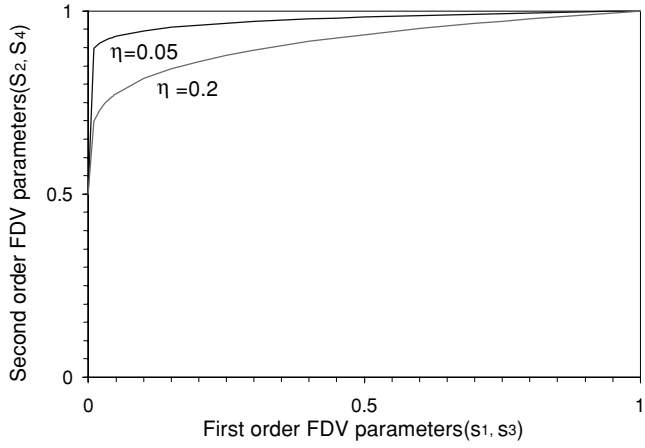

Figure 6.5.2 Relationship between the first and second order variation parameters $s_2 = (1 + s_1^{\eta})/2, s_4 = (1 + s_3^{\eta})/2,$ with $0.05 < \eta \leq 0.2$.

adjacent nodal points with α being the user-specified small number ($\alpha \cong 0.01$). The ranges of the second order FDV parameter exponent η are given, exponentially proportional to the first order FDV parameter, as shown in Figure 6.5.2. It appears that the range in $0.05 \leq \eta \leq 0.2$ is adequate in most of the examples that have been tested.

Diffusion FDV Parameters

$$s_3 = \begin{cases} \min(r, 1), & r > \alpha, \quad \alpha \cong 0.01 \\ 0 & r < \alpha, \quad \mathrm{Re}_{\min} \neq 0, \quad \text{or } Pe_{\min} \neq 0 \\ 1 & \mathrm{Re}_{\min} = 0, \quad \text{or } Pe_{\min} = 0 \end{cases} \tag{6.5.11a}$$

$$s_4 = \frac{1}{2}\left(1 + s_3^{\eta}\right), \quad 0.05 < \eta < 0.2 \tag{6.5.11b}$$

with

$$r = \sqrt{\mathrm{Re}_{\max}^2 - \mathrm{Re}_{\min}^2}\,/\mathrm{Re}_{\min} \quad \text{or } r = \sqrt{Pe_{\max}^2 - Pe_{\min}^2}\,/Pe_{\min} \tag{6.5.12a,b}$$

where the maximum and minimum Reynolds numbers or maximum and minimum Peclet numbers are calculated between the local adjacent nodal points, and α is a user-specified small number ($\alpha \cong 0.01$). If temperature gradients are large, it is possible that Peclet numbers instead of Reynolds numbers may dictate the diffusion FDV parameters. The larger value of s_3 is to be chosen, as obtained either from (6.5.12a) or (6.5.12b). Adequate ranges of η for the second order FDV variation parameter are the same as for the case of convection.

Relationships between the first and second order FDV parameters are graphically shown in Figure 6.5.3a. The ranges of these convection and diffusion FDV parameters for a typical compression corner high-speed flow are illustrated in Figure 6.5.3b. They represent the trend of an exhaustive numerical experimentation for various physical situations.

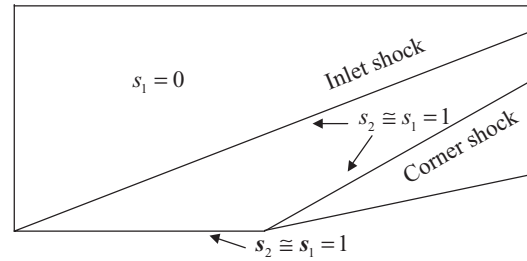

(a) Ranges of convection variation parameters

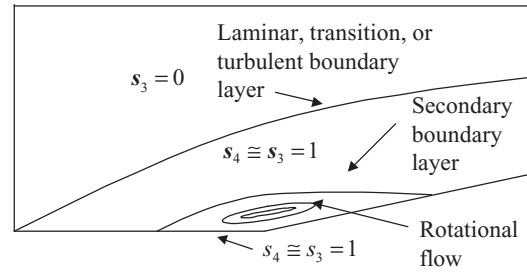

(b) Ranges of diffusion variation parameters

Figure 6.5.3 Typical ranges of first order (convection) and second order (diffusion) variation parameters for the compression corner high-speed flow.

6.5.3 FDV EQUATIONS

The final form of the FDV equations can be obtained by substituting the FDV parameters as defined in (6.5.8) through (6.5.12) into (6.5.7), leading to the residual of the form,

$$\begin{aligned}\mathbf{R} = \Delta\mathbf{U}^{n+1} - \Delta t\left[-\frac{\partial \mathbf{F}_i^n}{\partial x_i} - \frac{\partial \mathbf{G}_i^n}{\partial x_i} - s_1\frac{\partial \Delta\mathbf{F}_i^{n+1}}{\partial x_i} - s_3\frac{\partial \Delta\mathbf{G}_i^{n+1}}{\partial x_i}\right] \\ - \frac{\Delta t^2}{2}\left[\frac{\partial}{\partial x_i}(\mathbf{a}_i + \mathbf{b}_i)\left(\frac{\partial \mathbf{F}_j^n}{\partial x_j} + \frac{\partial \mathbf{G}_j^n}{\partial x_j}\right)\right] - \frac{\Delta t^2}{2}\left\{s_2\left[\frac{\partial}{\partial x_i}(\mathbf{a}_i + \mathbf{b}_i)\left(\frac{\partial \Delta\mathbf{F}_j^{n+1}}{\partial x_j}\right)\right]\right. \\ \left. + \frac{\partial}{\partial x_i}(\mathbf{a}_i + \mathbf{b}_i)\left(s_4\frac{\partial \Delta\mathbf{G}_j^{n+1}}{\partial x_j}\right)\right\} + \mathrm{O}(\Delta t^3) \qquad (6.5.13a)\end{aligned}$$

Now, rearranging and expressing the remaining terms associated with the FDV parameters in terms of the Jacobians, we have

$$\begin{aligned}\Delta\mathbf{U}^{n+1} + \Delta t\left[s_1\left(\frac{\partial \mathbf{a}_i \Delta\mathbf{U}^{n+1}}{\partial x_i}\right) + s_3\left(\frac{\partial \mathbf{b}_i \Delta\mathbf{U}^{n+1}}{\partial x_i} + \frac{\partial^2 \mathbf{c}_{ij}\Delta\mathbf{U}^{n+1}}{\partial x_i \partial x_j}\right)\right] \\ - \frac{\Delta t^2}{2}\left\{s_2\left[\frac{\partial^2(\mathbf{a}_i\mathbf{a}_j + \mathbf{b}_i\mathbf{a}_j)\Delta\mathbf{U}^{n+1}}{\partial x_i \partial x_j}\right] + s_4\left[\frac{\partial^2(\mathbf{a}_i\mathbf{b}_j + \mathbf{b}_i\mathbf{b}_j)\Delta\mathbf{U}^{n+1}}{\partial x_i \partial x_j}\right]\right\} \\ + \Delta t\left(\frac{\partial \mathbf{F}_i^n}{\partial x_i} + \frac{\partial \mathbf{G}_i^n}{\partial x_i}\right) - \frac{\Delta t^2}{2}\left[\frac{\partial}{\partial x_i}(\mathbf{a}_i + \mathbf{b}_i)\left(\frac{\partial \mathbf{F}_j^n}{\partial x_j} + \frac{\partial \mathbf{G}_j^n}{\partial x_j}\right)\right] + \mathrm{O}(\Delta t^3) = 0 \qquad (6.5.13b)\end{aligned}$$

Here, once again, the product of the diffusion gradient Jacobian with third order spatial derivatives is neglected and all Jacobians $\mathbf{a}_i$, $\mathbf{b}_i$, and $\mathbf{c}_{ij}$ are assumed to remain constant spatially within each time step and to be updated at subsequent time steps. For simplicity, we may rearrange (6.5.13b) in a compact form,

$$\mathbf{R} = \Delta\mathbf{U}^{n+1} + \frac{\partial}{\partial x_i}\left(\mathbf{E}_i \Delta\mathbf{U}^{n+1}\right) + \frac{\partial^2}{\partial x_i \partial x_j}\left(\mathbf{E}_{ij}\Delta\mathbf{U}^{n+1}\right) + \mathbf{Q}^n + O(\Delta t^3), \tag{6.5.13c}$$

or, lagging $\mathbf{E}_i$ and $\mathbf{E}_{ij}$ one time step behind,

$$\left(\mathbf{I} + \mathbf{E}_i^n \frac{\partial}{\partial x_i} + \mathbf{E}_{ij}^n \frac{\partial^2}{\partial x_i \partial x_j}\right)\Delta\mathbf{U}^{n+1} = -\mathbf{Q}^n \tag{6.5.14}$$

with

$$\mathbf{E}_i^n = \Delta t(s_1\mathbf{a}_i + s_3\mathbf{b}_i)^n \tag{6.5.15a}$$

$$\mathbf{E}_{ij}^n = \left\{\Delta t s_3 \mathbf{c}_{ij} - \frac{\Delta t^2}{2}[s_2(\mathbf{a}_i\mathbf{a}_j + \mathbf{b}_i\mathbf{a}_j) + s_4(\mathbf{a}_i\mathbf{b}_j + \mathbf{b}_i\mathbf{b}_j)]\right\}^n \tag{6.5.15b}$$

$$\mathbf{Q}^n = \frac{\partial}{\partial x_i}\left[\Delta t\left(\mathbf{F}_i^n + \mathbf{G}_i^n\right)\right] - \frac{\partial^2}{\partial x_i \partial x_j}\left[\frac{\Delta t^2}{2}(\mathbf{a}_i + \mathbf{b}_i)\left(\mathbf{F}_j^n + \mathbf{G}_j^n\right)\right] \tag{6.5.15c}$$

Note that the Beam-Warming scheme [1978] discussed in Section 6.3.2 can be written in the form similar to (6.5.14) with the following definitions of $\mathbf{E}_i$, $\mathbf{E}_{ij}$, and $\mathbf{Q}^n$:

$$\mathbf{E}_i = m\Delta t(\mathbf{a}_i + \mathbf{b}_i), \quad \text{with } m = \theta/(1+\xi) \tag{6.5.16a}$$

$$\mathbf{E}_{ij} = m\Delta t\mathbf{c}_{ij} \tag{6.5.16b}$$

$$\mathbf{Q}^n = \frac{\Delta t}{1+\xi}\left(\frac{\partial \mathbf{F}_i^n}{\partial x_i} + \frac{\partial \mathbf{G}_i^n}{\partial x_i}\right) + \frac{\xi}{1+\xi}\Delta\mathbf{U}^n \tag{6.5.16c}$$

where the cross-derivative terms appearing in $\mathbf{Q}^n$ for the Beam-Warming scheme are included in the second derivative terms on the left-hand side. The Beam-Warming scheme is seen to be a special case of the FDV equations if we set $s_1 = s_3 = m$, $s_2 = s_4 = 0$, in (6.5.14), with adjustments of $\mathbf{Q}^n$ on the right-hand side as in (6.5.16c). The stability analysis of the Beam-Warming scheme requires $\xi \geq 0.385$ and $\theta = 1/2 + \xi$. This will fix the FDV parameter m to be $0.639 \leq m \leq 0.75$.

We realize that all physical phenomena are dictated by the FDV parameters in the FDV equations (6.5.14). Either FDM, FEM, or FVM approximations can be applied to (6.5.14). However, their roles are merely to provide different options of discretization, with physics governed by the FDV theory itself. Furthermore, the FDV equations are capable of producing many existing FDM and FEM schemes as special cases, as demonstrated in Chapter 16.

For FDM applications, the first derivative for $\mathbf{E}_i\Delta\mathbf{U}^{n+1}$ and the second derivative for $\mathbf{E}_{ij}\Delta\mathbf{U}^{n+1}$ in (6.5.14) may be approximated by many options of finite difference equations including high order accuracy schemes introduced in Section 3.7 or using the flux vector splitting for the term involved in $\mathbf{a}_i$ for $\mathbf{E}_i$ in (6.5.14). However, the physical aspects accommodated in the FDV theory through the various FDV parameters are unique and they play important roles, as elaborated next.

6.5.4 INTERPRETATION OF FLOWFIELD-DEPENDENT VARIATION PARAMETERS

The flowfield-dependent variation (FDV) parameters as defined earlier are capable of allowing various numerical schemes to be automatically generated. They are summarized as follows:

(1) *First order FDV parameters*. The first order FDV parameters s_1 and s_3 control all high gradient phenomena such as shock waves and turbulence. These parameters as calculated from the changes of local Mach numbers and Reynolds (or Peclet) numbers within each element and are indicative of the actual local element flowfields. The contours of these parameters closely resemble the flowfields themselves, with both s_1 and s_3 being large (close to unity) in regions of high gradients, but small (close to zero) in regions where the gradients are small. The fact that the contours of s_1 and s_3 resemble the flowfield (Mach number or density contours) is demonstrated in Figure 13.7.3.2. The basic role of s_1 and s_3 is to provide computational accuracy.

(2) *Second order FDV parameters*. The second order FDV parameters s_2 and s_4 are also flowfield dependent, exponentially proportional to the first order FDV parameters. However, their primary role is to provide adequate computational stability (artificial viscosity) as they were originally introduced into the second order time derivative term of the Taylor series expansion of the conservation flow variables $\mathbf{U}^{n+1}$.

(3) *Parabolic/elliptic* ($s_1 = 0$). The s_1 terms represent convection. This implies that if $s_1 \cong 0$ then the effect of convection is small. The computational scheme is automatically altered to take this effect into account, with the governing equations being predominantly parabolic-elliptic.

(4) *Hyperbolic* ($s_3 = 0$). The s_3 terms are associated with diffusion. Thus, with $s_3 \cong 0$, the effect of viscosity or diffusion is small and the computational scheme is automatically switched to that of Euler equations where the governing equations are predominantly hyperbolic.

(5) *Mixed elliptic/parabolic/hyperbolic* ($s_1 \neq 0, s_3 \neq 0$). If the first order FDV parameters s_1 and s_3 are nonzero, this indicates a typical situation for the mixed hyperbolic, parabolic, and elliptic nature of the Navier-Stokes system of equations, with convection and diffusion being equally important. This is the case for incompressible flows at low speeds. The unique property of the FDV scheme is its capability to control pressure oscillations adequately without resorting to the separate hyperbolic elliptic pressure Poisson equation for pressure corrections. The capability of the FDV scheme to handle incompressible flows is achieved by a delicate balance between s_1 and s_3 as determined by the local Mach numbers and Reynolds (or Peclet) numbers. If the flow is completely incompressible ($M = 0$), the criteria given by (6.5.9) leads to $s_1 = 1$, whereas the variation parameter s_3 is to be determined according to the criteria given in (6.5.11). Make a note of the presence of convection-diffusion interaction terms given by the product of $\mathbf{b}_i\mathbf{a}_j$ in the s_2 terms and $\mathbf{a}_i\mathbf{b}_j$ in the s_4 terms. These terms allow interactions between convection and diffusion in the viscous incompressible and/or viscous compressible flows.

(6) *High temperature gradient flow*. If temperature gradients rather than velocity gradients dominate the flowfield, then s_3 is governed by the Peclet number rather

than by the Reynolds number. Such cases arise in high-speed, high-temperature compressible flows close to the wall.

(7) *Transition to turbulence*. The transition to turbulence is a natural flow process as the Reynolds number increases, causing the gradients of any or all flow variables to increase. This phenomenon is physical instability and is detected by the increase of s_3 if the flow is incompressible, but by both s_3 and s_1 if the flow is compressible. Such physical instability is likely to trigger the numerical instability, but will be countered by the second order FDV parameters s_2 and/or s_4 to ensure numerical stability automatically. In this process, these flowfield dependent variation parameters are capable of capturing relaminarization, compressibility effect or dilatational turbulent energy dissipation, and turbulent unsteady fluctuations. They are characterized by the product of s_3 and the fluctuations of stress tensor $(s_3\Delta\tau_{ij})$ in which the stresses consist of mean and fluctuation parts. As a consequence, some regions of the flow domain such as in boundary layers may always be unsteady $(\Delta\tau_{ij} \neq 0)$, even though the steady state may have been reached away from the wall. However, in order for these fluctuation parts to be correctly determined, it is necessary that Kolmogorov scales be resolved in sufficiently refined grids such as in the direct numerical simulation (DNS). Thus, for a coarse mesh, the advantage of FDV process cannot be expected.

6.5.5 SHOCK-CAPTURING MECHANISM

The shock-capturing mechanism is built into the FDV equations of continuity, momentum, and energy. For example, let us examine (6.5.7) or (6.5.13) and write the momentum equations, with all diffusion terms neglected.

$$\begin{aligned}\Delta(\rho v_j)^{n+1} &+ \Delta t[(\rho v_i v_j)_{,i} + p_{,j}]^n \\ &= -s_1\Delta t(\Delta\rho v_i v_j + \Delta p\delta_{i,j})^{n+1}_{,i} + s_2\frac{\Delta t^2}{2}\left(a_k^{(m)} + b_k^{(m)}\right)[\Delta(\rho v_i v_j)_{,i} + \Delta p_{,j}]^{n+1}_{,k} \\ &+ \frac{\Delta t^2}{2}\left(a_k^{(m)} + b_k^{(m)}\right)[(\rho v_i v_j)_{,i} + p_{,j}]^n_k \end{aligned} \tag{6.5.17}$$

where $a_k^{(m)}$ and $b_k^{(m)}$ denote the convection and diffusion Jacobians, respectively. To identify the shock capturing mechanism in the FDV formulation as compared to the TVD finite difference scheme, let us rewrite (6.5.17) for the 1-D momentum equation, retaining only the convection flux without the pressure gradients.

$$\Delta u^{n+1} = -\Delta t s_1\frac{\partial a\Delta u^{n+1}}{\partial x} + \frac{\Delta t^2}{2}s_2 a^2\frac{\partial^2\Delta u^{n+1}}{\partial x^2} - \Delta t\frac{\partial f^n}{\partial x} + \frac{\Delta t^2}{2}a\frac{\partial^2 f^n}{\partial x^2} \tag{6.5.18a}$$

or

$$\begin{aligned}\Delta u^{n+1} = &-\Delta t\frac{\sqrt{M_{\max}^2 - M_{\min}^2}}{M_{\min}}\frac{\partial a\Delta u^{n+1}}{\partial x} + \frac{\Delta t^2}{2}\left(\frac{\sqrt{M_{\max}^2 - M_{\min}^2}}{M_{\min}}\right)^{\eta} a^2\frac{\partial^2\Delta u^{n+1}}{\partial x^2} \\ &- \Delta t\frac{\partial f^n}{\partial x} + \frac{\Delta t^2}{2}a\frac{\partial^2 f^n}{\partial x^2}\end{aligned} \tag{6.5.18b}$$

where f is the convection flux and a is the 1-D convection Jacobian or speed of sound.

The FDM analog of (6.5.18) at node i becomes

$$\frac{\Delta u_i^{n+1}}{\Delta t}=-s_1 a\frac{1}{\Delta x}\left(\Delta u_i^{n+1}-\Delta u_{i-1}^{n+1}\right)+s_2 a^2\Delta t\frac{1}{2\Delta x^2}\left(\Delta u_i^{n+1}-2\Delta u_{i-1}^{n+1}+\Delta u_{i-2}^{n+1}\right)$$
$$-\frac{1}{\Delta x}\left(f_i^n-f_{i-1}^n\right)+a\Delta t\frac{1}{2\Delta x^2}\left(f_i^n-2f_{i-1}^n+f_{i-2}^n\right) \tag{6.5.19}$$

The second order TVD semi-discretized scheme (6.2.110) with limiter functions (6.2.111) is written at node i as

$$\frac{du_i}{dt}=-\frac{a^+}{\Delta x}\left[1+\Psi_{i-1/2}^+-\frac{1}{2}\frac{\Psi_{i-3/2}^+}{r_{i-3/2}^+}\right](u_i-u_{i-1})$$
$$-\frac{a^-}{\Delta x}\left[1+\Psi_{i+1/2}^--\frac{1}{2}\frac{\Psi_{i+3/2}^-}{r_{i+3/2}^-}\right](u_{i+1}-u_i) \tag{6.5.20}$$

where Ψ and r denote the limiter function and velocity ratio, respectively,

$$r_{i-3/2}^+=\frac{u_i-u_{i-1}}{u_{i-1}-u_{i-2}},\qquad r_{i+3/2}^-=\frac{u_{i+1}-u_i}{u_{i+2}-u_{i+1}} \tag{6.5.21}$$

Inserting (6.5.21) into (6.5.20) yields

$$\frac{du_i}{dt}=-\frac{a^+}{\Delta x}\left[(u_i-u_{i-1})+\frac{1}{2}\Psi_{i-1/2}^+(u_i-u_{i-1})-\Psi_{i-3/2}^+(u_{i-1}-u_{i-2})\right]$$
$$-\frac{a^-}{\Delta x}\left[(u_{i+1}-u_i)+\frac{1}{2}\Psi_{i+1/2}^-(u_{i+1}-u_i)-\Psi_{i+3/2}^-(u_{i+2}-u_{i+1})\right] \tag{6.5.22}$$

Let us assume that, for positive-going waves,

$$u_i=u_i^n+s\Delta u_i^{n+1},\qquad a^-=0,\qquad a^+=a,\qquad \Psi_{i-1/2}^+=2\Psi_{i-3/2}^+=-\Psi$$

Substituting the above into (6.5.22), the TVD equation may be expressed as

$$\frac{\Delta u_i^{n+1}}{\Delta t}=-sa\frac{1}{\Delta x}\left(\Delta u_i^{n+1}-\Delta u_{i-1}^{n+1}\right)+\frac{\Psi\Delta x}{2\Delta x^2}\left(\Delta u_i^{n+1}-2\Delta u_{i-1}^{n+1}+\Delta u_{i-2}^{n+1}\right)$$
$$-\frac{1}{\Delta x}\left(f_i^n-f_{i-1}^n\right)+\frac{\Psi\Delta x}{2\Delta x^2}\left(f_i^n-2f_{i-1}^n+f_{i-2}^n\right) \tag{6.5.23}$$

If we set

$$s_1=s,\quad s_2=\frac{s\Delta x\Psi}{a\Delta t},\quad \Psi=\frac{a\Delta t}{\Delta x},\quad s_2=s_1$$

it is seen that the FDV equation (6.5.19) becomes identical to the TVD equation (6.5.23). Note that in TVD either a^+ or a^- must be chosen from the flowfield and the FDV parameters s_1 and s_2 in FDV are automatically calculated. Of course, the precise shock-capturing mechanism of both methods is not exactly the same, because all the assumptions made above are not true in general. However, it is interesting to note that the first order convection FDV parameter s_1 is related to the TVD limiter function Ψ as

$$s_1=\frac{s\Delta x}{a\Delta t}\Psi$$

in which it is shown that the convection FDV parameters (s_1, s_2) are proportional or equivalent to the TVD limiter functions. A similar process can be shown also for negative-going waves $(a^- = a, a^+ = 0)$.

Considering that the motivations and procedures of derivation are completely different, the analogy between the TVD scheme and FDV formulation as demonstrated above is remarkable. Notice that, beyond this analogy, the FDV formulation is to couple the convection variation parameters (s_1, s_2) with all other variation parameters (s_3, s_4) so that shock wave interactions with all other physical properties can be resolved. They are involved also in transitions and interactions of compressible/incompressible, inviscid/viscous, and laminar/turbulent flows.

In the TVD methods, the resulting Euler equations are based on positive and negative eigenvalues or Jacobians, either $a^- = 0$ or $a^+ = 0$, which will switch the scheme to either backward differenceing for positive waves or forward differencing for negative waves in one dimension, respectively.

To illuminate the consequence of the FDV theory, it is infomative to write (6.5.18a) in the form,

$$u_i^{n+1} = u_i^n - s_1 a^{(+,-)} \frac{\Delta t}{\Delta x} \left(\delta u_i^{(+,-)n+1} - \delta u_i^{(+,-)n} \right) - s_2 a^2 \frac{\Delta t^2}{2\Delta x^2} \times \left[\left(\delta^2 u_i^{(+,-)} \right)^{n+1} - \left(\delta^2 u_i^{(+,-)} \right)^n \right] - \frac{\Delta t}{2\Delta x} \left(\delta f_i^{(+,-)} \right)^n + \frac{a \Delta t^2}{2\Delta x^2} \left(\delta^2 f_i^{(+,-)} \right)^n \tag{6.5.24a}$$

where the flux vector splitting scheme is used with $a = a^+ + a^-$ and the following definitions:

$$\begin{aligned}
&\text{For} \quad M > 1, \quad a^+ = a, \quad a^- = 0, \quad \delta u_i^+ = u_i - u_{i-1}, \quad \delta f_i^+ = f_i - f_{i-1}, \\
&\delta^2 u_i^+ = u_i - 2u_{i-1} + u_{i-2}, \quad \delta^2 f_i^+ = f_i - 2f_{i-1} + f_{i-2}, \\
&\text{For} \quad M < 1, \quad a^+ = 0, \quad a^- = a, \quad \delta u_i^- = u_{i+1} - u_i, \quad \delta f_i^- = f_{i+1} - f_i, \\
&\delta^2 u_i^- = u_{i+2} - 2u_{i+1} + u_i, \quad \delta^2 f_i^- = f_{i+2} - 2f_{i+1} + f_i,
\end{aligned}$$

Thus, the finite-differenced FDV equation takes the form

$$\begin{aligned}
&u_i^{n+1} + s_1 a^{(+,-)} \frac{\Delta t}{\Delta x} \delta u_i^{(+,-)n+1} + s_2 a^2 \frac{\Delta t^2}{2\Delta x^2} \left(\delta^2 u_i^{(+,-)} \right)^{n+1} \\
&\quad = u_i^n + s_1 a^{(+,-)} \frac{\Delta t}{\Delta x} \delta u_i^{(+,-)n} + s_2 a^2 \frac{\Delta t^2}{2\Delta x^2} \left(\delta^2 u_i^{(+,-)} \right)^n \\
&\qquad - \frac{\Delta t}{2\Delta x} \left(\delta f_i^{(+,-)} \right)^n + \frac{a \Delta t^2}{2\Delta x^2} \left(\delta^2 f_i^{(+,-)} \right)^n
\end{aligned} \tag{6.5.24b}$$

The main difference between the finite-differenced FDV theory and the TVD schemes lies in the fact that in FDV methods variation parameters control the shock capturing mechanism and play the role similar to the limiters in TVD.

In the finite-differenced FDV methods, calculated variation parameters affect the convection and diffusion Jacobians associated with E_1^n and E_{ij}^n in (6.5.15a,b) based on the Mach number and Reynolds number changes between adjacent nodes in multidimensions. Thus, for high values of the variation parameters indicative of high gradients

of variables, characterize the discontinuous physical behavior of the variables. The contours of these variation parameters closely resemble the flowfield itself (see Figure 13.7.3.2). An example for a triple shock wave boundary layer interaction problem using FDV-FDM is shown in Figures 6.8.21 through 6.8.24. Other examples of the FDV methods are demonstrated in Sections 13.7, 15.3, and 27.3.

6.5.6 TRANSITIONS AND INTERACTIONS BETWEEN COMPRESSIBLE AND INCOMPRESSIBLE FLOWS

One of the most significant aspects of the FDV scheme is that, for low Mach numbers (incompressible flow), the scheme will automatically adjust itself to prevent pressure oscillations by ensuring the conservation of mass. This can be evidenced by the presence of the second derivatives of pressure arising in the equations of momentum, continuity, and energy. We note that the FDV momentum equations given by (6.5.17) may be rearranged in the form,

$$\frac{\partial}{\partial t}(\rho \mathrm{v}_j)^{n+1} + (\rho \mathrm{v}_i \mathrm{v}_j + p\delta_{ij} - \tau_{ij})^n_{,i} = S_j(m) \tag{6.5.25}$$

with

$$\begin{aligned} S_j(m) = &-\lfloor s_1(\Delta\rho \mathrm{v}_i \mathrm{v}_j + \Delta p\delta_{ij}) - s_3\Delta\tau_{ij}\rfloor^{n+1}_{,i} \\ &+ \frac{\Delta t}{2}\left[\left(a_k^{(m)} + b_k^{(m)}\right)((\rho \mathrm{v}_i \mathrm{v}_j)_{,i} + p_{,j} - \tau_{ij,i})\right]^n_{,k} \\ &+ \frac{\Delta t}{2}\left[\left(a_k^{(m)} + b_k^{(m)}\right)(s_2(\Delta(\rho \mathrm{v}_i \mathrm{v}_j)_{,i} + \Delta p_{,j}) - s_4\Delta\tau_{ij,i})\right]^{n+1}_{,k} \end{aligned} \tag{6.5.26}$$

Similarly, the FDV equation for continuity becomes

$$\Delta\rho^{n+1} = \Delta t\left[-(\rho \mathrm{v}_i)^n_{,i} - s_1\Delta(\rho \mathrm{v}_j)^{n+1}_{,j}\right] + \frac{\Delta t^2}{2}\left[\left(a_i^{(c)}(\rho \mathrm{v}_j)_{,j}\right)_{,i} + s_2\left(a_i^{(c)}\Delta(\rho \mathrm{v}_j)_{,j}\right)_{,i}\right]^{n+1} \tag{6.5.27}$$

with $a_i^{(c)}$ being the convection Jacobian for the continuity equation. Substituting (6.5.17) into (6.5.27) and rearranging the differential equation of continuity,

$$\frac{\partial\rho^{n+1}}{\partial t} + (\rho \mathrm{v}_i)^n_{,i} = S(c) \tag{6.5.28}$$

with

$$\begin{aligned} S(c) = &\Delta t s_1[(\rho \mathrm{v}_i \mathrm{v}_j)_{,i} + p_{,j} - \tau_{ij,i}]^n_{,j} - \Delta t s_1[s_1(\Delta(\rho \mathrm{v}_i \mathrm{v}_j)_{,i} + \Delta p_{,j}) - s_3\Delta\tau_{ij,i}]^{n+1}_{,j} \\ &- \frac{\Delta t^2}{2}s_1\left[\left(a_k^{(m)} + b_k^{(m)}\right)((\rho \mathrm{v}_i \mathrm{v}_j)_{,i} + p_{,j} - \tau_{ij,i})\right]^n_{,kj} \\ &- \frac{\Delta t^2}{2}s_1\left[\left(a_k^{(m)} + b_k^{(m)}\right)(s_2(\Delta(\rho \mathrm{v}_i \mathrm{v}_j)_{,i} + \Delta p_{,j}) - s_4\Delta\tau_{ij,i})\right]^{n+1}_{,kj} \\ &+ \frac{\Delta t}{2}\left(a_i^{(c)}(\rho \mathrm{v}_j)^n_{,j}\right)_{,i} \end{aligned} \tag{6.5.29}$$

where the third derivative associated with s_2 is neglected. A glance at (6.5.26) and (6.5.29) reveals that the right-hand side terms $S(m)$ for momentum and $S(c)$ for continuity are the additional terms of higher order derivatives arising from the process of derivations of the FDV equations.

The FDV equation for energy is of the form,

$$\begin{aligned}\Delta(\rho E)^{n+1} = {} & \Delta t\lfloor -(\rho E\mathrm{v}_i + p\mathrm{v}_i)_{,i} + (\tau_{ij}\mathrm{v}_j)_{,i} + kT_{,ii}\rfloor^n \\ & - \Delta t\{s_1[\Delta(\rho E\mathrm{v}_i) + p\mathrm{v}_i]_{,i} - s_3\lfloor\Delta(\tau_{ij}\mathrm{v}_j) + kT_{,i}\rfloor_i\}^{n+1} \\ & + \frac{\Delta t^2}{2}\left\{\left(a_k^{(e)} + b_k^e\right)[(\rho E\mathrm{v}_i + p\mathrm{v}_i)_{,i} - (\tau_{ij}\mathrm{v}_j)_{,i} - kT_{,ii}]\right\}_k^n \\ & + \frac{\Delta t^2}{2}\left\{\left(a_k^{(e)} + b_k^e\right)[s_2\Delta(\rho E\mathrm{v}_i + p\mathrm{v}_i)_{,i} - s_4\Delta(\tau_{ij}\mathrm{v}_j + kT_{,i})_{,i}]\right\}_{,k}^{n+1}\end{aligned} \tag{6.5.30}$$

which leads to the reconstructed equation of energy,

$$\frac{\partial(\rho E)^{n+1}}{\partial t} + [-(\rho E\mathrm{v}_i + p\mathrm{v}_i)_{,i} + (\tau_{ij}\mathrm{v}_j)_{,i} + kT_{,ii}]^n = S(e) \tag{6.5.31}$$

with

$$\begin{aligned}S(e) = {} & -\left\{s_1[\Delta(\rho E\mathrm{v}_i) + p\mathrm{v}_i]_i - s_3[\Delta(\tau_{ij}\mathrm{v}_j) + kT_{,i}]_{,i}\right\}^{n+1} \\ & + \frac{\Delta t}{2}\left\{\left(a_k^{(e)} + b_k^e\right)[(\rho E\mathrm{v}_i + p\mathrm{v}_i)_{,i} - (\tau_{ij}\mathrm{v}_j)_{,i} - kT_{,ii}]\right\}_{,k}^n \\ & + \frac{\Delta t}{2}\left\{\left(a_k^{(e)} + b_k^{(e)}\right)[s_2\Delta(\rho E\mathrm{v}_i + p\mathrm{v}_i)_{,i} - s_4\Delta(\tau_{ij}\mathrm{v}_j + kT_{,i})_{,i}]\right\}_{,k}^{n+1}\end{aligned} \tag{6.5.32}$$

The physical implications of the right-hand side terms for all equations are quite complex. There exist not only the second derivatives of pressure for the terms having no variation parameters at the temporal station n, but also the inviscid/viscous interactions contributed by the s_2 and s_4 terms at the temporal station $n+1$. Thus, the transitions and interactions between compressible and incompressible flows are contributed by inviscid/viscous interactions or convection/diffusion interactions.

The most crucial aspect of the transition between compressible and incompressible flows is the relationship of the equation of state shared by both compressible and incompressible flows. To this end, consider that initially the fluid is a perfect gas and that the total energy is given by

$$E = c_p T - \frac{p}{\rho} + \frac{1}{2}\mathrm{v}_i\mathrm{v}_i \tag{6.5.33}$$

The momentum equation for steady-state incompressible rotational flow may be integrated to give

$$\int\left(p + \frac{1}{2}\rho\mathrm{v}_j\mathrm{v}_j\right)_{,i} dx_i = \int(\mu\mathrm{v}_{i,jj} + \rho\varepsilon_{ijk}\mathrm{v}_j\omega_k)dx_i \tag{6.5.34}$$

$$p + \frac{1}{2}\rho\mathrm{v}_j\mathrm{v}_j = p_0 + Q \tag{6.5.35}$$

with

$$Q = \frac{1}{n}\int (\mu v_{i,jj} + \rho \varepsilon_{ijk} v_j \omega_k) dx_i$$

where p_0 is the constant of integration, and n is the spatial dimension.

Substituting (6.5.33) into (6.5.35) leads to the following relationship:

$$p_0 = \rho(c_p T + \frac{1}{2} v_i v_i - E) - Q \tag{6.5.36}$$

If p_0 as given by (6.5.36) remains a constant, equivalent to a stagnation (total) pressure, then the compressible flow as assumed in the conservation form of the Navier-Stokes system of equations has now been turned into an incompressible flow, which is expected to occur when the flow velocity is sufficiently reduced (approximately $0.1 \leq M < 0.3$ for air). Thus, (6.5.36) serves as an equivalent equation of state for an incompressible flow. This can be identified nodal point by nodal point or element by element for the entire domain. Figure 13.7.4e,f shows that both density and stagnation pressure begin to vary in the cavity flow problem for $M = 0.1$, whereas they remain constant for $M = 0.01$.

We may begin with the condition given by (6.5.35) for compressible flows. If computations are involved in low-speed flows, then the governing equations and computational schemes initially intended for high-speed compressible flows are automatically switched to those for low-speed incompressible flows with p_0 remaining constant for all low Mach number flows (approximately $0.1 \leq M \leq 0.3$) based on the flowfield-dependent variation parameters. If the flow reverses to compressible, then the stagnation pressure becomes variable, allowing the density to change.

An advantage of the FDV scheme is to avoid the so-called pressure correction process, preconditioning approach, or the implementation of a separate hyperbolic-elliptic equation as is the case with other computational schemes designed to accommodate flows of all speed regimes. In the case of the FDV formulation, a computational scheme similar to pressure correction (keeping pressure from oscillating) automatically arises by means of the Mach number and Reynolds number-dependent variation parameters. This approach is particularly useful for the inviscid-viscous interaction regions and boundary layers close to the wall such as in hypersonic aircraft or shock wave turbulent boundary layer interactions in general.

6.5.7 TRANSITIONS AND INTERACTIONS BETWEEN LAMINAR AND TURBULENT FLOWS

When inviscid flow becomes viscous, we may expect that the flow may become laminar or turbulent through inviscid/viscous interactions across the boundary layer. Below the laminar boundary layer, if viscous actions are significant, then the fluid particles are unstable, causing the changes of Mach number and Reynolds number between adjacent nodal points (assuming they are closely spaced) to be irregular, the phenomenon known as transition instability prior to the state of full turbulence. How can these processes be modeled in FDV formulation?

Fluctuations due to turbulence are characterized by the presence of the terms in the equation of momentum, continuity, and energy such as

$$s_3 \Delta\tau_{ij} = \frac{\sqrt{\mathrm{Re}_{\max}^2 - \mathrm{Re}_{\min}^2}}{\mathrm{Re}_{\min}} \Delta\tau_{ij} \tag{6.5.37}$$

Physically, the above quantity represents the fluctuations of total stresses (physical viscous stresses plus Reynolds stresses) controlled by the Reynolds number changes between the local adjacent nodal points. Thus, the FDV solution contains the sum of the mean flow variables and the fluctuation parts of the variables.

Once the solution of the Navier-Stokes system of equations is carried out and all flow variables are determined, then we compute the fluctuation part, f' of any variable f,

$$f' = f - \overline{f} \tag{6.5.38}$$

where f and $\overline{f}$ denote the Navier-Stokes solution and its time or mass average, respectively. This process may be replaced by the fast Fourier transform of the Navier-Stokes solution. Unsteady turbulence statistics (turbulent kinetic energy, Reynolds stresses, and various energy spectra) can be calculated once the fluctuation quantities of all variables are determined.

Although the solutions of the Navier-Stokes system of equations using FDV are assumed to contain the fluctuation parts as well as the mean quantities, it will be unlikely that such information is reliable when the Reynolds number is very high and if mesh refinements are not adequate to resolve the Kolmogorov microscales. In this case, it is necessary to invoke the level of mesh refinements as required for the direct numerical simulation (DNS). It is expected that FDV methods lead to accurate solutions at high Mach number and high Reynolds number flows if the mesh refinements required for DNS are used.

It is important to recognize that unsteadiness in turbulent fluctuations may prevail in the vicinity of the wall, although a steady state may have been reached far away from the wall. This situation can easily be verified by noting that $\Delta\mathbf{U}^{n+1}$ will vanish only in the region far away from the wall, but remain fluctuating in the vicinity of the wall, as dictated by the changes of Reynolds number in the variation parameter s_3 between the nodal points and fluctuations of the stresses due to both physical and turbulent viscosities in $\Delta\tau_{ij}$ characterized by (6.5.37).

CONCLUDING REMARKS

Transitions and interactions between inviscid/viscous, compressible/incompressible, and laminar/turbulent flows can be resolved by the FDV theory. It is shown that variation parameters initially introduced in the Taylor series expansion of the conservation variables of the Navier-Stokes system of equations are translated into flowfield-dependent physical parameters responsible for the characterization of fluid flows. In particular, the convection FDV parameters (s_1, s_2) are identified as equivalent to the TVD limiter functions in a specialized case. The FDV equations are shown to contain the terms of fluctuation variables automatically generated in the course of developments, varying in time and space, but following the current physical phenomena. In addition, adequate numerical controls (artificial viscosity) to address both nonfluctuating and fluctuating parts of variables are automatically activated according to the current flowfield. It has been shown that some existing numerical schemes in FDM are the special cases of the FDV theory.

An example of three-dimensional triple shock wave boundary layer interactions is demonstrated in Section 6.8.2. Some simple problems of FDV methods for supersonic compression corner and driven cavity using FEM are shown in Section 13.7. Applications of FDV theory using FVM-FEM are demonstrated in Section 15.3. Finally, applications of FDV-FEM methods to relativistic astrophysical flows are presented in Section 27.3.

6.6 OTHER METHODS

6.6.1 ARTIFICIAL VISCOSITY FLUX LIMITERS

The convection flux vector may be written in the form [Jameson et al., 1981],

$$F_{j+1} = F\left(\frac{U_{j+1} + U_j}{2}\right) - d_{j+2} \tag{6.6.1}$$

with

$$d_{j+2} = \varepsilon^{(2)}_{j+1/2}(U_{j+1} - U_j) - \varepsilon^{(4)}_{j+1/2}(U_{j+2} - 3U_{j+1} + 3U_j - U_{j-1})$$
$$\varepsilon^{(2)}_{j+1/2} = k^{(2)} R_{j+1/2} \Psi_{j+1/2}$$
$$\varepsilon^{(4)}_{j+1/2} = \max\left(0, k^{(2)} R_{j+1/2} - \varepsilon^{(2)}_{j+1/2}\right)$$

where $k^{(2)}$ and $k^{(4)}$ are real numbers fixing the amount of diffusion brought up by the second and fourth order dissipative operators. $R_{j+1/2}$ is the spectral radius of the Jacobian $\partial \mathbf{F}/\partial \mathbf{U}$ at the cell face $j+1$. $\Psi_{j+1/2}$ is a limiter based on

$$\Psi_j = \frac{|\overline{p}_{j+1} - 2\overline{p}_j + \overline{p}_{j-1}|}{|\overline{p}_{j+1} + 2\overline{p}_j + \overline{p}_{j-1}|}$$
$$\Psi_{j+1/2} = \max\left(\Psi_j, \Psi_{j+1/2}\right) \tag{6.6.2}$$

Thus, the flux vectors may be written in terms of limiters in the form,

$$F_{j+1} = \frac{1}{2}(U_j \Psi_j + U_{j+1}\Psi_{j+1}) = \frac{1}{2}(U_j + U_{j+1})$$
$$F_{j-1} = \frac{1}{2}(U_{j-1}\Psi_{j-1} + U_j \Psi_j) = \frac{1}{2}(U_{j-1} + U_j) \tag{6.6.3}$$

Using the flux of the mean value, we obtain

$$F_{j+1/2} = \frac{1}{4}(U_j + U_{j+1})(\Psi_j + \Psi_{j-1})$$
$$F_{j-1/2} = \frac{1}{4}(U_{j-1} + U_j)(\Psi_{j-1} + \Psi_j) \tag{6.6.4}$$

which represents a semi-discrete equation using a skew-symmetric form of second order. It is designed to reduce the aliasing errors that are crucial in low order nondissipative schemes useful in problems such as large eddy simulations of turbulence (see Section 21.7.3).

6.6.2 FULLY IMPLICIT HIGH ORDER ACCURATE SCHEMES

The Navier-Stokes system of equations in terms of the primitive flow variables,

$$\mathbf{Q} = [\rho \quad v_i \quad p]^T$$

may be written as

$$\frac{\partial \mathbf{Q}}{\partial t} + \mathbf{A}_i \frac{\partial \mathbf{Q}}{\partial x_i} + \frac{\partial \mathbf{G}_i}{\partial x_i} = 0 \tag{6.6.5}$$

with

$$\mathbf{A}_i \frac{\partial \mathbf{Q}}{\partial x_i} = \mathbf{A}_i^+ \mathbf{Q}_{,i}^- + \mathbf{A}_i^- \mathbf{Q}_{,i}^+$$
$$\mathbf{A}_i^\pm = \mathbf{P}\, \Lambda_i^\pm\, \mathbf{P}^{-1} \tag{6.6.6}$$

where $\mathbf{A}_i$ is the convection flux Jacobian matrix.

The fully implicit finite difference approximations of (6.6.5) may be written as

$$\frac{3\mathbf{Q}^{n+1} - 4\mathbf{Q}^n + \mathbf{Q}^{n-1}}{2\Delta t} + (\mathbf{A}_i^+ \mathbf{Q}_{,i}^- + \mathbf{A}_i^- \mathbf{Q}_{,i}^+)^{n+1} + \left(\frac{\partial \mathbf{G}_i}{\partial x_i}\right)^{n+1} = 0 \tag{6.6.7}$$

The Newton-Raphson solution of (6.6.7) may be written in the form

$$\left(\mathbf{I} + \Delta \mathbf{t} \frac{\partial \mathbf{H}}{\partial \mathbf{Q}}\right) \Delta \mathbf{Q}^{m+1} = -\Delta \mathbf{Q}^m + \Delta t \mathbf{H}^m \tag{6.6.8}$$

with

$$\Delta \mathbf{Q}^{m+1} = \left(\frac{3}{2}\mathbf{Q}^{n+1} - 2\mathbf{Q}^n + \frac{1}{2}\mathbf{Q}^{n-1}\right)^{m+1}$$
$$\Delta \mathbf{Q}^m = \left(\frac{3}{2}\mathbf{Q}^{n+1} - 2\mathbf{Q}^n + \frac{1}{2}\mathbf{Q}^{n-1}\right)^{m}$$
$$\mathbf{H}^m = \left[-(\mathbf{A}_i^+ \mathbf{Q}_{,i}^- + \mathbf{A}_i^- \mathbf{Q}_{,i}^+) + \frac{\partial \mathbf{G}_i}{\partial x_i}\right]^m$$

where the superscript m represents the m-th iteration step, with $\mathbf{Q}^+$ and $\mathbf{Q}^-$ indicating the forward and backward finite differences. Rai and Moin [1993] used fifth order accurate finite differences for large eddy simulation calculations in compressible flows with a seven-point stencil,

$$\mathbf{Q}_x^- = \frac{-6\mathbf{Q}_{i+2} + 60\mathbf{Q}_{i+1} + 40\mathbf{Q}_i - 120\mathbf{Q}_{i-1} + 30\mathbf{Q}_{i-2} - 4\mathbf{Q}_{i-3}}{\mathbf{120}\Delta \mathbf{x}}$$
$$\mathbf{Q}_x^+ = \frac{4\mathbf{Q}_{i+3} - 30\mathbf{Q}_{i+2} + 120\mathbf{Q}_{i-2} - 40\mathbf{Q}_i - 60\mathbf{Q}_{i-1} + 6\mathbf{Q}_{i-2}}{\mathbf{120}\Delta \mathbf{x}} \tag{6.6.9}$$

on a grid that is equidistanced in the x-direction. The remaining convective terms are evaluated in a similar manner. The above scheme is used in Section 21.7.3.

6.6.3 POINT IMPLICIT METHODS

In order to circumvent stiff equations due to widely disparate time scales in source terms (such as occur in chemically reactive flows), it is advantageous to use the point implicit scheme in which the source terms are provided implicitly. Thus, the Navier-Stokes system of equations are written as

$$\frac{\Delta \mathbf{U}^{n+1}}{\Delta t} + \left(\frac{\partial \mathbf{F}_i}{\partial x_i} + \frac{\partial \mathbf{G}_i}{\partial x_i}\right)^n - \left(\mathbf{B}^n + \frac{\partial \mathbf{B}}{\partial \mathbf{U}} \Delta \mathbf{U}^{n+1}\right) = 0 \tag{6.6.10}$$

Rearranging, we obtain

$$\left(\mathbf{I} - \Delta \mathbf{t} \frac{\partial \mathbf{B}}{\partial \mathbf{U}}\right)^{n+1} \Delta \mathbf{U}^{n+1} = -\Delta t \left(\frac{\partial \mathbf{F}_i}{\partial x_i} + \frac{\partial \mathbf{G}_i}{\partial x_i} - \mathbf{B}\right)^n \tag{6.6.11}$$

where the source term Jacobian is evaluated implicitly. Note that derivatives of the convection and diffusion terms may be discretized with the fourth order accuracy finite difference scheme as used in Section 22.6.2.

6.7 BOUNDARY CONDITIONS

Mathematical theories of boundary conditions have been reported extensively in the literature. They include Kreiss [1970], Rudy and Strikwerda [1980], Gustafsson [1982], Dutt [1988], Oliger and Sundström [1978], and Nordström [1989], among others. Incorrect specifications of boundary conditions result in solution instability, nonconvergence of solutions, and/or convergence to inaccurate results. Boundary conditions must be correctly specified in accordance with speed regimes at inlet and outlet, viscous interactions on solid walls, one-dimensional or multidimensional geometries, reflecting and nonreflecting boundaries, and farfield boundaries.

Recall that derivations of Neumann boundary conditions and specification of boundary conditions in general for hyperbolic, parabolic, and elliptic equations were presented in Section 2.3. Discussions on boundary conditions associated with FEM will be included in Sections 10.1.2, 11.1, and 13.6.6. Multiphase flow boundary conditions are also presented in Section 22.2.6. In what follows, various boundary conditions involved in FDM are described.

6.7.1 EULER EQUATIONS

6.7.1.1 One-Dimensional Boundary Conditions

As mentioned in Section 6.2.1.3, the number of boundary conditions to be specified at inflow and outflow boundaries is determined by the eigenvalue spectrum of the Jacobian matrices (6.2.6) in terms of the primitive variables associated with boundary conditions normal to the surface. They are the characteristic variables or Riemann invariants $\mathbf{W}_1, \mathbf{W}_2$, and $\mathbf{W}_3$ in one dimension as given by (6.2.15) and (6.2.30). The general rule is that the number of Dirichlet boundary conditions for primitive variables is equal to the number of positive eigenvalues of the Jacobian matrix, which are prescribed as *physical boundary conditions*. In contrast, the negative eigenvalues

represent the *numerical boundary conditions* which must be extrapolated from the flowfield.

Propagation of flow quantities in a one-dimensional flow are shown for expansion and shock waves in Figure 6.2.3. Note that C_- wave is negative for subsonic flow whereas it is positive for supersonic flow in the domain of dependence. A summary of general boundary conditions is shown in Figure 6.7.1. At an inlet point, the characteristics C_0 and C_+ have slopes u and $u + a$, which are always positive for a flow in the positive x- direction. Thus, they will carry information from the boundaries toward the inside domain. The third characteristic C_- has a slope whose sign depends on the inlet Mach number. For the supersonic inlet, C_- has a positive sign, whereas it has a negative sign for subsonic flow. Therefore, no boundary conditions associated with C_- for the subsonic inlet can be specified. Similar considerations can be made for the outlet. Namely, no boundary conditions are to be specified for C_+ and C_0. As to C_-, however, we must provide boundary conditions for subsonic outlet, but not for supersonic outlet.

Note that each characteristic variable transports a given information and the quantities transported from the inside of the domain toward the boundary will dictate the situation along this boundary. Thus, only variables transported from the boundaries toward the interior are identified as physical boundary conditions. The remaining variables transported outside of the domain depend on the computed flow situations or part of the solution. This additional information, known as the numerical boundary conditions, can be linearly or quadratically extrapolated from the downstream (inflow) or upstream (outflow) flowfield information. These physical and numerical boundary conditions are summarized in Table 6.7.1.

Characteristic Boundary Conditions

If the full information on the incoming and outgoing characteristics is recovered from the imposed combinations of conservation variables $\mathbf{U}$ and primitive variables $\mathbf{V}$, then the problem is said to be well posed. Let us consider the subsonic outlet in which one physical boundary condition is allowed, say pressure p. From the relations (6.2.19) and (6.2.23) together with (6.2.28) we may write

$$\Delta\mathbf{W} = \begin{bmatrix} \Delta\mathbf{W}_a \\ \Delta\mathbf{W}_b \end{bmatrix} = \begin{bmatrix} \mathbf{L}_{aa}^{-1} & \mathbf{L}_{ab}^{-1} \\ \mathbf{L}_{ba}^{-1} & \mathbf{L}_{bb}^{-1} \end{bmatrix} \begin{bmatrix} \Delta\mathbf{V}_a \\ \Delta\mathbf{V}_b \end{bmatrix} = \begin{bmatrix} -1/\rho a & 0 & 1 \\ -1/a^2 & 1 & 0 \\ 1/\rho a & 0 & 1 \end{bmatrix}_0 \begin{bmatrix} \Delta p \\ \Delta\rho \\ \Delta u \end{bmatrix} \tag{6.7.1}$$

where the subscript 0 denotes end conditions, with a and b indicating the physical

Table 6.7.1 Physical and Numerical Boundary Conditions

		Subsonic	Supersonic
Inlet	Physical	W_1,W_2	W_1, W_2, W_3
	Numerical	W_3	None
Outlet	Physical	W_3	None
	Numerical	W_1, W_2	W_1, W_2, W_3

Supersonic Inflow

Supersonic Outflow

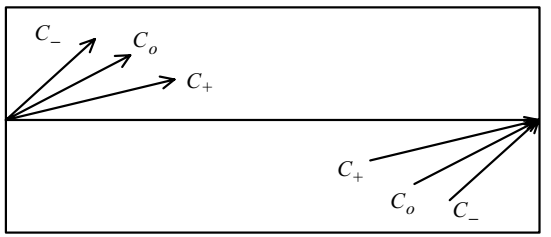

Three characteristics going into the domain. (Three physical boundary conditions required)

Three characteristics going out of the domain. (No physical boundary conditions. Instead, three numerical boundary conditions required)

	INFLOW		OUTFLOW	
	Euler	Navier-Stokes	Euler	Navier-Stokes
1-D	$\rho, \rho v_i, \rho E \quad (i = 1)$		Dirichlet, none (Set free) All variables extrapolated	
2-D	$\rho, \rho v_i, \rho E \quad (i = 1,2)$	$\rho, \rho v_i, \rho E \quad (i = 1,2)$	Dirichlet, none (Set free) $\rho E_{,i} n_i = 0$	Dirichlet, none (Set free) $\tau_{ij} n_j = 0 \quad (i = 1,2)$ $\rho E_{,i} n_i = 0$
3-D	$\rho, \rho v_i, \rho E \quad (i = 1,2,3)$	$\rho, \rho v_i, \rho E \quad (i = 1,2,3)$	Dirichlet, none (Set free) $\rho E_{,i} n_i = 0$	Dirichlet none (Set free) $\tau_{ij} n_j = 0 \quad (i = 1,2,3)$ $\rho E_{,i} n_i = 0$

(a)

Figure 6.7.1 Summary of boundary conditions for compressible flows. **(a)** Supersonic flow boundary conditions. **(b)** Subsonic flow boundary conditions.

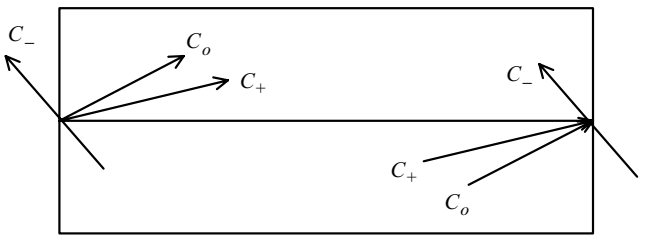

Two characteristics going into the domain, one characteristic going out of the domain. (One numerical and two physical boundary conditions required)

Two characteristics going out of the domain, one characteristic going into the domain. (One physical and two numerical boundary conditions required)

	INFLOW		OUTFLOW	
	Euler	Navier-Stokes	Euler	Navier-Stokes
1-D	$\rho, \rho E$ ρv_i extrapolated		$\rho v_i \quad (i = 1)$ All other variables extrapolated	
2-D	$\rho, \rho E$ ρv_i extrapolated	$\rho, \rho E$ ρv_i extrapolated	$\rho v_i \quad (i = 1, 2)$ All other variables extrapolated	$\rho v_i \quad (i = 1, 2)$ $\tau_{ij} n_j = 0 \quad (i = 1, 2)$ $\rho E_{,i} n_i = 0$
3-D	$\rho, \rho E$ ρv_i extrapolated	$\rho, \rho E$ ρv_i extrapolated	$\rho v_i \quad (i = 1, 2, 3)$ All other variables extrapolated	$\rho v_i \quad (i = 1, 2, 3)$ $\rho E_{,i} n_i = 0$

(b)

Figure 6.7.1 (*continued*)

(imposed variable) and numerical (free variable) boundary conditions, respectively.

$$\mathbf{W}_a = \mathbf{W}_3, \qquad \mathbf{W}_b = \begin{bmatrix} \mathbf{W}_1 \\ \mathbf{W}_2 \end{bmatrix}, \qquad \mathbf{V}_a = p, \qquad \mathbf{V}_b = \begin{bmatrix} \rho \\ u \end{bmatrix}$$

$$\mathbf{L}_{aa}^{-1} = -1/\rho a, \qquad \mathbf{L}_{ab}^{-1} = \begin{bmatrix} 0 & 1 \end{bmatrix}, \qquad \mathbf{L}_{ba}^{-1} = \begin{bmatrix} -1/a^2 \\ 1/\rho a \end{bmatrix}, \qquad \mathbf{L}_{bb}^{-1} = \begin{bmatrix} 1 & 0 \\ 0 & 1 \end{bmatrix}$$

Solving $\Delta \mathbf{V}_b$ from (6.7.1) yields

$$\Delta \mathbf{V}_b = \left(\mathbf{L}_{bb}^{-1}\right)^{-1} \left[\Delta \mathbf{W}_b - \mathbf{L}_{ba}^{-1} \Delta \mathbf{V}_a\right] \tag{6.7.2}$$

Obviously, the nonsingularity of $\mathbf{L}_{bb}^{-1}$ in (6.7.2) constitutes the condition for *well-posedness*. Thus, we require

$$\left|\mathbf{L}_{bb}^{-1}\right| \neq 0 \tag{6.7.3}$$

This can be applied for the various combinations of primitive variables at the boundaries. At a subsonic outlet it is shown by (6.7.1) that any of three variables ρ, u, p can be chosen as a physical boundary condition. This is because the first column of the transformation matrix in (6.7.1) contains all nonzero terms and thus none of the submatrices defining $\mathbf{W}_b$ is zero. For a subsonic inlet the physical boundary conditions $\mathbf{W}_a$ consist of ρ and u, with $\mathbf{W}_b = p$. This leads to

$$\Delta \mathbf{W} = \begin{bmatrix} \Delta \mathbf{W}_a \\ \Delta \mathbf{W}_b \end{bmatrix} = \begin{bmatrix} 1 & 0 & -1/a^2 \\ 0 & 1 & 1/\rho a \\ 0 & 1 & -1/\rho a \end{bmatrix}_0 \begin{bmatrix} \Delta\rho \\ \Delta u \\ \Delta p \end{bmatrix} \tag{6.7.4}$$

where it is seen that the bottom row of the transformation matrix has one zero term corresponding to the density ρ so that

$$\Delta \mathbf{W}_b = \Delta u - \frac{\Delta p}{(\rho a)_0} \tag{6.7.5}$$

which indicates that it is not possible to define $\Delta\rho$ at the boundary and the choice of u and p as a physical boundary condition is not well-posed. However, for any other combination involving ρ as a physical condition, one can determine the remaining free variable using (6.7.5).

Extrapolation Methods

For simplicity, let us use the variable Q to denote either the conservation variables (U), primitive variables (V), and characteristic variables (W) or any other combination, with the conditions for an inlet boundary designated as $i = 1, 2, 3 \ldots$ and outlet boundary as $i = p,\ p-1,\ p-2, \ldots$ The common practice is to use a linear (first order) extrapolations as follows:

Space extrapolation:

$$\begin{aligned} \mathbf{Q}_p^{n+1} &= 2\mathbf{Q}_{p-1}^{n+1} - \mathbf{Q}_{p-2}^{n+1} \\ \Delta \mathbf{Q}_p^{n} &= 2\Delta \mathbf{Q}_{p-1}^{n} - \Delta \mathbf{Q}_{p-2}^{n} \end{aligned} \tag{6.7.6a,b}$$

Space-time extrapolation:

$$\begin{aligned} \mathbf{Q}_p^{n+1} &= 2\mathbf{Q}_{p-1}^{n} - \mathbf{Q}_{p-2}^{n} \\ \Delta \mathbf{Q}_p^{n} &= 2\Delta \mathbf{Q}_{p-1}^{n-1} - \Delta \mathbf{Q}_{p-2}^{n-1} \end{aligned} \tag{6.7.7a,b}$$

Time extrapolation:

$$\begin{aligned} \mathbf{Q}_p^{n+1} &= 2\mathbf{Q}_p^{n} - \mathbf{Q}_p^{n-1} \\ \Delta \mathbf{Q}_p^{n} &= \Delta \mathbf{Q}_p^{n-1} \end{aligned} \tag{6.7.8a,b}$$

These schemes were studied by Griffin and Anderson [1977] and Gottlieb and Turkel [1978] for applications to the two-step Lax-Wendroff schemes. They show that the space-extrapolation methods do not stabilize these schemes nor reduce the stability limits.

Another approach is to discretize the equations at the boundary points in a one-sided manner such as (3.2.5) and to add this equation to the interior scheme. For instance, one could add a first order appropriate upwind equation in the Lax-Wendroff scheme and provide the missing information. Some of the examples for boundary conditions are shown in Figure 6.7.2.

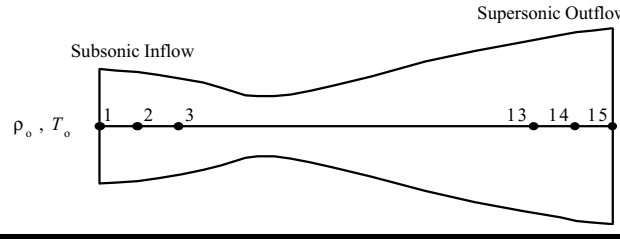

INFLOW	OUTFLOW
Physical boundary conditions, (ρ_1, T_1)	No physical boundary conditions
Numerical boundary conditions Extrapolate: $u_1 = 2u_2 - u_3$ Compute: $p = \rho RT$	Numerical boundary conditions Extrapolate: $u_{15} = 2u_{14} - u_{13}$, $\rho_{15} = 2\rho_{14} - \rho_{13}$, $T_{15} = 2T_{14} - T_{13}$
Initial conditions, $\rho(x,0) = T(x,0) = u(x,0) = 0$; If outflow is subsonic, specify p_{15} and set the others free.	

(a)

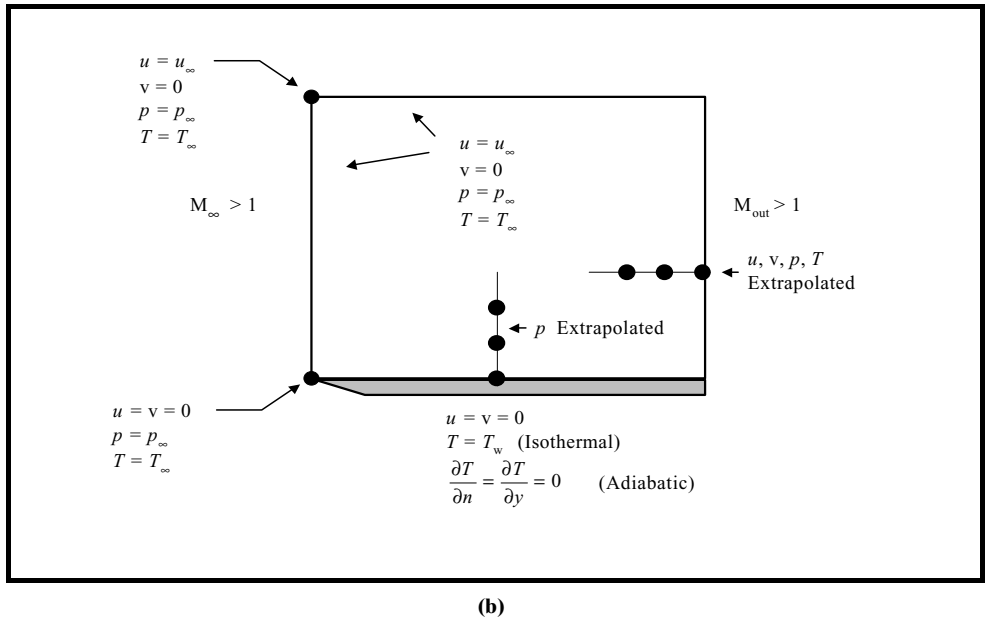

(b)

Figure 6.7.2 Examples for boundary conditions **(a)** 1-D boundary conditions for variable cross sections. **(b)** 2-D boundary conditions for a flat plate.

Characteristic Extrapolation Methods

This is an alternative method to the one-sided discretization of the compatibility equations corresponding to the outgoing characteristics [Yee, Beam, and Warming, 1982]. It follows from (6.7.2) that the numerical characteristic variables $\Delta \mathbf{W}_b$ are defined by an extrapolation such as in (6.7.6b):

$$\Delta \mathbf{W}_{b,p} = 2\Delta \mathbf{W}_{b,p-1} - \Delta \mathbf{W}_{b,p-2} \tag{6.7.9}$$

The values at $i = p-1$ and $i = p-2$ are obtained from the primitive variables by an explicit evaluation of (6.7.2):

$$\Delta \mathbf{W}_b = L_{ba}^{-1} \Delta \mathbf{V}_a + L_{bb}^{-1} \Delta \mathbf{V}_b \quad \text{for } i = p-1,\, p-2 \tag{6.7.10}$$

where the matrix elements are evaluated at time level n. By setting $\Delta \mathbf{V}_a = 0$ in (6.7.2) we obtain

$$\Delta \mathbf{V}_{b,p} = \left(L_{bb,p}^{-1}\right)^{-1} \Delta \mathbf{W}_{b,p} \tag{6.7.11}$$

where for time dependent problems $\Delta \mathbf{V}_a \neq 0$. This will be determined by the imposed time variation. The free variables $\mathbf{V}_{b,p}$ are transformed to the conservation variables through (6.2.7).

$$\Delta \mathbf{U}_p = \mathbf{M}_p \begin{bmatrix} \Delta \mathbf{V}_a \\ \Delta \mathbf{V}_{b,p} \end{bmatrix} = \mathbf{M}_p \begin{bmatrix} 0 \\ \Delta \mathbf{V}_{b,p} \end{bmatrix} \tag{6.7.12}$$

For subsonic outflow boundary with pressure imposed, we observe that

$$\Delta \mathbf{W}_{b,i} = \begin{bmatrix} \Delta w_1 \\ \Delta w_2 \end{bmatrix}_i = \begin{bmatrix} -1/a^2 \\ 1/\rho a \end{bmatrix} \Delta p_i + \begin{bmatrix} 1 & 0 \\ 0 & 1 \end{bmatrix} \Delta \begin{bmatrix} \rho \\ u \end{bmatrix}_i \tag{6.7.13}$$

$$\Delta \mathbf{W}_{b,p} = 2 \begin{bmatrix} -\Delta p/a^2 + \Delta \rho \\ \Delta p/\rho a + \Delta u \end{bmatrix}_{p-1} - \begin{bmatrix} -\Delta p/a^2 + \Delta \rho \\ \Delta p/\rho a + \Delta u \end{bmatrix}_{p-2} = \begin{bmatrix} \Delta w_1 \\ \Delta w_2 \end{bmatrix}_p \tag{6.7.14}$$

with $i = p-1, i = p-2$. It follows from (6.7.11) and (6.7.14) that

$$\Delta \mathbf{V}_{b,p} = \begin{bmatrix} \Delta \rho \\ \Delta u \end{bmatrix}_p = \begin{bmatrix} 1 & 0 \\ 0 & 1 \end{bmatrix} \begin{bmatrix} \Delta w_1 \\ \Delta w_2 \end{bmatrix}_p \tag{6.7.15}$$

Similarly, the corresponding conservation variables are given by (6.7.12),

$$\Delta \mathbf{U}_p = \mathbf{M} \begin{bmatrix} \Delta \rho \\ \Delta u \\ 0 \end{bmatrix}_p = \begin{bmatrix} \Delta \rho \\ \Delta(\rho u) \\ \Delta(\rho E) \end{bmatrix}_p \tag{6.7.16}$$

Thus the boundary condition equation for $(\Delta \rho)_p$ may be written as

$$(\Delta \rho)_p + 2\left(\frac{\Delta p}{a^2} - \Delta \rho\right)_{p-1} - \left(\frac{\Delta p}{a^2} - \Delta \rho\right)_{p-2} = 0 \tag{6.7.17}$$

This should be added to the interior point $p-1$. Similar equations can be written for $\Delta(\rho u)$ and $\Delta(\rho E)$.

6.7.1.2 Multi-Dimensional Boundary Conditions

Evaluation of multidimensional boundary conditions may be carried out similarly as in one dimension. The number of physical boundary conditions to be imposed at a boundary with the normal vector **n** pointing toward the flow domain is determined by the signs of the eigenvalues of the matrix **K** in terms of the primitive variable Jacobian $\mathbf{A}_i$ or the conservation variable Jacobian $\mathbf{a}_i$.

$$\begin{aligned} \mathbf{K} &= \mathbf{A}_i \kappa_i \qquad (i = 1, 2, 3) \\ \mathbf{K}^* &= \mathbf{a}_i \kappa_i \qquad (i = 1, 2, 3) \end{aligned} \tag{6.7.18a,b}$$

The eigenvalues Λ of both matrices **K** and $\mathbf{K}^*$ are equal,

$$\Lambda = \begin{bmatrix} \mathrm{v}_i \kappa_i & 0 & 0 & 0 & 0 \\ 0 & \mathrm{v}_i \kappa_i & 0 & 0 & 0 \\ 0 & 0 & \mathrm{v}_i \kappa_i & 0 & 0 \\ 0 & 0 & 0 & \mathrm{v}_i \kappa_i + a & 0 \\ 0 & 0 & 0 & 0 & \mathrm{v}_i \kappa_i - a \end{bmatrix} \tag{6.7.19}$$

in which the normal velocities $\mathrm{v}_i n_i = \mathrm{v}_i \kappa_i$ determine the signs of the eigenvalues.

Note that, for the inflow and outflow boundaries, if an eigenvalue λ is positive, the information carried by the corresponding characteristics propagates toward the interior domain and a physical boundary condition is to be imposed. If λ is negative, then the numerical boundary condition must be imposed. For example, at the subsonic inlet, two thermodynamic variables (temperature and pressure) and two velocity components are available as physical boundary conditions and one velocity component can be used as a numerical boundary condition.

For a solid wall, a single physical boundary condition is required as only one characteristic enters the flow boundaries. This is equivalent to

$$\begin{aligned} \mathrm{v}_i n_i &= 0 \\ p n_i &\neq 0 \end{aligned} \tag{6.7.20a,b}$$

Here, the wall pressure is numerically extrapolated from adjacent points.

Two-dimensional compatibility or characteristic relations are written as an extension of (6.2.28) as

$$\delta \mathbf{W} = \begin{bmatrix} \delta w_1 \\ \delta w_2 \\ \delta w_3 \\ \delta w_4 \end{bmatrix} = \begin{bmatrix} \delta \rho - \dfrac{\delta p}{a^2} \\ \kappa_y \delta u - \kappa_x \delta \mathrm{v} \\ n_i \delta \mathrm{v}_i + \dfrac{\delta p}{\rho a} \\ -n_i \delta \mathrm{v}_i + \dfrac{\delta p}{\rho a} \end{bmatrix} \tag{6.7.21}$$

which may be recast into (6.2.20) and (6.2.29). Thus, if the pressure and the velocity are uniform in the boundary surface, it is seen that we recover the one-dimensional condition given by (6.7.20).

6.7.1.3 Nonreflecting Boundary Conditions

Physical boundary conditions may be replaced by specification of nonreflecting boundary conditions. Let a constant pressure be imposed at a subsonic exit section as

$$\Delta p = p^{n+1} - p^n = 0 \tag{6.7.22}$$

This is equivalent to allowing perturbation waves to be reflected at the boundaries. Since the amplitude of the local perturbation wave carried by the incoming characteristic is $\Delta w_3 = \Delta u - \Delta p/\rho a$, imposing $\Delta p = 0$ amounts to the generation of an incoming wave of intensity $\Delta w_3 = \Delta u$ reflected from the exit boundary.

Engquist and Majda [1979] and Hedstrom [1979] proposed that the nonreflecting boundary conditions be implemented by making the local perturbations propagated along incoming characteristics vanish.

$$\frac{\partial w_k}{\partial t} = 0 \tag{6.7.23}$$

This will require that, for subsonic flows, we have

Inlet boundary conditions

$$\Delta w_1 = \Delta\rho - \frac{\Delta p}{a^{2n}} = 0 \tag{6.7.24a}$$

$$\Delta w_2 = \Delta u + \frac{\Delta p}{\rho^n a^n} = 0 \tag{6.7.24b}$$

Outlet boundary condition

$$\Delta w_3 = \Delta u - \frac{\Delta p}{\rho^n a^n} \tag{6.7.25}$$

These characteristic variables are not constant across a shock wave and will result in a reflection wave if a shock passes through a boundary.

Rudy and Strickwerda [1980] observed that the nonreflecting condition (6.7.23) does not ensure (6.7.22) or $p = p^*$ and that an ad hoc treatment may be to replace (6.7.23) for the incoming characteristic by, at the exit boundary,

$$\frac{\partial u}{\partial t} - \frac{1}{\rho a}\frac{\partial p}{\partial t} - \frac{\alpha}{\rho a}(p - p^*) = 0 \tag{6.7.26}$$

for $\alpha > 0$. The parameter α is problem dependent. For example, it has been suggested that we may choose $0.1 \leq \alpha \leq 0.2$ for $M = 0.8$ and $\alpha \cong 1$ for $M = 0.4$.

6.7.2 NAVIER-STOKES SYSTEM OF EQUATIONS

The Navier-Stokes system of equations may be considered as mixed hyperbolic, parabolic, and elliptic equations, or refered to as incompletely parabolic equations [Strikwerda, 1976; Gustafsson and Sundström, 1978]. Let us consider the Navier-Stokes system of equations in the form

$$\frac{\partial \mathbf{U}}{\partial t} + \mathbf{a}_i \frac{\partial \mathbf{U}}{\partial x_i} + \mathbf{b}_i \frac{\partial \mathbf{U}}{\partial x_i} + \mathbf{c}_{ij} \frac{\partial^2 \mathbf{U}}{\partial x_i \partial x_j} = 0 \tag{6.7.27}$$

which is obtained from (6.3.7) by inserting the convection Jacobian $\mathbf{a}_i$, diffusion Jacobian $\mathbf{b}_i$, and diffusion gradient Jacobian $\mathbf{c}_{ij}$. To determine the number of boundary condition, we must convert the conservation variables, $\mathbf{U} = [\rho \;\; \rho v_i \;\; \rho E]^T$ into nonconservation variables (primitive variables), $\mathbf{V} = [\rho \;\; v_i \;\; p]^T$ such that

$$\frac{\partial \mathbf{V}}{\partial t} + \mathbf{A}_i \frac{\partial \mathbf{V}}{\partial x_i} + \mathbf{B}_i \frac{\partial \mathbf{V}}{\partial x_i} + \mathbf{C}_{ij} \frac{\partial^2 \mathbf{V}}{\partial x_i \partial x_j} = 0 \tag{6.7.28}$$

Here, procedures similar to those employed for the case of the Euler equations in Section 6.2.1 may be followed to obtain the eigenvalues for the diffusion Jacobian $\mathbf{B}_i$ and the diffusion gradient Jacobian $\mathbf{C}_{ij}$ through the transformation matrix of the form (6.2.7)

$$\mathbf{M} = \frac{\partial \mathbf{U}}{\partial \mathbf{V}}$$

so that

$$\mathbf{A}_i = \mathbf{M}^{-1}\mathbf{a}_i\mathbf{M}, \quad \mathbf{B}_i = \mathbf{M}^{-1}\mathbf{b}_i\mathbf{M}, \quad \mathbf{C}_{ij} = \mathbf{M}^{-1}\mathbf{c}_{ij}\mathbf{M}$$

Introduce the oscillatory behavior in (6.7.28) with the wave number κ_i and frequency ω in the form,

$$\mathbf{V} = \overline{\mathbf{V}} e^{I(\kappa_i x_i - \omega t)} \tag{6.7.29}$$

leading to

$$(-\omega + \mathbf{A}_i\kappa_i + \mathbf{B}_i\kappa_i + \mathbf{C}_{ij}\kappa_i\kappa_j)\overline{\mathbf{V}} = 0 \tag{6.7.30}$$

which has a nontrivial solution if and only if

$$|\mathbf{K} - \lambda\mathbf{I}| = 0 \tag{6.7.31}$$

with

$$\lambda\mathbf{I} = \omega \tag{6.7.32}$$

$$\mathbf{K} = \mathbf{A}_i\kappa_i + \mathbf{B}_i\kappa_i + \mathbf{C}_{ij}\kappa_i\kappa_j \tag{6.7.33}$$

The eigenvalue problem similar to (6.7.31) was obtained by Nordström [1989], neglecting $\mathbf{B}_i\kappa_i$.

For multidimensional problems, the extra boundary conditions for the Navier-Stokes system of equations are obtained by

$$\int_\Omega \tau_{ij,i}\, d\Omega = \int_\Gamma \tau_{ij} n_i\, d\Gamma \tag{6.7.34}$$

with

$$\tau_{ij} n_i = \mu\left[(\mathrm{v}_{i,j} + \mathrm{v}_{j,i})n_i - \tfrac{2}{3}\mathrm{v}_{i,i} n_j\right] \tag{6.7.35}$$

where the velocity gradients are taken in the flow directions.

Unlike Euler equations, the Navier-Stokes system of equations require the no-slip boundary conditions at solid walls, resulting in the relative velocity between the fluid and the solid wall being zero.

For an adiabatic wall, we have

$$q_w = -kT_{,i}n_i = 0 \tag{6.7.36}$$

The wall temperature $T = T_w$ may also be fixed. The second thermodynamic variable at the solid wall can be obtained either by extrapolation from the inside or by applying the normal pressure equation

$$\frac{\partial p}{\partial n} = \tau_{ij,i} n_j \tag{6.7.37}$$

which vanishes for thin shear layers. A summary of boundary conditions for the Navier-Stokes system of equations is shown in Figure 6.7.2.

Since the exact form of eigenvalues of K in (6.7.33) depends on many different physical and geometrical conditions, the number of physical boundary conditions (positive eigenvalues) and the number of numerical boundary conditions (negative eigenvalues) cannot be determined exactly for all arbitrary physical and geometrical situations.

As mentioned earlier, the accuracy and convergence of numerical solution of the Navier-Stokes system of equations depend on correct applications of boundary conditions. Rudy and Strickwerder [1980] and Nordström [1989] examine various options of boundary conditions and evaluate the rates of solution convergence (well-posedness) associated with appropriate choices of boundary conditions. Other theoretical studies of boundary conditions include Kreiss [1970], Strickwerder [1976, 1977], Gustaffson and Sundström [1978], and Engquist and Gustaffson [1987], among others.

6.8 EXAMPLE PROBLEMS

Since benchmark problems using the central schemes, low and high order upwinding schemes including MUSCL, TVD, FCT, and ENO have been amply demonstrated in the literature, no attempt is made to include them here except for a simplest example for the benefit of the beginner. FDM applications of the FDV theory for high-speed flows have not appeared in the literature, and so they are illustrated in this section. Some incompressible and compressible flow problems using the FDV theory via FEM are presented in Section 13.7.

6.8.1 SOLUTION OF EULER EQUATIONS

In this example, solutions of Euler equations are given in a quasi–one-dimensional nozzle with variable cross section, NACA 1135, using McCormack explicit scheme and flux vector splitting method.

Given:

$$S(x) = 1.398 + 0.347 \tanh(0.8x - 4)\text{ft}^2 \text{ (NACA 1135)}$$

$$\gamma = 1.4$$

$$R = 1716 \frac{\text{ft}^2}{\text{sec}^2\, R}$$

Case 1

Supersonic inflow – supersonic outflow.

Boundary Conditions

Inflow

$M = 1.5$
$p = 1000$ psf
$\rho = 0.00237$ slug/ft^3
$\rho u = 2.7323$ slug/ft^3 sec
$\rho E = 4075$ slug/ft sec^2

Outflow. Full extrapolation of **U** is required since all eigenvalues are positive.

Initial Conditions

$$\begin{aligned} \rho &= 0.00237 \\ \rho u &= 2.7323 \qquad\qquad 0 \le x \le 10 \\ \rho E &= 4075 \end{aligned}$$

Case 2

Supersonic inflow – subsonic outflow.

Boundary Conditions

Inflow – same as before
Outflow – $u = 390.75$ ft/sec.

Other quantities are extrapolated since two eigenvalues are positive.

Initial Conditions

$$\text{for } x \le 2.8 \begin{cases} \rho = 0.00237 \\ \rho u = 2.7323 \\ \rho E = 4075 \end{cases}, \quad \text{for } x > 2.8 \begin{cases} \rho = 0.00237 \\ \rho u = 0.92608 \\ \rho E = 2680.93 \end{cases}$$

Results: The computational results for both the McCormack and flux vector splitting methods are shown in Figure 6.8.1.1a for Case 1 and Figure 6.8.1.1b for Case 2. The solution for both methods was obtained using a total of eighty grid points.

Case 1

Both schemes demonstrate a good level of accuracy, with the flux vector splitting scheme converging faster than the McCormack explicit scheme.

Case 2

Here again we find that the flux vector splitting scheme converges faster than the McCormack explicit scheme, but the level of accuracy is not as good as in the first case (supersonic outflow). In this case, the solution exhibits dispersion errors at the shock.

6.8.2 TRIPLE SHOCK WAVE BOUNDARY LAYER INTERACTIONS USING FDV THEORY

The FDV theory is utilized to analyze the flowfield produced from a triple shock/boundary layer interaction using 3-D FDM discretization [Schunk et al., 1999]. Flowfields of this nature are often encountered in the inlets of high-speed vehicles such as the scramjet engine of NASA's Hyper-X research vehicle. For this analysis, the FDV numerical results are compared to the experimental measurements and FDM calculations via $k - \varepsilon$ turbulent model reported by Garrison et al. [1994]. As indicated earlier, the FDV theory is expected to simulate turbulent flow accurately if DNS mesh refinements are provided. However, such mesh refinements are not available at the present time due to limited computer resources. No turbulence modeling is used in the present analysis.

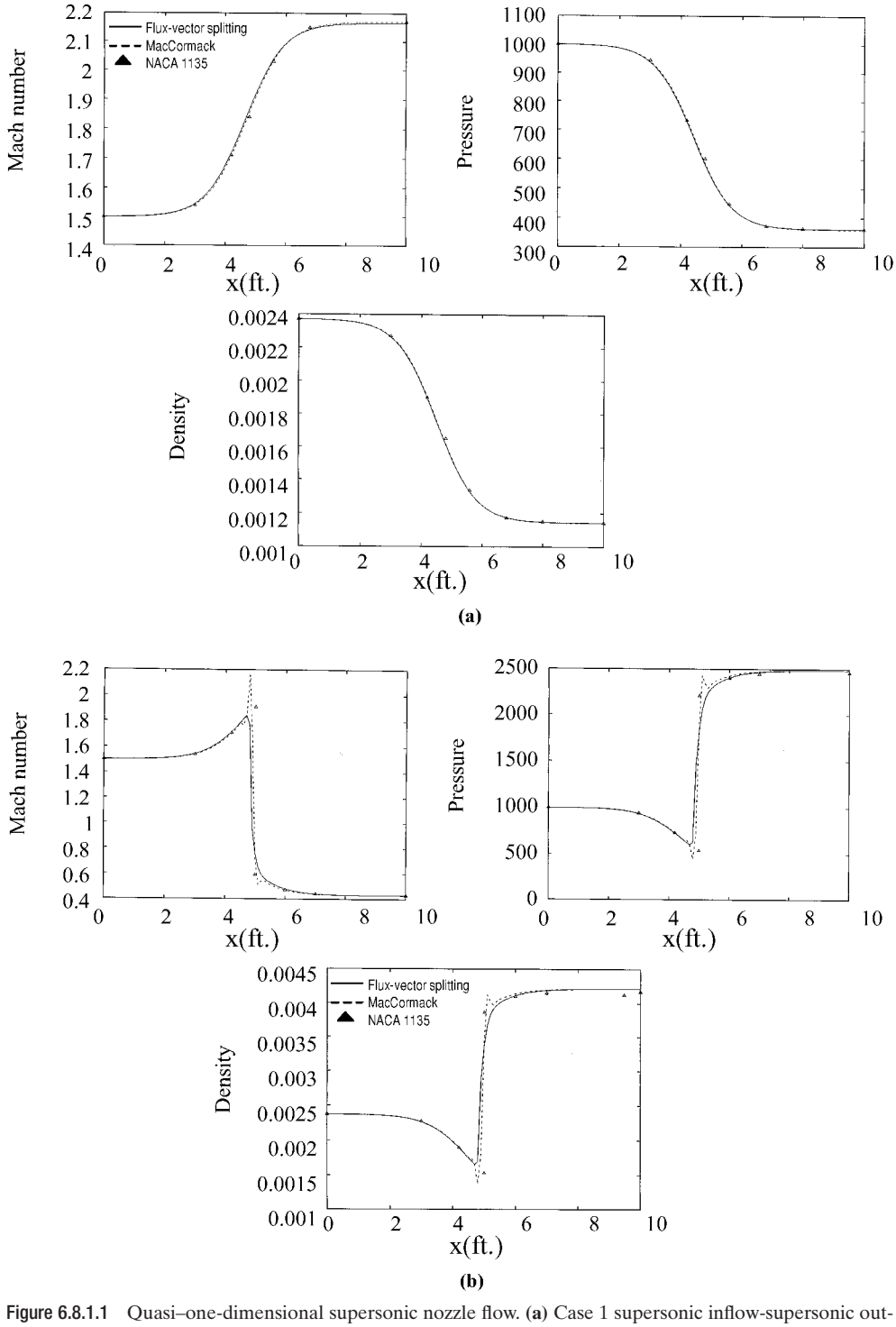

Figure 6.8.1.1 Quasi–one-dimensional supersonic nozzle flow. **(a)** Case 1 supersonic inflow-supersonic outflow. **(b)** Case 2 supersonic inflow-subsonic outflow.

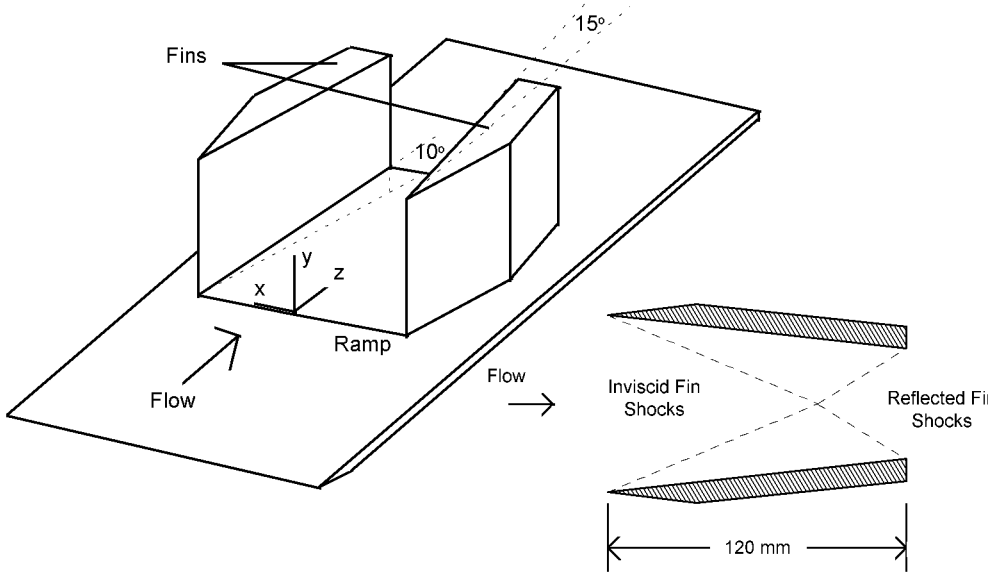

Figure 6.8.2.1 Hypersonic aircraft inlet. **(a)** Wind tunnel model. **(b)** Inviscid fin shock reflection (top view, x–z plane).

The wind tunnel model used to produce the triple shock/boundary layer interaction consists of two vertical fins and a horizontal ramp as shown in Figure 6.8.2.1. The angle of attack for the fins is 15° and the ramp is inclined at an angle of 10° with respect to the inlet flow. The inlet flow is at Mach 3.85 with a stagnation temperature and pressure of 295K and 1500 kPa, respectively. The fins are 82.5 mm high and are separated by a distance of 96.3 mm. The leading edge of the model is located 21 cm in front of the ramp inlet and produces a turbulent boundary layer with a thickness of 3.5 mm at the inlet to the model. Flow through the model is characterized by three oblique shocks originating from the leading edges of the ramp and the fins. Above the oblique ramp shock, the two inviscid fin shocks intersect and reflect as shown in Figure 6.7.1b. For the purposes of this analysis, the ramp is assumed to be 120 mm in length, the distance at which the reflected inviscid fin shocks are just incident upon the exit corners of each fin. According to inviscid flow theory, the fin shocks should intersect approximately 92 mm from the combined ramp and fin entrance. Measurements of the flowfield structure in the x–y plane are made via the Planar Laser Scattering (PLS) technique at various depths upstream of, coincident with, and behind the inviscid fin shock intersection [Garrison et al., 1996].

A detailed PLS view of the corner shock reflection physics is shown in Figure 6.8.2.2 [Garrison et al., 1996]. As shown in the figure, the inviscid fin (a) and ramp (b) shocks reflect to form the corner (c) shock. Both the embedded ramp (d) and fin (g) shocks split into separation (e,h) and rear (f,i) shocks above the ramp and fin boundary/separation layers. The ramp separated region (j) and the slip lines (k) dividing the different velocity regions as induced by the shock structure are also visible in the image.

Since the two fins are symmetric about the centerline, only half of the wind tunnel model is included in the computational model. Two finite difference computational grids, varying in resolution, are developed for the FDV analysis. The coarse grid model,

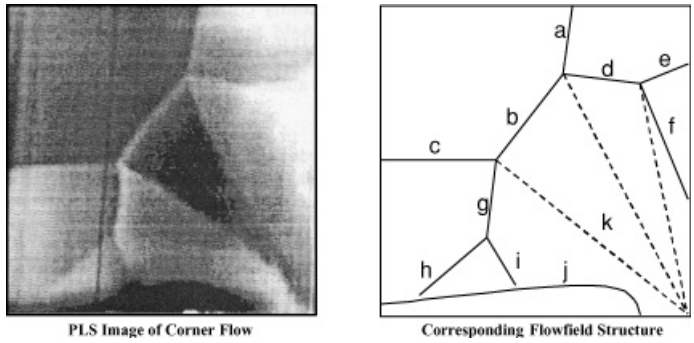

Figure 6.8.2.2 Fin/ramp shock structure in the x–y plane [Garrison et al., 1996], **a**) inviscid fin shock, **b**) corner shock, **c**) inviscid ramp shock, **d**) embedded ramp shock, **e**) ramp separation shock, **f**) ramp rear shock, **g**) embedded fin shock, **h**) separation fin shock, **i**) rear fin shock, **j**) separated region, **k**) sliplines.

consisting of a nonuniform nodal resolution of $31 \times 41 \times 55$ (in the x, y, and z directions) is shown in Figure 6.8.2.3. The viscous grid is clustered close to the fin and ramp surfaces. Results from the coarse grid analysis are used as the starting condition for the fine grid model. The fine grid model is obtained by interpolating the flow variables against the coarse mesh. Doubling the number of grid points in each direction produces a fine grid with over 538,000 nodal points ($61 \times 81 \times 109$). Recall that the most important aspect of the FDV theory is that the shock capturing mechanism and the transition and interaction between compressible/incompressible, viscous/inviscid, and laminar/turbulent flows are incorporated into the FDV formulation. No special treatments are required to simulate these physical phenomena. Thus, the finite difference discretization requires no special schemes. Simple central differences can be used to discretize the FDV equations given by (6.5.14).

The inlet conditions to the model are fixed with the freestream conditions described above ($M = 3.85$, $P_0 = 1500$ kPa, and $T_0 = 295$ K) and include a superimposed boundary layer 3.5 mm in height. At the fin and ramp surfaces, no-slip velocity boundary conditions are imposed and the normal pressure and temperature gradients are set to zero. In the symmetry plane and for the bounding surface on top (x-z plane), all of the

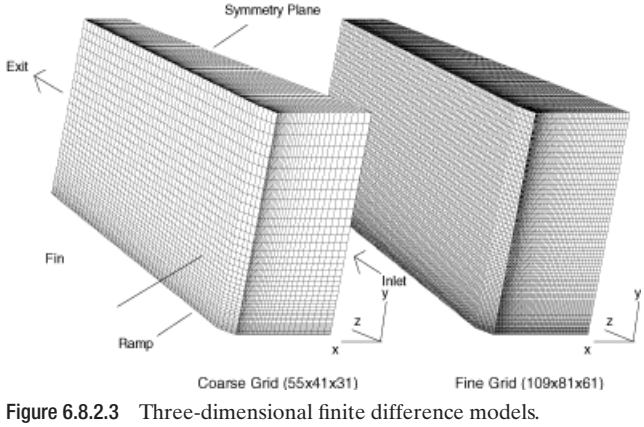

Figure 6.8.2.3 Three-dimensional finite difference models.

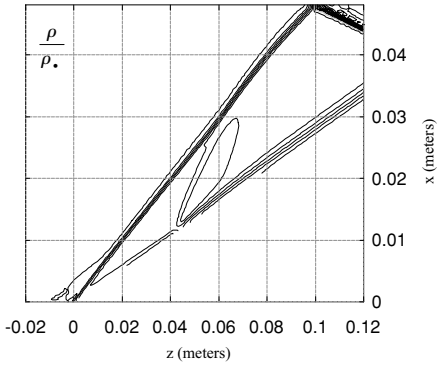

Figure 6.8.2.4 Inviscid fin shock interaction.

flow variables are computed such that the normal gradients vanish except for the normal flux, which is explicitly set to zero. At the exit, all of the flow variables are extrapolated from interior grid points.

In order to test the hypothesis that the FDV equations contain the necessary terms to model turbulence, no turbulence model is included in the analysis. It is theorized that turbulent fluctuations result from the interaction of the convective and diffusion Jacobians present in the second order terms of the FDV equations as dictated by the FDV parameters (s_1, s_2, s_3, s_4). The conclusions drawn from this study will be limited to predictions of the boundary layer separation height since the experimental results contain no measurements of turbulent statistics such as spectral energy density versus wave numbers, etc., since no Kolmogrov microscales are resolved in this analysis.

Density contours for the inviscid shock interaction (x-z plane, as viewed from above the wind tunnel model) are shown in Figure 6.8.2.4. The 15° fins produce inviscid shocks that are predicted to intersect and reflect approximately 97 mm from the ramp entrance (as opposed to 92 mm as predicted by inviscid flow theory). The reflected shock does not intersect with the exit corner of the ramp as expected. The discrepancy between the numerical prediction and inviscid flow theory could be due to the secondary oblique shock that is formed behind the fin shock (approximately 45 mm from the entrance). This is apparently an anomalous condition and could be due to the formation of a nonphysical boundary layer on the fin, possibly due to the discretization of the flowfield close to the fin wall.

Static pressure contours for flow in x-y planes located 70 mm (upstream of the inviscid shock intersection) and 97 mm (coincident with the inviscid shock intersection) from the combined fin/ramp entrance are shown in Figure 6.8.2.5. To match the experimental

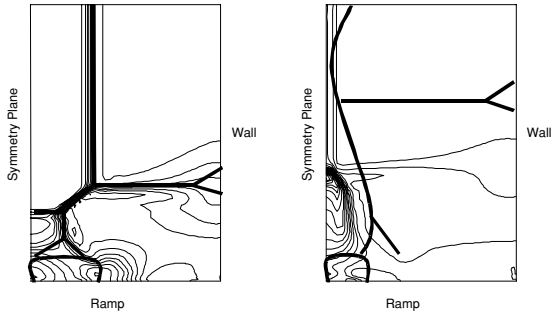

Figure 6.8.2.5 Static pressure contours in x–y plane before (left) and coincident (right) with the inviscid fin shock intersection.

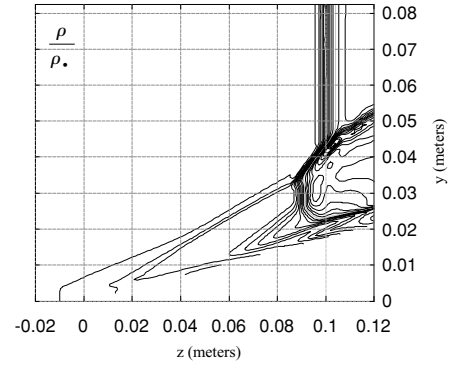

Figure 6.8.2.6 Boundary layer separation on the ramp.

images, the z locations of the x-y planes are scaled relative to the predicted inviscid fin shock intersection. The numerical predictions upstream of the fin shock intersection (left) correlate well with the experimental PLS images. Evident in the upstream figure are the inviscid ramp and fin shocks as well as the corner reflection. The flow separation from the ramp is also visible, appearing as concentric isobaric rings. Although not well resolved, it appears that both the embedded fin and ramp shocks split into separation and rear shocks above the respective surface separation/boundary layers. Coincident with the shock intersection (see right), the inviscid fin shocks merge together in the symmetry plane. No curvature of inviscid fin shock is observed in the numerical predictions as in the experimental results. The reflection of the corner shock about the symmetry plane is observed, but the ramp embedded shock is much lower relative to the height of the fin than in the experimental results. The ramp boundary layer separation is not strongly resolved in the static pressure contours. It is important to note that these results from the FDV theory qualitatively reveal the boundary layer separation predicted by Garrison et al. [1996] using a k-ε turbulence model.

An alternative view (Figure 6.8.2.6) of the flowfield in the symmetry plane (y–z plane, $x = 0$) shows the boundary layer separation and the reflection of the fin intersection shocks through the weaker ramp shock. No experimental imagery is available to compare to this figure, but it is nonetheless informative. Boundary layer separation appears to be approximately 5 mm at the exit.

More fundamental studies for validation of the FDV theory are presented in Chapter 13 using FEM. Contour plots of the FDV parameters are shown to resemble the actual flowfields of the supersonic compression corner flow. Transition between compressible and incompressible flows is also demonstrated for the driven cavity problems. Thus, these fundamental examples are not duplicated in this chapter. The reader is invited to examine Examples (3) and (4), Section 13.7, for details.

6.9 SUMMARY

History of compressible flow computations using potential equations, Euler equations, and the Navier-Stokes system of equations is long, and so is this chapter. Our focus was to study how to capture shocks in both inviscid flows and viscous flows. In compressible inviscid flows using Euler equations, we studied central schemes, first order upwind schemes, and second order upwind schemes. Specifically, we examined the flux vector splitting and Godunov method for the first order scheme and MUSCL, TVD, ENO,

and FCT for the second order scheme. For compressible viscous flows, it is necessary to solve the Navier-Stokes system of equations. We examined explicit methods, implicit methods, PISO methods, preconditioning methods, flowfield-dependent variation (FDV) methods, and other available methods. Exhaustive coverage of potential equation, Euler equations, and Navier-Stokes system of equations has been made available in many other texts, particularly in Hirsch [1990]. Thus, in this text, only a brief summary of these topics is provided. The emphasis has been placed on the FDV methods, anticipating that this theory be investigated more thoroughly in the future.

Currently, a limited amount of validation of the FDV theory is available. It has been verified that (1) the FDV parameters are equivalent to the TVD limiters, (2) FDV parameter contours resemble the flowfield (Mach number or density contours), and (3) transitions and interactions between inviscid/viscous flows, compressible/incompressible flows, and laminar/turbulent flows are characterized by the FDV process. Examples demonstrating these fundamental properties are presented in Section 13.7. An extensive and rigorous future research on FDV theory will be required not only for its own theoretical foundation, but also for closer examinations as to the relationships with other methods.

REFERENCES

Abgrall, R. [1994]. On essentially non-oscillatory schemes on unstructured meshes analysis and implementation. *J. Comp. Phys.*, 114, 45–58.

Beam, R. M. and Warming, R. F. [1976]. An implicit finite-difference algorithm for hyperbolic systems in conservation law form. *J. Comp. Phys.*, 22, 87–110.

———. [1978]. An implicit factored scheme for the compressible Navier-Stokes equations. *AIAA J.*, 16, 393–401.

Ben-Artzi, M. and Falcovitz, J. [1984]. A second order Godunov-type scheme for compressible fluid dynamics. *J. Comp. Phys.*, 55, 1–32.

Boris, J. P. and Book, D. L. [1973]. Flux corrected transport 1, SHASTA, a fluid transport algorithm that works., *J. Comp. Phys.*, 11, 38–69.

Briley, W. R. and McDonald, H. [1975]. Solution of the three-dimensional compressible Navier-Stokes equations by an implicit technique. Proc. Fourth International Conference on Numerical Methods in Fluid Dynamics, Lecture Notes in Physics, Vol. 35, Berlin: Springer-Verlag.

Casier, F., Deconinck, H. and Hirsch C. [1983]. A class of central bidiagonal schemes with implicit boundary conditions for the solution of Eulers equations. AIAA Paper 83-0126, AIAA 21st Aerospace Sciences Meeting. See also *AIAA J.*, 22, 1556–63.

Casper, J. [1992]. Finite volume implementation of high-order essentially nonoscillatory schemes in two dimensions. *AIAA J.* 30, 12, 2829–35.

Casper, J., Shu, C. W., and Atkins, H. [1994]. Comparison of two formulations for high-order accurate essentially nonoscillatory schemes. *AIAA J.*, 32, 10, 1970–77.

Choi, D. and Merkle, C. L. [1993]. The application of preconditioning for viscous flows. *J. Comp. Phys.*, 105, 203–23.

Chung, T. J. [1999]. Transitions and interactions of inviscid/viscous, compressible/incompressible, and laminar/turbulent flows. *Int. J. for Num. Meth. in Fl.,* 31, 223–46.

Courant, R., Isaacson, E., and Reeves, M. [1952]. On the solution of nonlinear hyperbolic differential equations by finite differences. *Comm. Pure Appl. Math.*, 5, 243–55.

Davis, S. F. [1984]. TVD finite difference schemes and artificial viscosity. ICASE Report 84-20, NASA CR-172373, NASA Langley Research Center.

Dutt, P. [1988]. Stable boundary conditions and difference schemes for Navier-Stokes equations. *SIAM J. Num. Anal.*, 25, 245–67.

Engquist, B. and Majda, A. [1979]. Radiation boundary conditions for acoustic and elastic wave calculations. *Comm. Pure Appl. Math.*, 32, 629–51.

Engquist, B. and Osher, S. [1980]. Stable and entropy satisfying approximations for transonic flow calculations. *Math. of Comp.*, 34, 45–75.

Garrison, T. J., Settles, G. S., Narayanswami, N., Knight, D. D., Horstman, C. C. [1996]. Flowfield surveys and computations of a crossing-shock wave/boundary-layer interaction. *AIAA J.*, 34, no. 1, 57–64.

Godunov, S. K. [1959]. Finite-difference method for numerical computation of discontinuous solutions of the equations of fluid dynamics., *Mat. Sb.*, 47, 271–306.

Godunov, S., Zabrodine, A., Ivanov, M., Kraiko, A. and Prokopov, G. [1979]. Resolution Numerique des Problems Multidimensionnels de la Dynamique des Gaz. Moscow, USSR: Editions MIR.

Gottlieb, D. and Turkel, E. [1978]. Boundary conditions for multistep finite difference methods for time-dependent equations. *J. Comp. Phys.*, 26, 181–96.

Griffin, M. D. and Anderson, J. D. [1977]. On the application of boundary conditions to time-dependent computations for quasi–one-dimensional fluid flows. *Comp. and Fl.*, 5, 127–37.

Gustafsson, B. [1982]. The choice of numerical boundary conditions for hyperbolic systems. *J. Comp. Phys.*, 48, 270–83.

Gustafsson, B. and Sundström, A. [1978]. Incompletely parabolic problems in fluid dynamics. *SIAM J. Appl. Math.*, 35, 343–57.

Harten, A. [1983]. High resolution schemes for hyperbolic conservation laws. *J. Comp. Phys.*, 9, 357–393.

———. [1984]. On a class of high resolution total variation stable finite difference schemes. *SIAM J. Num. Anal.*, 21, 1–23.

Harten, A. and Lax, P. D. [1981]. A random choice finite difference scheme for hyperbolic conservation laws. *SIAM J. Num. Anal.*, 18, 289–315.

Harten, A., Lax, P. D., and Van Leer, B. [1983]. On upstream differencing and Godunov-type schemes for hyperbolic conservation laws. SIAM Review, 25, 35–61.

Harten, A. and Osher, S. [1987]. Uniformity high-order accurate nonoscillatory schemes I. *SIAM J. Num. Anal.*, 24, 279–309.

Hedstrom, G. W. [1979]. Non-reflecting boundary conditions for non-linear hyperbolic systems. *J. Comp. Phys.*, 30, 222–37.

Hirsch, C. [1990]. *Numerical Computation of Internal and External Flows*. Vol. 2. New York: Wiley.

Holst, T. L. and Ballhaus, W. F. [1979]. Fast, conservative schemes for the full potential equation applied to transonic flows *AIAA J.*, 17, 145–52.

Issa, R. I., Gosman, A. D., and Watkins, A. P. [1986]. The computation of compressible and incompressible recirculating flows by a non-iterative schmes. *J. Comp. Phys.*, 62, 66–82.

Jameson, A. [1974]. Iterative solutions of transonic flows over airfoils and wings, including flows at Mach 1. *Comm. Pure Appl. Math.*, 27, 283–309.

Jameson, A., Schmidt, W., and Turkel, E. [1981]. Numerical simulation of the Euler equations by finite volume methods using Runge-Kutta time stepping schemes. AIAA Paper 81-1259, AIAA 5th Computational Fluid Dynamics Conference.

Kreiss, H. O. [1970]. Initial boundary value problem for hyperbolic systems. *Comm. Pure Appl. Math.*, 23, 273–98.

Lax, P. D. [1954]. Weak solutions of nonlinear hyperbolic equations and their numerical computation. *Comm. Pure Appl. Math.*, 7, 159–93.

Lax, P. D. [1973]. Hyperbolic systems of conservation laws and mathematical theory of shock waves. *Society for Industrial and Applied Mathematics*. Philadelphia, PA.

Lax, P. D. and Wendroff, B. [1960]. Systems of conservation laws. *Comm. Pure Appl. Math.*, 15, 363.

Lerat, A. [1979]. Numerical shock structure and nonlinear corrections for difference schemes in conservation form. Lecture Notes in Physics, 20, 345–51, New York: Springer-Verlag.
Lerat, A. [1983]. Implicit methods of second order accuracy for the Euler equations. AIAA Paper, 83–1925.
Lerat, A. and Peyret, R. [1974]. Noncentered schemes and shock propagation problems. *Comp. Fl.*, 2, 35–52.
MacCormack, R. W. [1969]. The effect of viscosity in hypervelocity impact cratering. AIAA Paper, 66–354.
MacCormack, R. W. and Paullay, A. J. [1972]. Computational efficiency achieved by time splitting of finite difference operators. AIAA Paper 72–154.
MacCormack, R. W. [1981]. A numerical method for solving the equations of compressible viscous flow, AIAA Paper, 81–0110.
Merkle, C. L., Sullivan, J. Y., Buelow, P. E. O., and Venkateswaran, S. [1998]. Computation of flows with arbitrary equations of state. *AIAA J.*, 36, 4, 515–21.
Moretti, G. [1979]. Conformal Mappings for the Computation of Steady Three-dimensional Supersonic Flows, Numerical/Laboratory Computer Methods in Fluid Mechanics. A. A. Pouring and V. I. Shah, eds. New York: ASME, 13–28.
Murman, E. M. and Cole, J. D. [1971]. Calculation of plane steady transonic flows. *AIAA J.*, 9, 114–21.
Nordström, J. [1989]. The influence of open boundary conditions on the convergence to steady state for the Navier-Stokes equations. *J. Comp. Phys.*, 85, 210–44.
Oliger, J. and Sundsröm, A. [1978]. Theoretical and practical aspects of some initial boundary value problems in fluid dynamics. *SIAM J. Appl. Math.*, 35, 419–46.
Osher, S. [1982]. Shock modelling in aeronautics. In K. W. Morton and M. J. Baines (eds.) *Numerical Methods for Fluid Dynamics*, London: Academic Press, 179–218.
———. [1984]. Riemann solvers, the entropy condition and difference approximations. *SIAM J. Num. Anal.*, 21, 217–35.
Osher, S. and Chakravarthy, S. R. [1984]. High resolution schemes and the entropy condition. *SIAM J. Num. Anal.*, 21, 955–84.
Osher, S., Hafez, M., and Whitlow, W. Jr. [1985]. Entropy condition satisfying approximations for the full potential equation of transonic flow. *Math. Comp.*, 44, 1–29.
Peyret, R. and Viviand, H. [1985]. Pseudo-unsteady methods for inviscid or viscous flow computations. *Recent Advances in the Aerospace Sciences, C. Casi (ed). Plenum, New York*.
Pletcher, R. H. and Chen, K. H. [1993]. On solving the compressible Navier-Stokes equations for unsteady flows at very low Mach numbers. AIAA Paper, 93-3368.
Rai, M. M. and Moin, P. [1993]. Direct numerical simulation of transitional and turbulence in a spatially evolving boundary layer. *J. Comp. Phys.*, 109, 169–92.
Raithby, G. D. [1976]. Skew upstream differencing schemes for problems involving fluid flow. *Comput. Meth. Appl. Mech. Eng.*, 9, 153–64.
Richtmyer, R. D. and Morton, K. W. [1967]. *Difference Methods for Initial-Value Problems*, 2nd ed., New York: Wiley, Interscience Publishers.
Roe, P. L. [1981]. Approximate Riemann solvers, parameter vectors and difference schemes. *J. Comp. Phys.*, 43, 357–372.
———. [1984]. Generalized formulation of TVD Lax-Wendroff schemes. ICASE Report 84-53. NASA CR-172478, NASA Langley Research Center.
———. [1985]. Upwind schemes using various formulations of the Euler equations. In F. Angrand et al. (eds.) *Numerical Methods for the Euler Equations of Fluid Dynamics*, Philadelphia, PA: SIAM Publications.
Rudy, D. H. and Strickwerda, J. C. [1980]. A non-reflecting outflow boundary condition for subsonic Navier-Stokes calculations. *J. Comp. Phys.*, 36, 55–70.
Schunk, R. G., Canabal, Heard, G. W., and Chung, T. J. [1999]. Unified CFD methods via flowfield-dependent variation theory. AIAA Paper, 99-3715.

Shu, C. W. and Osher, S. [1988]. Efficient implementation of essentially non-oscillatory shock-capturing schemes. *J. Comp. Phys.*, 77, 439–71.
Shu, C. W. and Osher, S. [1989]. Efficient implementation of essentially non-oscillatory shock-capturing schemes, II. *J. Comp. Phys.*, 83, 32–78.
Suresh, A. and Jorgenson, P. C. E. [1995]. Essentially nonoscillatory reconstructions via extrapolation. *AIAA Paper*, 95-0467.
Steger, J. L. and Warming, R. F. [1981]. Flux vector splitting of the inviscid gas-dynamic equations with applications to finite difference methods. *J. Comp. Phys.*, 40, 263–93.
Stanescu, D. and Habashi, G. [1998]. Essentially nonoscillatory Euler solutions on unstructured meshes using extrapolation. *AIAA J.*, 36, 8, 1413–16.
Strikwerda, J. C. [1976]. Initial boundary value problems for incompletely parabolic systems. Ph. D. dissertation, Standford University.
Strikwerda, J. C. [1977]. Initial boundary value problems for incompletely parabolic systems. *Comm. Pure Appl. Math.*, 30, 797–822.
Sweby, P. K. [1984]. High resolution schemes using flux limiters for hyperbolic conservation laws. *SIAM J. Num. Anal.*, 21, 995–1011.
Tannehill, J. C., Hoist, T. L., and Rakich, J. V. [1975]. Numerical computation of two-dimensional viscous blunt body flows with an impinging shock, AIAA Paper 75-154, Pasadena, California.
Van Leer, B. [1973]. Towards the ultimate conservative difference scheme. I. The quest of monotonicity. Lecture Notes in Physics, Vol. 18, 163–68. Berlin: Springer Verlag.
———. [1974]. Towards the ultimate conservative difference scheme. II. Monotonicity and conservation combined in a second order scheme. *J. Comp. Phys.*, 14, 361–70.
———. [1979]. Towards the ultimate conservative difference scheme. V. A second order sequel to Godunovs method. *J. Comp. Phys.*, 32, 101–36.
———. [1982]. Flux vector splitting for the Euler equations. Proc. 8th International Conference on Numerical Methods in Fluid Dynamics, Berlin: Springer-Verlag.
Woodward, P. R. and Colella, P. [1984]. The numerical simulation of two-dimensional fluid flow with strong shocks. *J. Comp. Phys.*, 54, 115–73.
Yanenko, N. N. [1979]. *The Method of Fractional Steps*. New York: Springer-Verlag. In J. R. Bunch and D. J. Rose (eds.), *Space Matrix Computations*, New York: Academic Press.
Yee, H. C. [1985]. On symmetric and upwind TVD schemes. Proc. 6th GAMM Conference on Numerical Methods in Fluid Mechanics, 399-407, Braunschweig: Vieweg.
Yee, H. C. [1986]. Linearized form of implicit TVD schemes for multidimensional Euler and Navier-Stokes equations. *Comp. Math. Appl.*, 12A, 413–32.
Yee, H. C., Beam, R. M., and Warming, R. F. [1982]. Boundary approximation for implicit schemes for one-dimensional inviscid equations of gas dynamics. *AIAA J.*, 20, 1203–11.
Zalesak, S. T. [1979]. Fully multidimensional flux corrected transport algorithm for fluids. *J. Comp. Phys.*, 31, 335–62.
Zhong, X. [1994]. Application of essentially nonoscillatory schemes to unsteady hypersonic shock-shock interference heating problems. *AIAA J.*, 32, 8, 1606–16.